UNIVERSIDADE DE LISBOA

FACULDADE DE CIÊNCIAS

DEPARTAMENTO DE BIOLOGIA VEGETAL

Study of the effects of the antifungal defensin *Ps*d1 in *Candida albicans* using atomic force microscopy and flow cytometry

Patrícia Maria de Oliveira e Silva

Dissertação

MESTRADO EM MICROBIOLOGIA APLICADA

2013

UNIVERSIDADE DE LISBOA

FACULDADE DE CIÊNCIAS

DEPARTAMENTO DE BIOLOGIA VEGETAL

Study of the effects of the antifungal defensin *Ps*d1 in *Candida albicans* using atomic force microscopy and flow cytometry

Patrícia Maria de Oliveira e Silva

Dissertação orientada por Doutora Sónia Gonçalves (IMM-FMUL)

e Prof.ª Doutora Ana Tenreiro (FCUL-BioFIG)

MESTRADO EM MICROBIOLOGIA APLICADA

2013

Study of the effects of the antifungal defensin *Ps*d1 in *Candida albicans* using atomic force microscopy and flow cytometry

Patrícia Maria de Oliveira e Silva

MASTER THESIS

2013

This thesis was fully performed at the Instituto de Medicina Molecular of the Faculty of Medicine of the University of Lisbon under the direct supervision of Dr. Sónia Gonçalves and Prof. Nuno C. Santos.

Prof. Ana Tenreiro was the internal designated supervisor on the context of the *Master in Applied Microbiology* of the Faculty of Sciences of the University of Lisbon.

Table of Contents

Preface

The work presented in this thesis is integrated in the Master in Applied Microbiology from the *Faculdade de Ciências da Universidade de Lisboa* (FCUL, Lisbon, Portugal) and was developed in the Biomembranes Unit of the *Instituto de Medicina Molecular* (IMM), *Faculdade de Medicina da Universidade de Lisboa* (FMUL, Lisbon, Portugal), under the supervision of Dr. Sónia Gonçalves (IMM / FMUL), Prof. Nuno C. Santos (IMM / FMUL) and Prof. Ana Tenreiro (BioFIG / FCUL). The present work is focused on the study of a plant defensin *Pisum sativum* defensin 1 (*Ps*d1), with antifungal properties against the human pathogen *Candida albicans*. Altogether, the results obtained by biophysical and flow cytometry analysis provide new information about the mode of action and the effects of *Ps*d1 as an alternative antifungal agent.

The results of a one year work integrated in the Biomembranes Unit as part of a research project already ongoing before my arrival, are gathered in this thesis. In the Introduction there is state-of-the-art information regarding *Candida albicans* as a human pathogen, antimicrobial peptides and their mode of action, resistance and function in the host organism, as well as the aims of this study. The Methodology section contains the theoretical and practical basis of the techniques and procedures employed in this work. Next, the results obtained are presented and discussed, and finally the conclusions to which this work led to are presented.

The involvement in this project greatly increased my research expertise and allowed me to apply my knowledge in the microbiology area and acquire valuable scientific knowledge. I participated in four short courses of biomedical interest:

- Flow Cytometry Workshop, 17th-21st June 2013, IMM;
- Requimte Atomic Force Microscopy Workshop 2013, 25th-28th March 2013, Centro de Química da Universidade do Porto;
- Nanomedicine - CAML PhD Advanced Course, 18th-20th February 2013, IMM;
- Beating the Blood-Brain and Other Blood Barriers Workshop, 6th-8th February 2013, IMM.

I also participated in a scientific meeting, the 9th European Biophysics Congress - EBSA 2013, 13th-17th July 2013 (Lisbon, Portugal), in which the results of the present work were presented in two communications on poster format (one of them presented by myself), with the two abstracts being published in the European Biophysical Journal (please consult the Appendix - Outcomes of the present thesis):

- Silva PM, Gonçalves S, Medeiros LN, Kurtenbach E, Santos NC. Antifungal defensin *Ps*d1 increases membrane roughness and promotes apoptosis in *Candida albicans*. Abstract published in (2013) *Eur Biophys J*, **42** (Suppl 1):S106.

- Gonçalves S, Silva PM, Medeiros LN, Kurtenbach E, Santos NC. Biofilm formation by different *Candida albicans* variants and their antifungal agents' susceptibility. Abstract published in (2013) *Eur Biophys J*, **42** (Suppl 1):S167.

In addition, I have already co-authored two manuscripts, one of them, as first author (a review with a subject closely related to this thesis work). The second manuscript, although not related to this thesis, employs some of the same techniques to study another antimicrobial agent (please consult abstracts in the Appendix - Outcomes of the present thesis):

- Silva PM, Gonçalves S, Santos NC. Defensins - antifungal lessons from eukaryotes (manuscript under editorial revision – acceptable with minor changes). Submitted for publication in the journal Frontiers in Antimicrobials, Resistance and Chemotherapy;

- Domingues MM, Silva PM, Franquelim HG, Carvalho FA, Castanho M, Santos NC. Antimicrobial protein $rBPI_{21}$-induced surface changes on Gram-negative and Gram-positive bacteria (manuscript submitted, under editorial revision after the submission of a revised version – acceptable with minor changes). Submitted for publication in the journal Nanomedicine (NBM).

Furthermore, the data presented in this thesis will also be converted in an additional manuscript, to be submitted to another international peer-reviewed journal during the upcoming months.

Acknowledgements

I wish to thank all my colleagues at the Biomembranes and the Physical Biochemistry Units of IMM, who were always helpful and welcoming since I became a part of the Biomembranes Unit. I am especially grateful to Dr. Sónia A. Gonçalves, my supervisor at the IMM, who directly and continuously worked with me and guided me throughout all the steps of this thesis work, and also to Prof. Nuno C. Santos, head of the Unit and my co-supervisor. The encouragement and support I always felt from both Sónia and Nuno were really important to me, by helping me to build up my self confidence in my work and my critical thinking towards my results. I am also thankful to Peter Eaton, Filomena A. Carvalho and Diana Gaspar for excellent and valuable discussions about Atomic Force Microscopy imaging and force spectroscopy.

My acknowledgements are also due to the professors of the Master in Applied Microbiology, for having inspired me and helped me in having a better understanding of the evolution and adaptation of the microbes surrounding us.

Candida albicans clinical isolate, from a donor of Hospital de Santa Maria, was a kind gift from Prof. Mário Ramirez (Instituto de Microbiologia, IMM, FMUL). *C. albicans* WT and Δ*gcs* as well the defensin *Ps*d1 were a kind gift from Prof. Eleonora Kurtenbach and Dr. Luciano N. de Medeiros (Instituto de Biofísica Carlos Chagas Filho, Universidade Federal do Rio de Janeiro, Rio de Janeiro, Brazil)

This work was funded by Fundação para a Ciência e a Tecnologia – Ministério da Educação e Ciência (FCT-MEC, Portugal) and by the FP7 IRSES project MEMPEPACROSS (European Union).

Amigalhaços, os antigos, os novos, os que estiveram mais presentes/ausentes por motivos incontornáveis da vida, os peixinhos e os flipados, obrigada pelas gargalhadas e pelos momentos, obrigada pelas músicas e pelos cafés!

À minha família, obrigada pelo apoio. Apesar das distâncias, que têm vindo a aumentar ao longo dos anos, vamos estar sempre perto.

Pedro, obrigada por sempre me puxares p'ra cima e por me dares forças. O teu apoio, carinho e amor são sem dúvida especiais e essenciais para mim e garantiram que eu nunca tivesse desistido quando o cansaço era mais forte. "Caribou".

Esta tese é dedicada ao meu pai.

Throw your thoughts back many years
To the time when there was life with every morning
Perhaps a day will come when the light will be as clear as on that morning

And if you want to stay for a little bit
Rest your aching limbs for a little bit
...

Pink Floyd - The Narrow Way Part III

David Gilmour, 1969
Ummagumma, The Man and the Journey

Abstract

*Ps*d1 is a defensin, isolated from *Pisum sativum* seeds, previously shown to have a strong interaction with fungal-specific membrane components. *Candida albicans* is an important human pathogen, causing oral, genital and systemic opportunistic infections, which are especially relevant clinically in immunocompromised patients, such as HIV-infected individuals.

We tested the effects of this antimicrobial peptide against three *C. albicans* strains, of which one was a mutant that lacked the capability to produce glucosylceramide. We compared *Ps*d1 with the antifungal drugs amphotericin B and fluconazole, at the minimal inhibitory concentration (MIC) and at a 10-fold higher concentration. Using atomic force microscopy (AFM) imaging and force spectroscopy, we assessed morphological changes and alterations in membrane stiffness on *C. albicans* planktonic cells. To determine whether *Ps*d1 has an apoptosis triggering effect in the pathogen, a flow cytometry analysis was performed on *Ps*d1 treated cells, after staining with propidium iodide and annexin V conjugated to FITC.

Our results show that, with increasing incubation times and *Ps*d1 concentrations, there is an increased surface roughness with the appearance of membrane features, such as blebs, cell size alterations, loss of volume and leakage of cellular contents. Also, *Ps*d1 causes a loss of stiffness in the cell membrane and increases the percentage of apoptotic cells. In a general way, *Ps*d1 has less antifungal action against the mutant strain, leading to assign glucosylceramide as one of its molecular targets in *C. albicans*. We were able to study the action of *Ps*d1 against a relevant fungal human pathogen, aiming at its possible use as a natural antimycotic agent.

Keywords: antimicrobial peptides, *Ps*d1, *Candida albicans*, atomic force microscopy, flow cytometry.

Resumo

As defensinas são um dos maiores grupos de péptidos antimicrobianos (AMPs) e têm sido alvo de investigação intensiva nos últimos anos. Os AMPs são péptidos encontrados no sistema imunitário de eucariotas, que têm uma larga atividade antibacteriana, antifúngica, antiviral e também anticancerígena. Estes péptidos são uma possível alternativa aos antibióticos utilizados hoje em dia, que com o decorrer dos anos têm perdido eficácia e cujos microrganismos contra os quais são utilizados têm desenvolvido cada vez mais mecanismos de resistência. A *Ps*d1 é uma defensina com propriedades antifúngicas isolada de sementes de *Pisum sativum*. Tem 46 resíduos de aminoácidos e uma estrutura secundária composta por uma hélice α e folhas β, estabilizada por quatro pontes persulfureto. Foi recentemente demonstrado que este péptido tem grande afinidade, com elevada especificidade, para membranas modelo enriquecidas em ergosterol, o principal esterol presente nas membranas de fungos, e glucosilceramida, o glicoesfingolípido mais comum em fungos. Contrariamente, não existe interação entre o péptido e membranas modelo enriquecidas em colesterol, que simulam células de mamífero, levando a uma toxicidade reduzida para células humanas.

A ação antifúngica da *Ps*d1 foi anteriormente testada contra diferentes fungos, tendo sido descoberto em estudos com *Neurospora crassa* que tem afinidade para uma proteína relacionada com o controlo do ciclo celular, a ciclina F. Ao se ligar à ciclina F, a *Ps*d1 provoca uma paragem no ciclo celular, promovendo endorreduplicação e perturbando a migração nuclear. Foi também testada por outros autores a sua ação contra duas estirpes de *Candida albicans*, uma estirpe nativa (WT) e uma estirpe derivada da WT e mutante na glucosilceramida sintetase, tendo-se demonstrado que a *Ps*d1 causa uma menor inibição no crescimento da estirpe mutante. Estes resultados demonstram que a ação antifúngica da *Ps*d1 envolve uma elevada afinidade para componentes na membrana em *C. albicans*, como as glucosilceramidas.

Candida albicans é um importante agente patogénico que causa infeções oportunistas orais, genitais e sistémicas em humanos, sendo especialmente relevante em pacientes imunocomprometidos, tais como indivíduos infetados com o vírus HIV. Este fungo normalmente existe como comensal na microflora gastrointestinal e nas mucosas bucal ou vaginal. Mais de 50% da população humana pode ser portadora de *C. albicans* como comensal sem ter qualquer efeito negativo. Contudo, este fungo pode alternar o seu estado de comensal para invasivo, dependendo de alguns fatores relacionados com o hospedeiro, tais como perturbação da microflora normal de algumas mucosas, imunossupressão ou disrupção de funções protetoras de barreiras como a pele. *C. albicans* possui vários fatores de virulência que possibilitam a sua patogenicidade. Estes incluem dimorfismo morfológico, expressão de adesinas e invasinas à superfície celular, tigmotropismo, formação de biofilmes, *switching* fenotípico, secreção de enzimas hidrolíticas e atributos relacionados com aptidão biológica, como resposta ao *stress* mediada por proteínas de choque térmico (HSPs) ou excreção de amónia para alcalinizar o ambiente extracelular.

Em organismos unicelulares, a apoptose é um processo de morte celular programada que pode ser encarado como um processo em que a morte altruísta de algumas células pode ser benéfica para a população como um todo ao promover a sua sobrevivência. A apoptose é regulada por uma complexa

rede de proteínas (caspases) e de processos metabólicos. Em fungos existe pelo menos um ortólogo das caspases de mamíferos: a metacaspase YCA1 (*yeast caspase 1*). Alguns efeitos que definem este processo incluem alterações proteómicas nas mitocôndrias, libertação de citocromo c no citosol, aumento de produção de espécies reativas de oxigénio, aparecimento de marcadores apoptóticos, tais como vesículas membranares, ou perda de volume celular. Testes de rotina para a deteção de caraterísticas apoptóticas são utilizados para a identificação de células que estejam a passar por um processo apoptótico após tratamento com agentes antifúngicos. Esta prática é comum quando se estudam os efeitos de péptidos antimicrobianos em *C. albicans*.

Neste trabalho, testámos os efeitos da *Ps*d1 em três estirpes de *C. albicans*, um isolado clínico e as duas estirpes referidas anteriormente, a WT e a mutante na glucosilceramida sintetase, para determinar se a ausência deste glicoesfingolípido interfere na ação da defensina, sob o ponto de vista biofísico e das características estudadas nesta tese. Comparámos a *Ps*d1 com as drogas antifúngicas anfotericina B e fluconazol, um polieno e um azol, respetivamente. A anfotericina B é um composto que se liga irreversivelmente ao ergosterol presente na membrana celular de fungos, formando poros que levam à perda de conteúdos intracelulares e, posteriormente, à morte celular. O fluconazol necessita entrar dentro da célula para surtir o seu efeito, que consiste na perturbação da síntese de ergosterol, ao impedir que o seu percursor, lanosterol, seja desmetilado. Para as três estirpes de *C. albicans* foi determinada a concentração mínima inibitória (MIC) destes compostos com atividade antifúngica, que foram posteriormente testados à concentração correspondente à MIC e a uma concentração 10 vezes superior. Utilizando imagens de microscopia de força atómica (AFM) e espetroscopia de força baseada em AFM, avaliámos alterações na morfologia, tais como rugosidade da superfície da célula e perda de volume celular, e alterações biomecânicas de células plantónicas de *C. albicans*, ao nível da rigidez membranar. Para determinar se a *Ps*d1 tem a capacidade de provocar apoptose neste agente patogénico, foi efetuada uma análise de citometria de fluxo em células tratadas com *Ps*d1, após marcação com as sondas fluorescentes iodeto de propídeo e anexina conjugada a FITC.

Os nossos resultados demonstram que, com o aumento de concentração e o tempo de incubação com *Ps*d1, há um aumento da rugosidade da membrana celular, verificado pela visualização e pela análise de imagens de altura obtidas por AFM. Através de imagens de AFM obtidas em modo de erro, verificou-se também o aparecimento de caraterísticas associadas à apoptose, tais como vesículas membranares, alterações de tamanho e perdas de volume e de conteúdos celulares. Pôde-se também visualizar que as células parecem ter uma menor capacidade de adesão após tratamento com o péptido, o que pode indicar que a *Ps*d1 tem a capacidade de interferir com a formação de biofilmes, visto que esta caraterística é determinante para a formação destes consórcios microbianos. Considerando as alterações morfológicas causadas pela defensina, o modelo que melhor explica o mecanismo de interação do péptido com a membrana é o modelo de carpete, com um efeito de detergente e micelização da membrana, em que há uma perturbação da organização e homogeneização membranar, sem a formação de poros na membrana. Pelos dados obtidos por espetroscopia de força baseada em AFM, foi calculado o módulo de Young, verificando-se uma diminuição da rigidez celular após tratamento com a defensina ou com qualquer dos

outros compostos antifúngicos, o que também foi visualizado em imagens de AFM em modo de contraste de fase. Foi também possível determinar que a rigidez média das células de *C. albicans* mutante é intrinsecamente menor que a de células de *C. albicans* WT, o que está de acordo com o facto de as membranas ricas em ceramidas serem mais rígidas. Através de dados de citometria de fluxo, foi registado um aumento na percentagem de células apoptóticas.

De um modo geral, a *Ps*d1 tem menor ação antifúngica contra a estirpe mutante, indicando que a glucosilceramida possa ser um dos seus alvos moleculares em *C. albicans*. Foi assim possível adquirir um conhecimento mais alargado da ação da *Ps*d1 contra um agente patogénico humano importante, apontando para o seu possível uso como um agente antimicótico de origem natural.

Palavras-chave: péptidos antimicrobianos, *Ps*d1, *Candida albicans*, microscopia de força atómica, citometria de fluxo.

List of figures and tables

Abbreviations, acronyms and symbols

The acronyms used are expanded on first usage and whenever seemed necessary to improve clarity. Very common acronyms, such as "DNA" or HIV, are not extended nor described. Amino acid residues are indicated using the one-letter code.

APD	Antimicrobial Peptide Database
AFM	Atomic force microscopy
AMP	Antimicrobial peptide
Amph B	Amphotericin B
Annexin V-FITC	Annexin V conjugated to fluorescein isothiocyanate
APS	American Phytopathological Society
BioFIG	Center for Biodiversity, Functional and Integrative Genomics
BP	Bubble protein
CAML	Centro Académico Médico de Lisboa
DF	Dilution factor
E	Young's modulus
EBSA	European Biophysical Societies' Association
F	Force
FCT	Fundação para a Ciência e a Tecnologia
FCUL	Faculdade de Ciências da Universidade de Lisboa
FCZ	Fluconazole
FMUL	Faculdade de Medicina da Universidade de Lisboa
FSC	Forward scatter
GlcCer	Glucosylceramide
GCS	Glucosylceramide synthase
GSL	Glycosphingolipids
HEPES	4-(2-hydroxyethyl)-1-piperazieethanesulfonic acid
Hog1	High osmolarity glycerol mitogen-activated protein
Hsps	Heat shock proteins
IMM	Instituto de Medicina Molecular

LPS	Lipopolysaccharide
MAPK	Mitogen-activated protein kinase
MEC	Ministério da Educação e Ciência
MIC	Minimal inhibitory concentration
MOPS	3-Morpholinopropanesulfonic acid
NMR	Nuclear magnetic resonance
PBS	Phosphate buffer saline
PCD	Programmed cell death
PI	Propidium iodide
PLL	Poly-L-lysine
PS	Phosphatidylserine
***Ps*d1**	*Pisum sativum* defensin 1
PZT	Piezoelectric transducer
rBPI$_{21}$	Recombinant 21kD fragment of Bactericidal/Permeability-increasing protein
RMS	Root mean square
ROS	Reactive oxygen species
RP-HPLC	Reverse-phase high performance liquid chromatography
RPMI	Roswell Park Memorial Institute broth
SEM	Scanning electron microscopy
SSC	Side scatter
STM	Scanning tunneling microscopy
TEM	Transmission electron microscopy
WT	Wild type
YCA1	Yeast caspase-1
YPD	Yeast potato dextrose culture medium
α	Half angle to face
δ	Indentation
ν	Poisson's ratio

Introduction

1. *Candida albicans*

Candida albicans is an important human pathogen, causing oral, genital and systemic opportunistic infections, which are especially relevant clinically in immunocompromised patients, such as HIV-infected individuals, making this one of the most important pathogenic fungi (Berman, 2012). *C. albicans* normally exists as a commensal as part of mucosal microflora, such as the oral cavity, the gastrointestinal tract or the vagina (Ruhnke and Maschmeyer, 2002; Calderone and Clancy, 2012). More than 50% of the human population may carry *C. albicans* as a commensal without having any negative effect. However, this fungi can switch from commensal to invasive state, depending on some host factors, such as the disruption of normal mucosal flora, impaired barrier protective functions and immunosuppression (Mayer et al., 2012). Despite the existence of currently available antifungal therapies, mortality and morbidity caused by this pathogen are still inadmissibly high (Behnsen et al., 2008).

1.1. *Candida albicans* pathogenicity

C. albicans possesses a number of major virulence factors (Figure 1), which enable its pathogenicity. These include morphological dimorphism, which consists in the transition between yeast and hyphal forms (Figure 1 B) (Berman and Sudbery, 2002; Zheng and Wang, 2004); the expression of adhesins and invasins on the cell surface, which permit the adherence to host cell surfaces (Figure 1 A) (Verstrepen and Klis, 2006; Wachtler et al., 2011) and induce endocytosis uptake of the fungus (Phan et al., 2005; Zhu and Filler, 2009), respectively; thigmotropism, i.e., directed growth stimulated by contact with host cells (Figure 1 C) (Brand et al., 2007; Kumamoto, 2008); biofilm formation possible due to the attachment of planktonic yeast cells to abiotic, e.g., catheters, or biotic surfaces, e.g., host cells, with yeast cells in the lower part and hyphal cells in the upper part of the biofilm (Figure 1 E) (Nobile et al., 2009; Finkel and Mitchell, 2010); a second form of phenotypic switching (plasticity) between white and opaque forms, which exhibit marked differences in their ability to undergo filamentation; and the secretion of hydrolytic enzymes (Figure 1 D) (Mayer et al., 2012; Poulain, 2012; Si et al., 2013).

In addition to these virulence factors, fitness attributes include stress response mediated by heat shock proteins (Hsps) (Lindquist, 1992), auto-induction of hyphal formation through amino acid uptake (Vylkova et al., 2011), excretion of ammonia (NH_3) and subsequent extracellular alkalinization, uptake of different compounds as carbon and nitrogen sources (Brock, 2009; Fleck et al., 2011) and essential metals like iron, zinc, copper and manganese (Figure 1 F) (Heymann et al., 2002; Marvin et al., 2003; Citiulo et al., 2012; Mayer et al., 2012).

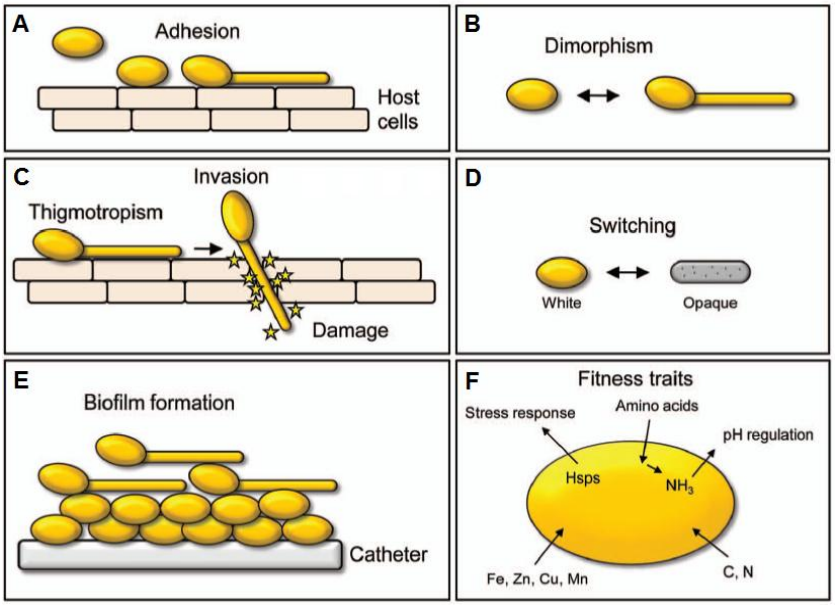

Figure 1. Overview of the major pathogenicity mechanisms of *Candida albicans*. Image adapted from Mayer et al., 2012.

1.2. Fungal targets for antifungal drugs

Fungi possess a unique cell wall and cell membrane that can serve as targets for antifungal agents. The fungal cell membrane is similar to that of other eukaryotic cells, composed of a lipid bilayer with proteins embedded within it (Katzung et al., 2011). Sterols are major components of fungal membranes and this component is absent in all prokaryotes. The sterol present in higher eukaryotic membranes is cholesterol, but in fungal membranes the main sterol present is ergosterol, which provides stability and flexibility to the cell membrane (Thevissen et al., 1999; Thevissen et al., 2003).

Polyenes, such as amphotericin B target the cell membrane. Amphotericin B is a lipophylic molecule that crosses the cell wall and aggregates closely and irreversibly with ergosterol, forming a pore in the membrane (Figure 2), resulting in loss of intracellular contents and, ultimately, in total impairment of cell membrane function, leading to cell death (Carrillo-Munõz et al., 2006). The azoles, such as fluconazole or itraconazole, are a family of drugs that also target the cell membrane, although indirectly, because they need to enter the cell to exert their function (Figure 2). Lanosterol serves as a precursor for ergosterol and although many enzymes are a part of this reaction, 14-α demethylase is responsible for the demethylation of lanosterol and is an essential enzyme that serves as a target for azole antifungal agents. 14-α demethylase requires cytochrome P450 mediation to exert its function; the azoles bind to this cytochrome inhibiting the demethylation of lanosterol and, thus, the synthesis of ergosterol (Ghannoum and Rice, 1999). The lack of ergosterol in the fungal cell membrane makes it very unstable, eventually leading to breakdown, cell shrinkage and the organism death.

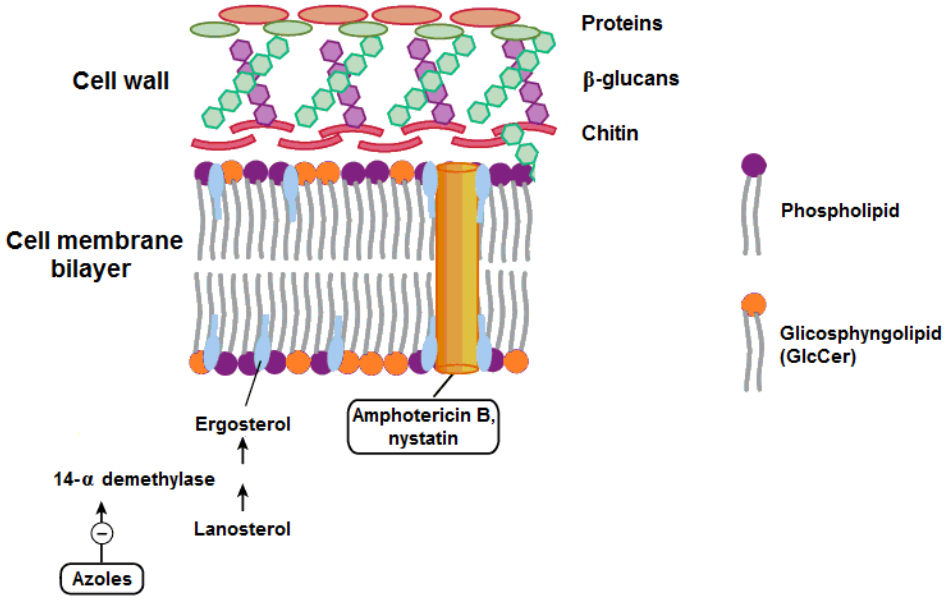

Figure 2. Fungal cell wall and cell membrane representation. Targets for polyenes and azoles are shown here, polyenes form pores in the membrane and azoles inhibit the formation of ergosterol. Image adapted from Katzung et al., 2011.

Glycosphingolipids (GSL) are a family of lipids that act as key components of biological membranes. They exist in animals, plants and fungi (Leipelt et al., 2001; Halter et al., 2007; Daniotti and Iglesias-Bartolome, 2011). GSL were initially described as components of the architecture of cell membranes, straightly connected with fluidity and stability (Feinstein et al., 1975; Aaronson and Martin, 1983; Campanella, 1992). Recently, however, it was demonstrated that their role goes clearly beyond the initial concept, since these molecules are major components of specialized membrane domains called lipid rafts (Bagnat et al., 2001; Hakomori, 2003; Hakomori, 2008). GSL have been characterized as important structures in cell-cell interaction, cell signaling and protein sorting (Bagnat et al., 2000; Bagnat and Simons, 2002; Nimrichter et al., 2008; Staubach and Hanisch, 2011). Lipid rafts are more ordered and tightly packed than the surrounding bilayer and serve as organizing centers for the assembly of signaling molecules, influencing membrane fluidity and membrane proteins trafficking (Chiantia and London, 2013).

The most common GSL found in fungi is glucosylceramide (GlcCer) (Figure 2), present in the membranes of most fungi, such as *Pichia pastoris*, *C. albicans*, *Cryptococcus neoformans*, *Aspergillus fumigatus*, *Sporothrix schenckii* and *Neurospora crassa* (Saito et al., 2006). Large amounts of this glycosphingolipid have also been found in the fungal cell wall (Nimrichter and Rodrigues, 2011). GlcCer has been identified as a fungal component decades ago. Its functions during fungal growth/dimorphism, lipid raft formation and correlation with virulence have been reported (Rittershaus et al., 2006). In fact, it was recently shown to be required for virulence in *C. albicans* (de Medeiros et al., 2010; Noble et al., 2010; de Coninck et al., 2013).

Work published by Karin Thevissen and coworkers strongly suggested that targeting fungal GlcCer with the AMPs RsAFP2 and HsAFP1 could initiate a cell signaling response in fungal organisms, with

formation of reactive oxygen species (ROS) and subsequent cell death by apoptosis (Thevissen et al., 2004; Aerts et al., 2007; Aerts et al., 2009; Aerts et al., 2011). The use of anti-GlcCer antibodies was shown to block germ tube formation in *C. albicans*, *Colletotrichum gloeosporioides* and *Pseudallescheria boydii* (Pinto et al., 2002; da Silva et al., 2004), and also to protect mice in lethal infection of *C. neoformans* (Rodrigues et al., 2007).

The crescent knowledge of GlcCer functions in eukaryotes (may these be related to virulence, growth or morphological transitions), together with the findings described above, can be connected to specific and essential structural features and particular biosynthetic steps to validate these GSL as potential targets on the development and discovery of new antifungal drugs (Nimrichter and Rodrigues, 2011; Gonçalves et al., 2012b).

1.3. Apoptosis in yeast

Apoptotic cell death seemed like a process that was absent in yeast, until the unexpected discovery of an apoptotic phenotype in a yeast, over a decade ago (Madeo et al., 1997). Until then, the development and conservation of a programmed cell death (PCD) did not make sense for a unicellular organism, since that would mean the death of the organism. So the fact that yeast apoptosis follows the same physiological purpose known for multicellular organisms, namely eliminating superfluous cells, demanded a conceptual change.

Yeast populations should not be interpreted just as a group of partitioned unicellular organisms that do not communicate among each other, but rather as a multicellular community of interacting individuals. Under certain circumstances, the death of a single cell might be beneficial for the whole population, thus promoting the survival of the clone. Several physiological scenarios in which altruistic death of single cells promotes survival of the population as a whole support this idea (Buttner et al., 2006). For example, death of older cells helps to preserve vanishing resources, stimulating the survival of younger and fitter cells (Vachova and Palkova, 2005). Apoptosis may also occur to clear the population of non-recombinant cells after meiosis, infertile cells or damaged haploid cells (guaranteeing the adaptive benefit of the diploid state) (Severin and Hyman, 2002). Several stimuli can trigger apoptotic pathways. Internal triggers may be aging and mutations such as DNA damage and replication failure (Weinberger et al., 2005).

Apoptosis is regulated by a complex network of proteins and metabolic pathways. The central core of this process is regulated by a family of proteins named caspases. Yeasts have at least one ortholog of mammalian caspases: the metacaspase YCA1 (yeast caspase 1) (Madeo et al., 2002).

Apoptosis may be defined as a process that causes proteomic alterations in mitochondria, release of cytochrome c to the cytosol, DNA fragmentation, phosphatidylserine (PS) externalization, chromatin condensation, increased ROS production, and development of apoptotic markers such as membrane blebs or cell shrinkage (Figure 3) (Carmona-Gutierrez et al., 2010; Cho et al., 2012). Routinely used assays aiming at the detection of these apoptotic features are used for the identification of fungal cells

undergoing apoptosis after treatment with antifungal agents. This practice is common when studying the effect of antimicrobial peptides (AMPs) on *C. albicans*.

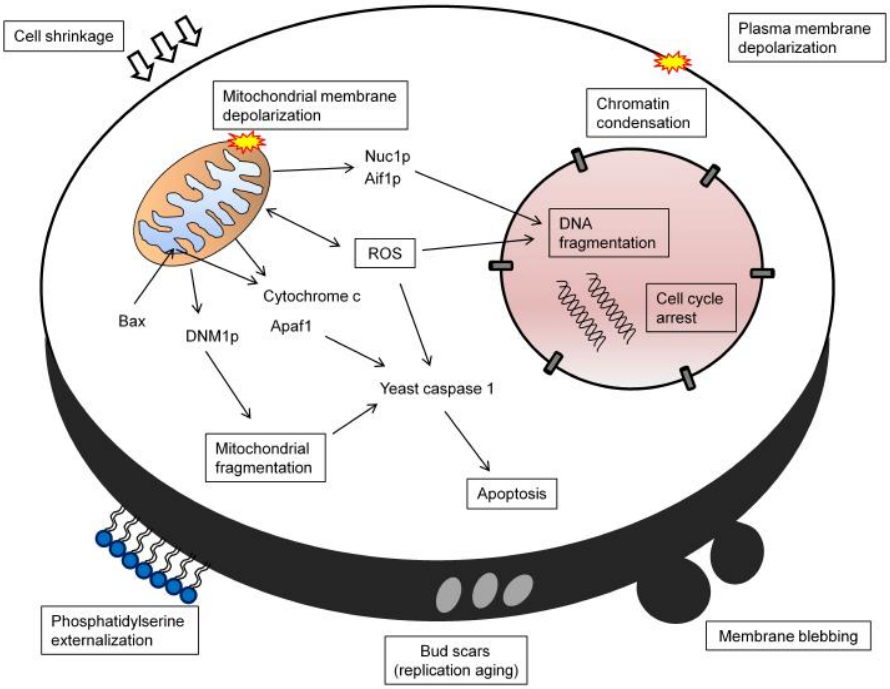

Figure 3. Apoptotic pathways in yeast cells. Image from Cho et al., 2012.

C. albicans is clinically relevant and, lately, research on antimicrobial peptides using this fungal pathogen as target has been increasing. *Rs*AFP2 (Terras et al., 1992; Aerts et al., 2007; Aerts et al., 2009; Thevissen et al., 2012), *Hs*AFP1 (Osborn et al., 1995; Aerts et al., 2011), human β-defensins 1-3 (Schroder and Harder, 1999; Sahl et al., 2005), coprisin (Hwang et al., 2009; Lee et al., 2012), juruin (Fry et al., 2009; Ayroza et al., 2012) and crotamine (Gonçalves and Polson, 1947; Nicastro et al., 2003; Fadel et al., 2005; Yamane et al., 2013) are just a few examples of research on possible alternatives to the most commonly used antifungal therapies.

2. Antimicrobial Peptides

Naturally occurring AMPs probably represent one of the first evolved and successful forms of chemical defense of eukaryotic cells against bacteria, protozoa, fungi and viruses (Ganz and Lehrer, 1998; Lehrer and Ganz, 1999; Zasloff, 2002; Mookherjee and Hancock, 2007; Lai and Gallo, 2009; Guo et al., 2012), being also active against cancer cells (Hoskin and Ramamoorthy, 2008; Gaspar et al., 2013). Currently commercialized antibiotics are mostly of microbial origin or synthesized from those. These antibiotics are losing efficacy as a result of high selection pressure and rapid emergence of resistance in many important human pathogens, threatening to put an end to the golden age of antibiotics (Clardy et al., 2009). The use of antifungal treatments has increased as a consequence of the increase of immunocompromised patients, mostly due to improvements in oncology and transplant fields (Mehra et

al., 2012), leading to more frequent resistances to the drugs used. An alternative to this problem can be found in the innate immune system of plants (Thomma et al., 2002; Lay and Anderson, 2005; Gonçalves et al., 2012b), fungi (Mygind et al., 2005; Schneider et al., 2010; Oeemig et al., 2012), invertebrates (Bulet and Stocklin, 2005; Ayroza et al., 2012) and vertebrates (Ganz, 2004; Sahl et al., 2005; van Dijk et al., 2008; Gonçalves et al., 2012a), where AMPs are found, presenting a broad spectrum of antimicrobial activities.

AMPs have variable amino acid composition and size (ranging from less than 10 to more than 100 amino acid residues), commonly being cationic and amphipathic molecules. To date, nearly 2300 AMPs have been identified (either natural or synthetic), as listed by the Antimicrobial Peptide Database (APD; http://aps.unmc.edu/AP/main.php), of which over 1800 have antibacterial activity and more than 800 have antifungal activity. This discrepancy, however, may be redundant and antibacterial AMPs may also have antifungal activity that has not yet been investigated.

According to structural classification, AMPs are divided into four families: β-strand, such as protegrin (Aumelas et al., 1996); α-helix, such as dermaseptin (Mor et al., 1991); αβ-motif, such as drosomicin (Landon et al., 1997); and non-αβ or extended, such as indolicidin (Ladokhin et al., 1999). Although some AMPs have had their target unveiled, many mechanisms of antifungal action still remain unclear. AMPs may target membranes, and induce their effect by disrupting them (Shai, 1999), or they may enter the cell and exert their action intracellularly (Hancock and Rozek, 2002; Oberparleiter et al., 2003).

3. Models of membrane activity – mechanism of action of AMPs

Besides GlcCer, fungal membranes are also rich in phosphomannans and in the negatively charged phospholipids phosphatidylinositol (PI), PS and diphosphatidylglycerol (DPG), which confer high negative charge surface to the membranes (Pasupuleti et al., 2011).

The biological activity of AMPs is strongly influenced by peptide-membrane interaction. To explain differential membrane affinity, biological activities and modes of action of some AMPs as a function of their concentration, interaction of defensins with models of fungal membranes have been reported, showing a strong dependence on lipid composition (de Medeiros et al., 2010; Gonçalves et al., 2012a; Gonçalves et al., 2012b). As with other AMPs, the mechanism of action of some plant defensins with antifungal activity involves membrane binding, leading to its permeabilization, binding to the cell wall, interaction with intracellular targets which would lead to apoptosis, membrane permeabilization and receptor-mediated internalization (van der Weerden et al., 2013).

The mode of action of some defensins has been studied by using synthetic lipid vesicles mimicking the lipid composition of fungal, bacterial and mammal membranes (de Medeiros et al., 2010; Wimley and Hristova, 2011; Gonçalves et al., 2012a; Gonçalves et al., 2012b). The permeabilization models used to explain the mode of action of defensins could be classified into two main groups: transmembrane pore formation, such as the barrel-stave and toroidal models, and non-pore formation, such as the carpet, aggregate channel, Shai-Matsuzaki-Huang, lipid clustering and interfacial activity models (Alba et al.,

2012). The carpet model can evolve to disrupt the membrane through pore formation models or through a detergent-like mechanism, with micellization of the membrane (Bechinger and Lohner, 2006; Chang et al., 2008; Hoskin and Ramamoorthy, 2008). There are currently at least three different commonly accepted models describing possible AMPs mode of action: the barrel-stave pore model, the toroidal pore model, and the carpet model (Shai, 2002; Chang et al., 2008; Hoskin and Ramamoorthy, 2008; Alba et al., 2012).

Most defensins are amphipathic molecules with clusters of positively charged amino acid residues side chains and hydrophobic amino acid side chains (Lehrer and Lu, 2011). This structural behavior allows them to interact with microbial membranes both at the level of the negatively charged phospholipids head groups and of the hydrophobic fatty acid chains. The orientation of the peptide on the membrane surface depends on the specific peptide-lipid system, but it is common for the AMP to stay at the membrane interface until a threshold peptide concentration is reached (Yang et al., 2000; Yount and Yeaman, 2005; Pasupuleti et al., 2011).

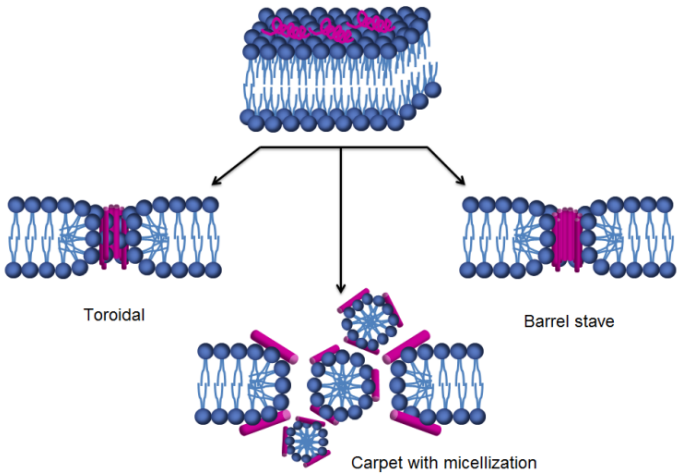

Figure 4. Models of lipid membrane permeabilization by AMPs. Initially, the peptide (magenta) is adsorbed at the membrane surface. After an initial recognition of the surface, a conformation change of the peptide occurs. Image from Silva et al., 2013 (submitted, under editorial revision).

In the barrel stave model (Figure 4), once the critical threshold concentration of peptide is reached, peptides self-aggregate in the membrane resulting in the formation of a transmembrane pore lined by peptide, which dissipates proton and ionic gradients (Ehrenstein and Lecar, 1977; Reddy et al., 2004), but the membrane thickness and homogeneity do not change (Chang et al., 2008). The toroidal pore model is a variant of the barrel stave model, claiming that, at some critical peptide concentration, curvature strain induces membranes to curve inward, resulting in the formation of a pore that is lined by both peptides and lipid headgroups (Figure 4). Toroidal pores seem to have varying lifetimes and longer-lived pores may have a lethal effect similar to barrel-stave pores, with dissipation of protonic and ionic gradients. This type of mechanism of AMPs action also causes a decrease in membrane thickness and a slightly decreased surface homogeneity (Chang et al., 2008). In the carpet model (Figure 4), peptides bind to phospholipid head groups by electrostatic interactions and align themselves parallel to the membrane surface in a carpet-like fashion until a critical threshold concentration is reached. When a detergent-like membrane micellization takes place, a strong decrease of membrane homogeneity occurs (Chang et al.,

2008; Hoskin and Ramamoorthy, 2008; Epand et al., 2010; Hazlett and Wu, 2011; Pasupuleti et al., 2011; Li et al., 2012).

4. Resistance

Like antibiotics resistance, it is easily conceivable that AMPs resistance is a key characteristic for increased virulence of pathogenic strains. Despite this fact, and contrary to antibiotics that act through a single approach (meaning that microbes can evade them through a single resistance system), AMPs follow a multidimensional strategy against microbial invasion (Lai and Gallo, 2009) (issue further developed in the text, in section 5.1 - Immunomodulatory function). Therefore, selective pressures on microbes are avoided, reducing the development of resistant strains (Zasloff, 2002).

A synergistic effect between different AMPs in the host is also possible, as evidenced by the fact that the MIC of AMPs in vitro are usually higher than the physiological concentrations of those AMPs in vivo (Lai and Gallo, 2009). Another example is that two distinct AMPs may have their combined MIC much lower than when acting isolated, strongly suggesting heterologous host defense peptide interactions (Westerhoff et al., 1995).

AMPs frequently have the ability to disrupt microbial membranes and to inhibit their synthesis; thus, strategies to escape the action of those AMPs follow the redesign of cell membranes and have been described for both Gram-negative and Gram-positive bacteria (Gunn et al., 2000; Li et al., 2007). Other evasion mechanism includes affecting the correct function of the AMP by turning off its expression, releasing plasmid DNA in epithelial cells, a strategy adopted by highly contagious bacteria from the *Shigella* genus that cause dysentery (Islam et al., 2001). Since AMPs frequently rely on transmembrane potential to interact with and exert their mechanism of action against microbial pathogens, it is probable that another strategy for evading AMPs could be to alter their transmembrane energy status (Yeaman and Yount, 2003). *C. albicans* resistance to some AMPs is regulated by the protein Ssd1 (Gank et al., 2008), combined with the transcription factor Bcr1 (Jung et al., 2013). This combination gives resistance to the α-helical cationic polypeptide protamine, frequently used to screen for antimicrobial peptide susceptibility (Yeaman et al., 1996), the synthetic antimicrobial peptide RP-1, modeled upon the C-terminal α-helical domain existent in the human platelet factor-4 kinocidins, domain which is responsible for its microbicidal activity, (Bourbigot et al., 2009) and human β-defensin-2, by maintaining mitochondrial energetics and reducing membrane permeabilization, thus allowing the fungus to counteract the negative effects of these AMPs (Jung et al., 2013). The Hog1 (high osmolarity glycerol) MAPK pathway, which provides a response to osmotic, oxidative and heavy-metal exposure stresses in fungal cells, was shown to be activated in the presence of antimicrobial peptides (Yeaman et al., 1996; Vylkova et al., 2007; Argimon et al., 2011). This MAPK triggers a transcriptional response upon exposure to histatin-5, a salivary cationic AMP that has a role in keeping *C. albicans* in its commensal state, and human β-defensins 2 and 3.

Another strategy for evading AMP function is to enzymatically degrade them before they take action, by producing proteases and peptidases involved in tissue degradation, as described for *C. albicans*

secreted aspartic proteases (Saps). Namely, histatin-5 is a host-specific substrate of Sap9, enabling the transition of the fungus from commensal to pathogenic in HIV^+ individuals, who have lower levels of this isoenzyme in the saliva, causing an increased incidence of oral candidiasis (Meiller et al., 2009; Khan et al., 2013). Also regarding histatin-5, a transport mechanism of efflux mediated by the flu-1 transporter has been described for *C. albicans*, rendering the pathogen the ability to reduce the isoenzyme cytosolic concentration and fungicidal activity (Li et al., 2013). The LL-37 cathelicidin and histatins bind to cell wall carbohydrates, preventing adhesion of *C. albicans* to host cells; thus, the release of AMP-binding proteins acts as a decoy for these AMPs, diverting them from binding to fungal cell surface (den Hertog et al., 2005; den Hertog et al., 2006; Mochon and Liu, 2008). Msb2 is a *C. albicans* surface protein, highly soluble and proteolytically stable, which is shed to the extracellular environment, acting as a basal AMP-resistance strategy by avoiding killing by LL-37 and histatin-5 (Szafranski-Schneider et al., 2012).

The above characteristics decrease microbes' susceptibility to AMPs and indicate that microbial pathogens have developed some structure-specific and energy-dependent mechanisms to subvert the action of host defenses.

5. Defensins

Defensins comprise one of the largest groups of AMPs. These peptides are cysteine-rich and have diverse sequences and structures, stabilized into compact shapes by three or four conserved cysteine disulphide bridges, have at least two positive charges (lysine or arginine residues) and are small, ranging approximately from 12 to 50 amino acid residues (2-6 kDa) (Ganz, 2003; Ren et al., 2011; Gao and Zhu, 2012).

Vertebrate's defensins are divided in three subfamilies: α-, β- and θ-defensins. α-defensins are present in mammals such as humans, monkeys and several rodent species (Ouellette and Selsted, 1996; Ganz and Lehrer, 1998; Lehrer and Ganz, 1999). β-defensins are found in a wide range of vertebrates, presenting a cysteine-stabilized αβ-motif composed of an antiparallel β-sheet and an α-helix. θ-defensins, present only in Old World monkeys, are cyclic and derived from α-defensins (Lehrer, 2004; Lehrer and Lu, 2011; Semple and Dorin, 2012). In Figure 5, some conserved amino acids between defensins from different kingdoms are shown.

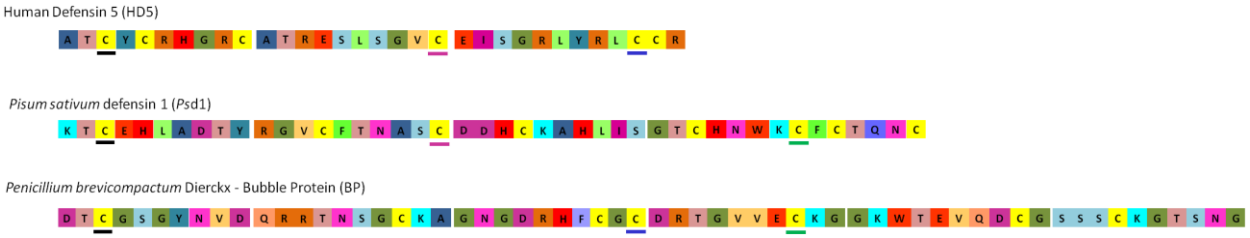

Figure 5. Amino acid residues sequence examples of defensins with antifungal activity. Animal, plant and fungi origin: human defensin 5 (HD5), *Pisum sativum* defensin 1 (*Ps*d1) and *Penicillium brevicompactum* Dierckx bubble protein (BP), respectively. Colored bars underline the conserved cysteines among defensins from different kingdoms. Image from Silva et al., 2013 (submitted, under editorial revision).

Plants, fungi and many invertebrates produce defensin-like peptides structurally similar to the β-defensins from vertebrates (Thomma et al., 2002; Bulet and Stocklin, 2005; Mygind et al., 2005; Sahl et al., 2005; van Dijk et al., 2008; Ayroza et al., 2012; Oeemig et al., 2012). These observations enabled to assume that all defensins and defensin-like peptides evolved from a common precursor (Zhu and Gao, 2013). The relatively recent identification of three defensins in lower eukaryotes, plectasin from *Pseudoplectania nigrella* (Mygind et al., 2005), eurocin from *Eurotium amstelodami* (Oeemig et al., 2012) and bubble protein from *Penicillium brevicompactum* Dierckx (Seibold et al., 2011), is important to demonstrate the wide distribution of defensins over diverse eukaryotic lineages, which suggests that ancestral defensin genes existed over 1500 million years ago, before Fungi, Plantæ and Animalia kingdoms diverged (Wang et al., 1999). It is quite likely that these antimicrobial weapons have been fundamental to the evolution of multicellular organisms within the microbial environment.

Although defensins were initially identified as antimicrobial peptides, recent studies have demonstrated that they have a much broader range of action, including immunomodulatory function (Ulm et al., 2012).

5.1. Immunomodulatory function

Defensins may be produced constitutively or have their expression triggered when there is an inflammatory process by the recognition of microbial conserved structures, such as lipopolysaccharide (LPS) and lipoteichoic acid, or inflammatory effectors, like cytokines. These AMPs are expressed differentially depending on the peptide itself and on the tissue or cell type (Ulm et al., 2012).

Defensins, besides their AMP action, are also immunomodulatory molecules and inhibitors of virulence factors. Thus, they can enhance the host's immune system, with this multifunctional character rendering these peptides a lower probability of becoming tolerated by microorganisms (Mehra et al., 2012)

Pro-inflammatory mediation has been recognized in some of these molecules, as they can bind to chemokine receptors, being able to recruit immune cells, thus enhancing the immune response (Mookherjee and Hancock, 2007; Lai and Gallo, 2009; Alba et al., 2012; Semple and Dorin, 2012; Ulm et al., 2012; Zhu and Gao, 2013). Surprisingly, some defensins are also able to attenuate pro-inflammatory responses whenever these can be harmful for the organism (Lande et al., 2007; Yamasaki et al., 2007). These antagonistic effects depend on the level of expression, disease state and pathogen exposure. It has been demonstrated that human β-defensin 3 (mainly expressed in epithelial cells), when in basal concentration, has an immunosuppressive effect in the presence of LPS, contributing to the maintenance of a non-inflammatory environment over continual low-level exposure to microorganisms, commensal or pathogenic (Semple et al., 2010). Due to this multifunctionality, AMPs have also been referred to as host defense peptides (HDPs) (Ulm et al., 2012).

5.2. *Pisum sativum* defensin 1

Many fungi are phytopathogenic, with species such as *Fusarium* spp., *Cladosporium* spp., *Pythium* spp., *Curvularia* spp., *Aspergillus flavus* and *Puccinia pittieriana* affecting potato, rice, corn, wheat, tobacco and cotton crops by causing wilt, mold, crown rot, mildew and rust, just to name a few plant diseases (The American Phytopathological Society, APS - https://www.apsnet.org/). These diseases can deplete entire crops, bearing enormous costs for agriculture due to the difficulty in eliminating fungal infections from plants, once they appear. Soils harbor plants for most of their life cycle, but also a considerable amount of bacteria, fungi and parasites, many of which can be phytopathogenic. Plants need to have good defenses against these microorganisms, thus it is easy conceivable to consider plants as major AMPs producers. In fact, much research has been made to screen for these molecules in plants.

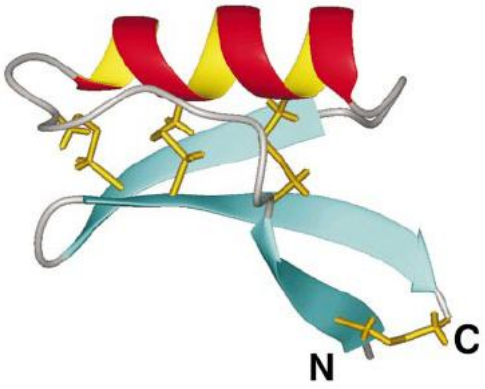

Figure 6. Representation of the secondary structure elements of *Ps*d1 mean structure. The β-strands are represented by blue arrows and the α-helix by a red ribbon. The four disulphide bridges are shown in stick representation. Image from Almeida et al., 2002.

Pisum sativum defensin 1 (*Ps*d1) was firstly characterized in 2000 (Almeida et al., 2000). A fraction with antifungal activity against *Aspergillus niger* was isolated from seeds of the garden pea (*Pisum sativum*) by ammonium sulfate fractionation followed by gel filtration on Sephadex G-75. Further purification was performed by reverse-phase high performance liquid chromatography (RP-HPLC). Full details of purification process and molecular characterization of *Ps*d1 are found in Almeida et al., 2000. At present, the peptide used is recombinant, having the same folding and antifungal activity when compared to native *Ps*d1 (Cabral et al., 2003).

This peptide has 46 amino acid residues and its secondary structure comprises a globular fold composed of β-sheets and an α-helix stabilized by four disulphide bridges, i.e., cysteine-stabilized αβ-motif (Figure 6) (Almeida et al., 2002). Its three-dimensional structure was determined by nuclear magnetic resonance (NMR) and is identical to the backbone structure of other defensins and neurotoxins (Kobayashi et al., 1991; Cornet et al., 1995). Through surface topology studies, it was suggested by Almeida et al., 2002, that *Ps*d1 might have a sodium channel inhibiting activity, due to presenting several common features with potassium channel inhibitors. The peptide has also been shown to cause a growth inhibition of 100% on *C. albicans* WT, when using a concentration of 20 μM, against a growth inhibition of 70% on a *C. albicans* strain mutant in the GlcCer synthase gene (de Medeiros, 2009). These results point out to the hypothesis that GlcCer may be a possible target for *Ps*d1.

As demonstrated by a yeast two-hybrid screening system, *Ps*d1 has affinity to a *Neurospora crassa* protein related to the cell cycle control, cyclin F (Lobo et al., 2007). Using a developing retinal tissue of neonatal rats as a model to study this interaction, it was proven that *Ps*d1 impairs the correct cell cycle progression, by blocking cyclin F role in the transition of S to G2 phases of the cell cycle, promoting endoreduplication and disturbing nuclear migration.

Recently, it has been demonstrated through partition studies that *Ps*d1 has a high affinity, with high specificity, to model membranes enriched in ergosterol, the main sterol present in fungal membranes, and GlcCer (Gonçalves et al., 2012b). On the contrary, there is no interaction between the defensin and model membranes enriched in cholesterol, which simulate mammalian cells, leading to a reduced *Ps*d1 toxicity to human cells.

Aims and Goals

Despite what is already known about *Ps*d1, further insight on its mode of action and effect in *C. albicans* are yet to be known. The aim of this thesis, which is integrated in the work already under development at the host laboratory (IMM Biomembranes Unit), was to study the effects of *Ps*d1 on the human pathogen *C. albicans*, using an AFM-based biophysical approach to determine alterations in external appearance and biomechanical properties of the cell after treatment with *Ps*d1. In order to determine if the defensin induces apoptosis, flow cytometry was also used. Given the recent evidence that *Ps*d1 interacts with GlcCer (Gonçalves et al., 2012b), a fungal strain mutant in GlcCer synthase was used, as well as its wild-type counterpart, to assess the effects of *Ps*d1 on the cell when this GSL is lacking in the membrane.

Methodology

The basic theoretical aspects of the main techniques employed in this study are introduced in this chapter, followed by a description of experimental procedures and materials used.

1. Atomic Force Microscopy

Atomic Force microscopy (AFM) first instrument, from 1986, was built by Binnig, Quate and Gerber (Binnig et al., 1986) and it is currently in the Science Museum in London, UK. This microscope is the successor of the scanning tunnelling microscope (STM), invented in 1981 by Binnig and Rohrer (Binnig and Rohrer, 1982). The technique behind how these microscopes work is nothing like the normal imaging microscopes that form images by capturing light or electrons from surfaces. The AFM and STM are based in a surface profiler invented in the 1920s, the stylus profiler or profilometer, which had a sharp tip on the edge of a small cantilever and this tip was dragged through a surface placed upon a moving stage. The tip's vertical movement was due to a spring on the opposite end of the cantilever, fixed to a stage. The vertical movement of the tip was monitored through the recording of a light signal reflected through a mirror in the back of the tip to a photographic film.

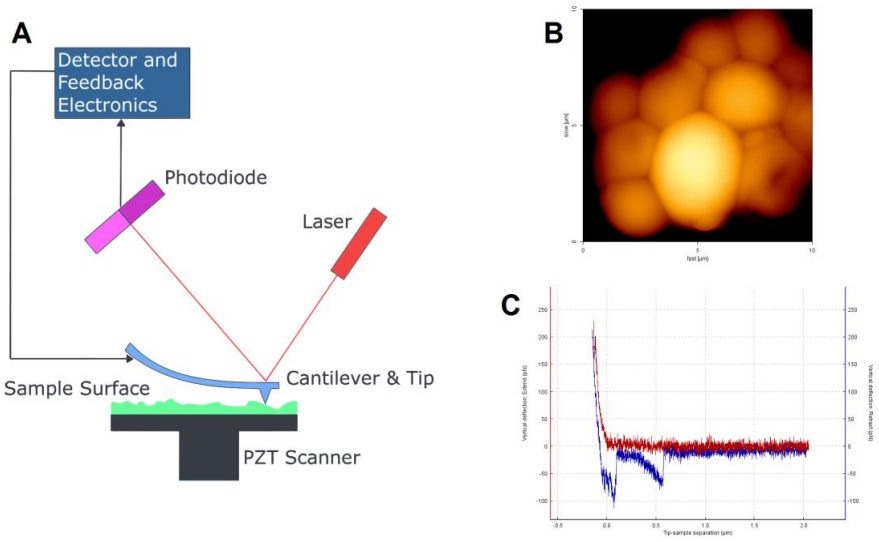

Figure 7. Atomic force microscopy. A) Schematic representation of the AFM mechanism; B) Height image of *C. albicans* cells made with AFM; C) Approach (red) and retraction (blue) force-distance curves obtained over a *C. albicans* cell.

AFM works very similarly to the stylus profiler, despite their different topographic scales. There is a tip in the end of a cantilever and this cantilever is attached to a probe, represented in Figure 7 A. The tip scans across a surface, in contact mode or intermittent contact mode. The latter prevents drift of higher and or/softer samples. The movements made by this tip, however, are much more controlled by the user than the movements of the original cantilever of the stylus profiler, which relied only on a spring at the end of the cantilever. The AFM probe is supported on a mechanism of piezoelectric transducers (PZTs),

which consist of crystals that change size when an electric charge is applied to them, thus controlling the X, Y and Z movements of the probe over the surface. X movements are often called fast and Y movements slow (Figure 7 B - axis legends). Some AFMs have the PZTs in the sample holder and not in the probe holder.

The final pseudo-tridimensional images are the result of a convolution of the probe with the surface and this information is acquired through the photodetection of a laser pointing at a mirror in the back of the cantilever end that holds the sharp tip. Any movement made by the tip in consequence of "feeling" a topographic feature, called deflection, alters the position of the laser in the photo detector, which channels this information to feedback electronics, the proportional-integral-derivative controllers (PID controllers), that allow AFM to keep a constant force and distance to the sample, this is called the feedback loop. The photo detector is connected to electronic signal transducers that convert the signal into the output information, i.e., digital data that is later analyzed by the user, e.g. images (Figure 7 B) or force-distance curves (Figure 7 C).

There are AFM probes with cantilevers and tips of various shapes, sizes, frequency resonances, spring constants, coatings, materials, among other very characteristic features. The combination of these characteristics is a very important step of the design of an experiment, because the user needs to have in consideration the type of sample, i.e., for soft samples, soft cantilevers should be used, with low resonance frequencies and low spring constants; when imaging in contact mode, softer cantilevers have to be used because in this mode the tip is always in touch with the sample and the cantilever, being softer, adapts easier to changes in sample's topography. On the contrary, intermittent contact appropriate cantilevers have to be longer and stiffer, with higher resonance frequencies, so they can endure being in constant vibration over the sample without causing excessive vibration amplitude.

The amount of information contained in one AFM image is enormous and the user can know the height of a chosen point of the image, the contrast phase which allows to see the distribution of harder and softer areas in an apparently homogeneous surface, the lateral and vertical deflections suffered by the cantilever due to the contact with the surface, among others. Through height images it is possible to know the roughness of a certain surface. It is quantified by the vertical deviations of a real surface from its ideal form. If these deviations are large, the surface is rough; if they are small the surface is smooth. To know this, small crops are performed over the cells surface, these crops are plane fitted to remove any concavities or convexities existent in the membrane that are due to the cells shape, resulting in a flat image of the membrane crop with only the small features that make the membrane more or less rough. Afterwards, the root mean square value of the height irregularities is computed from data variance and roughness is calculated as follows:

$$R_{RMS} = \sqrt{\frac{1}{n}\sum_{i=1}^{n} y_i^2} \qquad (1)$$

where n represents the equally spaced, ordered points along the trace of the roughness profile, and y_i is the vertical distance from the mean line to the i^{th} point (DeGarmo et al., 2003).

As far as what concerns AFM-based force spectroscopy, the principle used is the same as for images, but in this case, instead of scanning an area of the sample to form images, the tip is placed over a specific area where there may be a preliminary recognition of sample topography through force maps (similar to height images but with much less resolution and with a different acquiring process) followed by the selection of the desired points of the sample where the user wants to perform the force-distance curve acquisition.

Force-distance curves consist of two parts (Figure 7 C), the approach curve, which represents the deflection of the cantilever when approaching the sample, and the retraction curve, which represents the opposite movement. Depending on the objective of the study, it may be taken in consideration only one part of the force-distance curve, e.g. forces of interaction between molecules are measured with retraction curves (Carvalho et al., 2013; Franquelim et al., 2013) and forces necessary to perform a given nanoindentation on cells are measured with approach curves (Eaton et al., 2012). Nanoindentation is a technique used to measure the hardness of small volumes of material, invented in the mid-1970s (Ternovskii et al., 1974; Bulychev et al., 1975). To perform nanoindentation to *C. albicans* in the present work, silicon nitride tips with a quadratic pyramid shape were used, as shown in Figure 8.

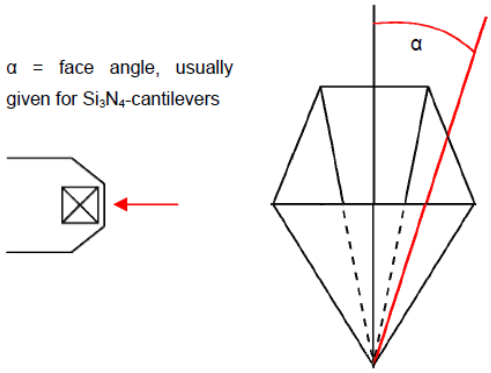

Figure 8. Four-sided pyramid silicon nitride tip representation. Half angle to face is the value α to use in formula (2). Image adapted from JPK Application Report on determining the elastic modulus of biological samples using atomic force microscopy.

The Young's modulus, or elastic modulus, is a measure of an elastic material's stiffness, meaning that a stiff material has a high Young's modulus and a soft material has a low Young's modulus. Assuming that the indenter used is indeformable and that there are no interactions between indenter and sample, the Young's Modulus of the sample can be calculated using the Hertzian model. This model considers the shallow contact of two spherical bodies; thus, some modifications to the model had to be made for each different shape of indenter used (Lin et al., 2007). The following formula is used when the indenter tips has a quadratic pyramidal shape:

$$F = \frac{E}{1 - v^2} \frac{\tan \alpha}{\sqrt{2}} \delta^2 \qquad (2)$$

where E is the Young's modulus, F is the force applied to the sample, v is the Poisson's ratio and the parameter that describes the sample (for biological samples this parameter is usually set to 0.5) and δ is the indentation performed in the sample. The Hertz model assumes that the indentation is neglectable comparing to sample thickness. Therefore, it is only valid for small indentations around 5 to 10% of cells height.

AFM is a powerful tool of nowadays state of the art research in the several different areas of science, like biochemistry, medicine, nanotechnology, physics, material sciences, among others, allowing scientist to come up with a biophysical approach (Santos and Castanho, 2004). For some examples of AFM applications, consult the following references: protein folding and functionality, such as fibrinogen-erythrocyte interactions (Carvalho et al., 2010; Carvalho et al., 2011; Carvalho and Santos, 2012; Carvalho et al., 2013) or dengue virus capsid protein and low-density lipoproteins interaction (Faustino et al., 2013); elasticity and stiffness of cells (Kuznetsova et al., 2007), for example leukemia cells (Rosenbluth et al., 2006; Lam et al., 2007) or malaria infected hepatocytes (Eaton et al., 2012); surface perturbation of microbial cells after treatment with antimicrobial peptides or other antimicrobial agents (Alves et al., 2010; Kim et al., 2011); HIV biophysical studies, like the immature HIV-1 entry regulation by virion stiffness (Pang et al., 2013) or membrane interactions of HIV-1 fusion inhibitors (Franquelim et al., 2013); study of tribological properties (tribology is a branch of mechanical engineering and materials science that studies the principles of friction, lubrication and wear of interacting surfaces in relative motion (Norris et al., 2008)) of chemically and mechanically stable materials with relevance in electronic and biomedical applications (Pujari et al., 2013); and thickness control of graphene films with aerospace applications (Kuzhir et al., 2013).

2. Flow Cytometry

Flow cytometers are impedance-based devices that use the Coulter principle, discovered in 1940 by Wallace H. Coulter (Graham, 2003; Simson, 2013). The Coulter principle states that particles produce a change in impedance when pulled through an orifice, concomitantly with an electric current. This change in impedance is proportional to the volume of the particle crossing the orifice and originates from the displacement of electrolytes caused by the particle (Simson, 2013). Flow cytometry devices are composed of several parts, as shown in Figure 9.

At the interrogation point (Figure 9 b), it is important that only one particle at the time crosses the laser beam, allowing for more accurate data collection. This is accomplished due to the injection of the sample solution in a flowing stream of sheath fluid (Figure 9 a), which is then compressed into a very narrow passage for the cells to pass (hydrodynamic focusing). Cells with a size range of less than a micrometer to several dozens of micrometers can be analyzed by flow cytometry, as long as the user makes sure to set the machine with the proper settings, such as speed of sample flow, and also that the sample is as clean of debris as possible. In cases when the sample is somewhat contaminated with debris, it is possible to use a threshold or cut-off value to exclude those particles from the analysis and assure that the majority of events that are collected by the cytometer correspond to the cells of interest.

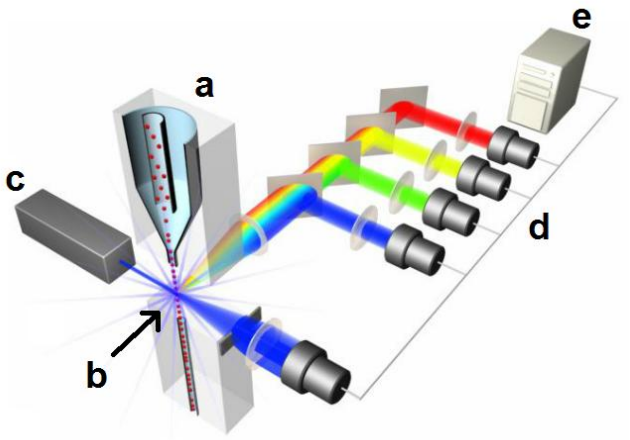

Figure 9. Flow cytometry instrumentation overview. a) the fluidics system, which presents samples to b) the interrogation point and takes away the waste, c) the lasers, which are the light source for scatter and fluorescence, d) the optics filters and detectors, which gather and detect the light resultant from the intersection of the sample and the lasers in the interrogation point, and e) the peripheral electronics and computer system, which converts the signals into digital data. Image adapted from probes.invitrogen.com/resources/education.

When cells are hit by the laser, there is a scatter of light in all directions. Light that is scattered in the forward direction is called the forward scatter (FSC) and the magnitude of this signal is proportional to the size of the cell that is struck by the laser. Light that is scattered to the sides of the cell is called side scatter (SSC) and the magnitude of this signal is proportional to the granularity and structural complexity inside the cell. Signals collected by FSC and SSC detectors are translated into a voltage pulse and this information can be represented in one or two-dimensional plots (Figure 10).

Figure 10. One and two-dimensional representations of flow cytometry data. When considered alone, one-dimensional histograms may not be informative of the complexity of the populations present in a sample, so the user may think there is only one population, when in fact there are multiple populations, which can only be distinguished by looking at the data in a second dimension. This can be done using two-dimensional dot or scatter-plots. Image adapted from: probes.invitrogen.com/resources/education.

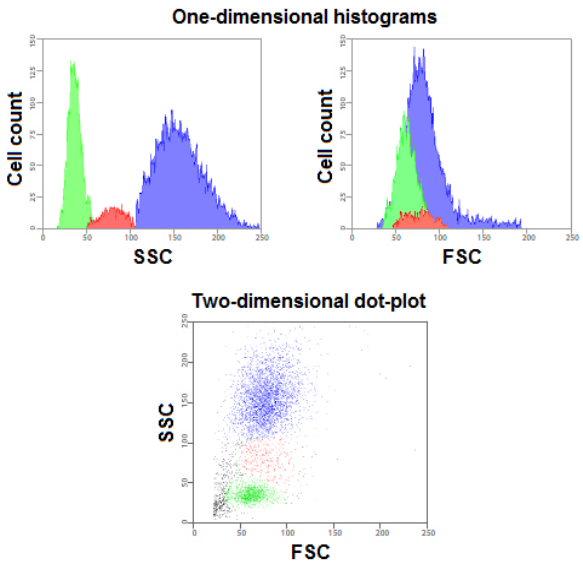

The next level of discrimination of cells is through the emitted fluorescence after excitation by the laser. This fluorescence is emitted by fluorescent dyes, which are molecules that have the capacity to emit fluorescence after being excited. These dyes can bind to the cells' surface or they may enter the cell and find their target intracellularly.

Each dye has specific excitation and emission wavelengths and spectral profile bandwidth. According to this, the laser and detectors set used differs and the choice of which set to use is made in the flow cytometry software interface. Sometimes, due to experimental constraints, dyes with close emission spectra have to be used and, consequently, there will be fluorescence bleed-through or spectral overlap into each of the filters used. This means that some of the fluorescence emitted by the dye A may be captured by the detector of the dye B, resulting in an erroneous measure of the intensity of the fluorescence of the dye B. It is possible to surpass this problem by adding a few controls to the experiment, the single stains. With this, using a process called compensation, the user can excite a sample stained with the dye A and collect the fluorescence emitted by it with the detector of the dye B, thus knowing the amount of bleed-through of the dye A into the dye B filter, making it possible to remove this bleed-through and to collect discrete fluorescence data.

Similarly to FSC and SSC, fluorescence data collected by the detectors is also translated into voltage pulses and this information can be represented in one or two-dimensional plots (Figure 11). When using multiple dyes, a three-dimensional plot can also be used. It is possible nowadays to a few laboratories in the world to collect up to 18 colors simultaneously. Such requirement of a large number of dyes is mostly used in immunology studies.

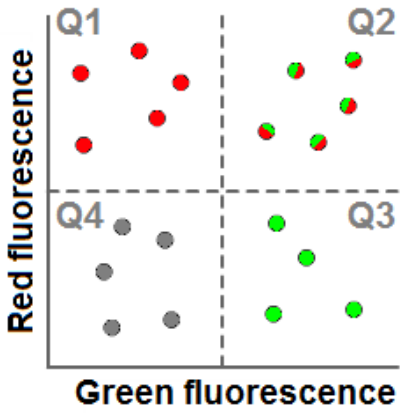

Figure 11. Flow cytometry two-dimensional dot plot of green versus red fluorescence. Q stands for quadrant and each quadrant represents a different population: in Q1 and Q3 are dots corresponding to cells that exhibit red and green fluorescence, respectively; in Q2 are dots corresponding to cells that exhibit both colors (double positives); Q4 is the quadrant where the double negatives locate. Not always the separation among populations is as clear as in this example. Image adapted from: probes.invitrogen.com/resources/education.

Flow cytometry is a unique tool that provides the possibility to gather statistic data of a large number of cells and use that information to correlate multiple parameters within a cell population. These characteristics make it an important tool in a number of fields, such as microbiology, pathology, immunology, molecular biology, plant biology and others (Rodrigues et al., 2007; Caiado et al., 2013; Chen et al., 2013; De, 2013; Derrick et al., 2013; Maurya et al., 2013; Rahman, 2013)

Materials and Methods

Unless mentioned otherwise, all reagents were of analytical grade and were purchase from Sigma-Aldrich (St. Louis, MO, USA).

1. Cell Suspension

The strains used were a *C. albicans* clinical isolate (CI) from a patient of Hospital de Santa Maria (Lisbon, Portugal), *C. albicans* SC5314 (WT) and *C. albicans* SC5314 CAI4 (Δ*gcs*). In Δ*gcs* strain the GlcCer synthase gene was disrupted (molecular genetics details of mutant and WT counterpart in Leipelt et al., 2001). Strains stocks were kept at -80ºC, with 15% glycerol. 10 µl of the cells in stock, previously thawed, were inoculated onto Yeast Peptone Dextrose (YPD) agar and incubated for 48 h at 37ºC. After this period, an isolated fungal colony was suspended in YPD broth and allowed to grow overnight at 25ºC, with 180 rpm agitation. The cells were then centrifuged at 1882 *g* for 10 min and washed three times under the same conditions using 10 mM HEPES buffer, pH 7.4, with 150mM NaCl. Afterwards, cells were counted on hemocytometer to determine cell concentration and the initial suspension was then diluted to the concentration necessary for each experiment.

2. Antifungal susceptibility – minimal inhibitory concentration determination

In vitro antifungal susceptibility tests were performed to determine the minimal inhibitory concentrations. RPMI 1640 medium (Gibco-Life Technologies, UK) was used, supplemented with L-glutamine and 2% glucose, buffered to pH 7.4, with 0.165 M MOPS (3-morpholinopropanesulfonic acid) (AppliChem, Gmbh, Germany). The antifungal drugs tested were Amph B FCZ, which were diluted in RPMI 1640 medium and final drugs concentration ranged from 0.001 to 62.5 µg/ml, over 17 wells, in a volume of 100 µl per each well. Afterwards, 80 µl of RPMI1640 and 20 µl of 10^4 cell/ml were added. Final volume in each well was 200 µl and final cell concentration was 10^3 cell/ml. The MIC was determined by the microdilution method, performed in a 96-well polystyrene flat-bottom plate (TPP, Trasadingen, Switzerland) following the guidelines of the Clinical Laboratory Standard Institute (CLSI, Wayne, PA, USA). Wells with RPMI1640 and cell inoculum were included as positive control and wells with RPMI1640 without inoculum were included as negative control. 200 µl of deionized sterile water were placed in all of periphery wells to minimize evaporation inside the plate. Plates were incubated for 48 h, at 37ºC, after which optical density was read at 540 nm. MIC was defined as the minimal concentration of a drug that, after incubation, causes 100% growth inhibition of an organism (Andrews, 2001). Experiments were performed in triplicate and values were analyzed with GraphPad Prism 5, using the Gompertz equation for MIC determination (Lambert and Pearson, 2000). Due to sample restrictions, MIC values for *Ps*d1 were not determined. However, at a concentration of 20 µM (or 90.0 µg/ml) of *Ps*d1, it has been previously described a growth inhibition of 100% and 70% for both C. albicans WT and mutant strains, respectively (de Medeiros, 2009).

3. Atomic Force Microscopy (AFM)

AFM studies were conducted using a JPK NanoWizard II (Berlin, Germany) mounted on a Zeiss Axiovert 200 inverted microscope (Jena, Germany).

3.1. Imaging

C. albicans washed suspensions were incubated at 25ºC in HEPES buffer, with agitation, with Amph B, FCZ or *Ps*d1, for 6 and 24 h. Antifungic final concentrations were equal to the MIC and 10-fold higher than the MIC. Cell final concentration was set to 10^5 cell/ml and control samples were incubated without any treatment. Cells used in this procedure were resuspended with HEPES buffer, after having been washed. A 100 µL droplet of each test sample was applied onto a poly-L-lysine (PLL)-coated glass slide and left at 25°C for 2 h. After deposition, the samples were rinsed 10 times with deionized sterile water and air-dried at 25°C.

Measurements were carried out in intermittent contact mode, at room temperature, using uncoated silicon ACL cantilevers (Applied NanoStructure, Santa Clara, CA, USA). These cantilevers have typical resonance frequencies of 145-230 kHz and spring constants of 20-90 N/m. The scan rate was set to less than 1 Hz for imaging and image resolution was set to 512 pixel^2 for all images. Height, error signal (often called amplitude) and phase contrast images were recorded, and line-fitted as required. Height and size information was acquired with the JPK Data Processing software 4.2.27.

Roughness analysis of AFM height images was performed using the Gwyddion 2.31 software (free software). Roughness was calculated from the root mean square value (RMS, i.e., standard deviation of distribution of heights over 1 µm^2 crop image). The results of this processing were statistically analyzed using analysis of variances (ANOVA) and Bonferroni post-tests.

3.2. Force Spectroscopy

C. albicans washed suspensions were incubated at room temperature, with agitation, with Amph B, FCZ or *Ps*d1, for 24 h. Antifungic final concentrations were 10-fold higher than the MIC. Cell final concentration was set to 10^6 cell/ml and control samples were incubated without any treatment. 100 µL of sample were placed onto a PLL-coated glass slide and left at 25°C for 2 h. After deposition, the samples were rinsed 3 times with HEPES buffer to remove any cells that had not adhered to the PLL-coated glass slide. 100 µL of HEPES buffer were added to the adhered cells to avoid sample drying. Measurements were carried out in HEPES buffer at 25º C, using the 200 µm long gold reflex coated silicon-nitride OMCL-TR400PSA-1 cantilevers (Olympus, Tokio, Japan). These cantilevers have typical resonance frequencies of 8-14 kHz and spring constants of approximately 0.02 N/m.

First, to have a prior overview of the cells shape and height, force maps were performed using a 10 µm/s approach and retraction speed, Z length of 3 µm and a relative set-point of 0.4 V. The coordinates on the map were then chosen (Figure SF1 in the Appendix - Supplementary data section). Afterwards, one location per each cell was chosen and force-distance measurements were conducted over those

coordinates, in triplicate, using a 3 µm/s approach and retraction speed, Z length of 3 µm and a relative set-point of 0.4 V. These conditions of height and applied force ensure that the indentation ranged is 5 to 10% of cells height, mandatory requirement for measuring cell stiffness. Retraction force-distance curves were processed with the JPK Data Processing software 4.2.27. After processing, the four-sided pyramid Hertz modified equation was applied to the curves and the Young's modulus obtained. The results of this processing were statistically analyzed using analysis of variances (ANOVA) and Bonferroni post-tests.

4. Flow Cytometry

To determine if *Ps*d1 triggers apoptosis in *C. albicans*, a flow cytometry analysis was performed using annexin V conjugated to fluorescein isothiocyanate (annexin V-FITC) and propidium iodide (PI) (Invitrogen, Carlsbad, CA, USA). Annexin V is a human anticoagulant, with high affinity to PS. Annexin V is coupled with FITC, which emits green fluorescence, making it possible to identify apoptotic cells by binding to PS in the outer leaflet (Koopman et al., 1994). Live cells and apoptotic cells are impermeable to PI, but dead cells are stained with red fluorescence through the dye binding to nucleic acids in the cell. After the staining process with annexin V and PI, apoptotic cells show green fluorescence, dead cells show red fluorescence and dead cells that went through an apoptotic process before dying show red and green fluorescence; these are called necrotic cells (Fink and Cookson, 2005).

C. albicans washed suspensions were incubated at 25ºC, with agitation, with Amph B, FCZ or *Ps*d1, for 24 h. Antifungic final concentrations were equal to the MIC. Cell concentration was set to 10^7 cell/ml and control samples were incubated without any treatment. After the incubation, cells were harvested and washed with cold PBS. After centrifuging and discarding the supernatant, cells were resuspended with annexin-binding buffer (Invitrogen, Carlsbad, CA, USA) and final cell concentration was set to 10^6 cell/ml. Afterwards, annexin V-FITC in a 5:100 proportion and PI in a 1 µg/ml final concentration were added to the samples. Incubation took place at room temperature for 15 min. After the incubation period, 400 µl of annexin-binding buffer were added and samples were kept on ice until being analyzed by flow cytometry. In order to visualize and discriminate the distribution of live (double negatives), dead (PI positive and annexin V FITC-negative), necrotic (double positives) and apoptotic (annexin V-FITC positive and PI negative) cells in the dot-plot of flow cytometry data, both annexin V FITC and PI were separately incubated with a mixture of live cells and cells killed by heat, for 15 min at 80ºC, in a live:dead cells proportion of 1:1. This type of staining is called single staining and is used to determine the limits between each condition in the dot-plots.

Measurements were performed in a BD LSRFortessa Flow Cytometer (BD Biosciences, San Jose, CA, USA), using a blue (488 nm) laser to excite stained cells. Green fluorescence (annexin V-FITC) emission was detected with a 530/30 bandpass filter and red fluorescence (PI) emission was detected with a 695/40 bandpass filter. Fluorescence emissions were acquired in biexponential scale and data were collected for 10 000 events using BD FACSDiva v. 6.2 (BD Biosciences). All flow cytometry results were analyzed using FlowJo Software version 9 (Tree Star Inc., Ashland, OR, USA).

Results

1. Susceptibility of planktonic *C. albicans* cells to Amph B, FCZ and *Ps*d1

The activity of Amph B and FCZ against the three *C. albicans* strains selected was determined by measuring their susceptibility to the antifungal drugs. The minimal inhibitory concentration (MIC) was calculated from the susceptibility curves obtained (shown in Fig. SF 2, in the Appendix - Supplementary data section). As shown in Table 1, the MICs of Amph B and FCZ show differences depending on the strain studied. The clinical isolate displays lower MIC values when compared to WT and Δ*gcs*. Growth inhibitory concentration values reported for *Ps*d1 are more than 20-fold higher for WT and Δ*gcs* strains than those obtained for the same strains with different antifungal drugs.

Table 1. Amph B, FCZ and *Ps*d1 growth inhibitory concentrations used on the different *C. albicans* strains.
* *Ps*d1 concentration values obtained from Luciano de Medeiros Doctoral Thesis, Instituto de Biofísica Carlos Chagas Filho, Universidade Federal do Rio de Janeiro, Rio de Janeiro, Brazil (2009). *n.d.* - not determined.

	Clinical isolate	**WT**	**Δ*gcs***
Amphotericin B	1.0 μg/ml	4.0 μg/ml	4.0 μg/ml
Fluconazole	1.5 μg/ml	4.0 μg/ml	4.0 μg/ml
***Ps*d1**	*n.d.*	90.0 μg/ml *	90.0 μg/ml *

Due to sample restrictions, susceptibility curves of the selected strains to *Ps*d1 were not determined and the value considered was 90.0 μg/ml for both WT and Δ*gcs* strains (Figure SF 3, in the Appendix – Supplementary data), previously determined by Luciano de Medeiros (de Medeiros, 2009). This was the value that fully inhibited *C. albicans* WT growth and caused an inhibition of 70% of *C. albicans* Δ*gcs* growth. Although the value of the MIC for *Ps*d1 on the clinical isolate was not determined, the value considered for all experiments was the same as used for WT and Δ*gcs*.

As seen in Table 1, the three *C. albicans* strains were sensitive to the selected drugs, Amph B and FCZ. For the clinical isolate, differences on MIC values of these drugs were related with the antifungal drug tested, contrary to WT and Δ*gcs* isolates that showed equal resistance (MIC values) for the same antifungic tested.

2. Amph B, FCZ and *Ps*d1 cause morphological alterations in *C. albicans*

AFM imaging on intermittent contact mode was used to evaluate the effects suffered by *C. albicans* planktonic cells after incubation with Amph B, FCZ or *Ps*d1. Antifungic concentrations tested were equal and 10-fold higher than MIC values determined previously (Table 1). Figures 12 and 13 show AFM images of *C. albicans* clinical isolate cells, after 6 and 24 h incubation periods, respectively, without (control) and after incubation with Amph B, FCZ or *Ps*d1. Effects of these treatments show morphological changes in *C. albicans* cells. As seen, untreated cells have a smooth surface, a regular

shape and cells gather in groups of 5 or more units (Figures 12 and 13, control). Regarding amphotericin B effects on clinical isolate, cells lose volume and membranes appear rougher. These effects increase in severity in a time-dependent manner, as seen in Figures 12 and 13, A-B. After a 24 h incubation with Amph B, cells are more wrinkled than after a 6 h incubation. After 6 h it is possible to observe small irregularities in the membrane (blebs) at an antifungic concentration 10-fold higher than the MIC (Figure 12 B). It is also possible to observe that there are small vesicles deposited over and around the cells, on the glass slide, giving the appearance that the blebs are being released from the cells. Of the three treatments, Amph B is the one that induces a more extensive cell deformation.

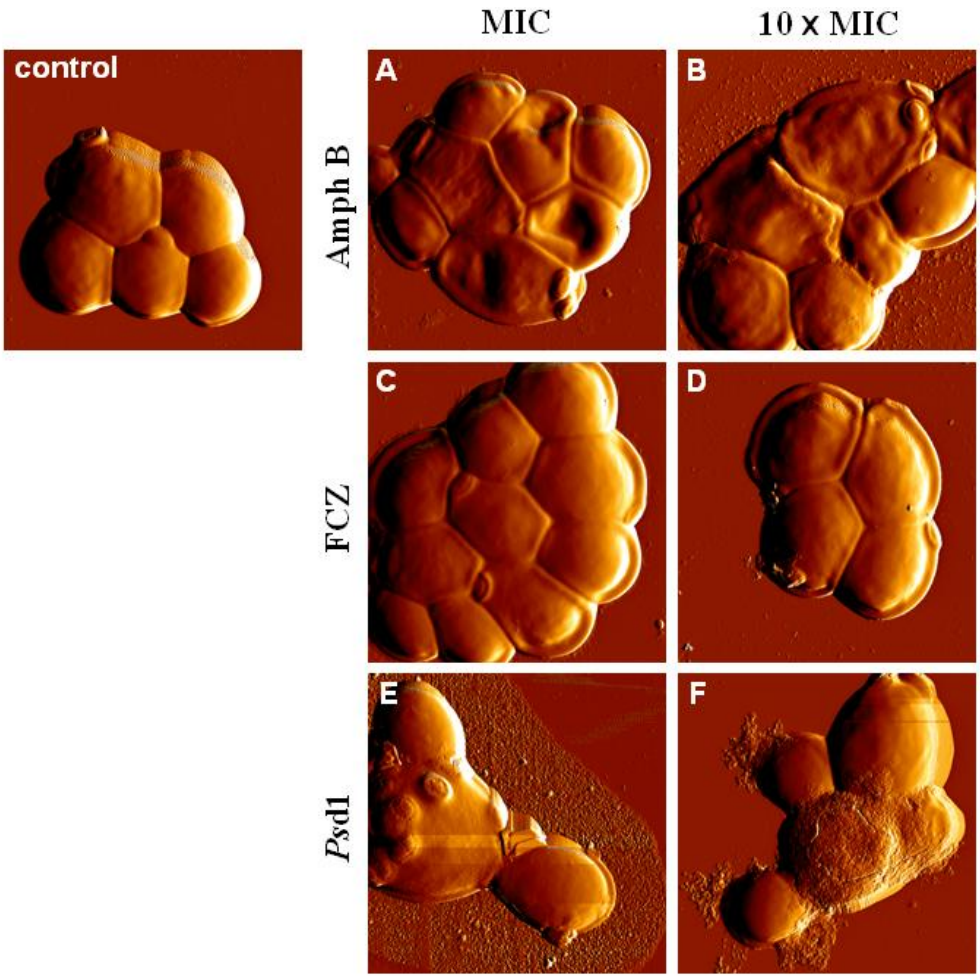

Figure 12. AFM error signal images of clinical isolate cells after 6 h incubation with Amph B, FCZ or *Ps*d1. All images are 10 µm^2.

The clinical isolate seems to be less affected by FCZ, at both times of incubation and concentration of drug used (Figures 12 and 13, C-D), only with some irregularities in the cells membranes appearing after 24 h of incubation (Figure 13 C-D).

Unlike Amph B and FCZ, *Ps*d1 effects appear to be more severe. After 6 h of incubation (Figure 12 E-F) and at both concentrations, the cells exhibit blebs in the membrane and, as it can be observed in Figure 12 F, one cell is completely covered of multiple blebs; probably the internal cell content is released along with the blebs that surround the cells. The height of the blebs, which is around 10 nm, is

shown in detail in Figure 14 and the pseudo-3D representation reveals that the blebs accumulate over each other, forming a bulk structure on top of the cell. After 24 h of incubation (Figure 13 E-F), however, unlike the 6 h incubation blebbing effect, the cells exhibit a peel-off-like morphology, as if small pieces of the membrane were breaking in between them and being removed from the surface of the cells. This effect is strongly prominent when the concentration of peptide is equal to the MIC (Figure 13 E).

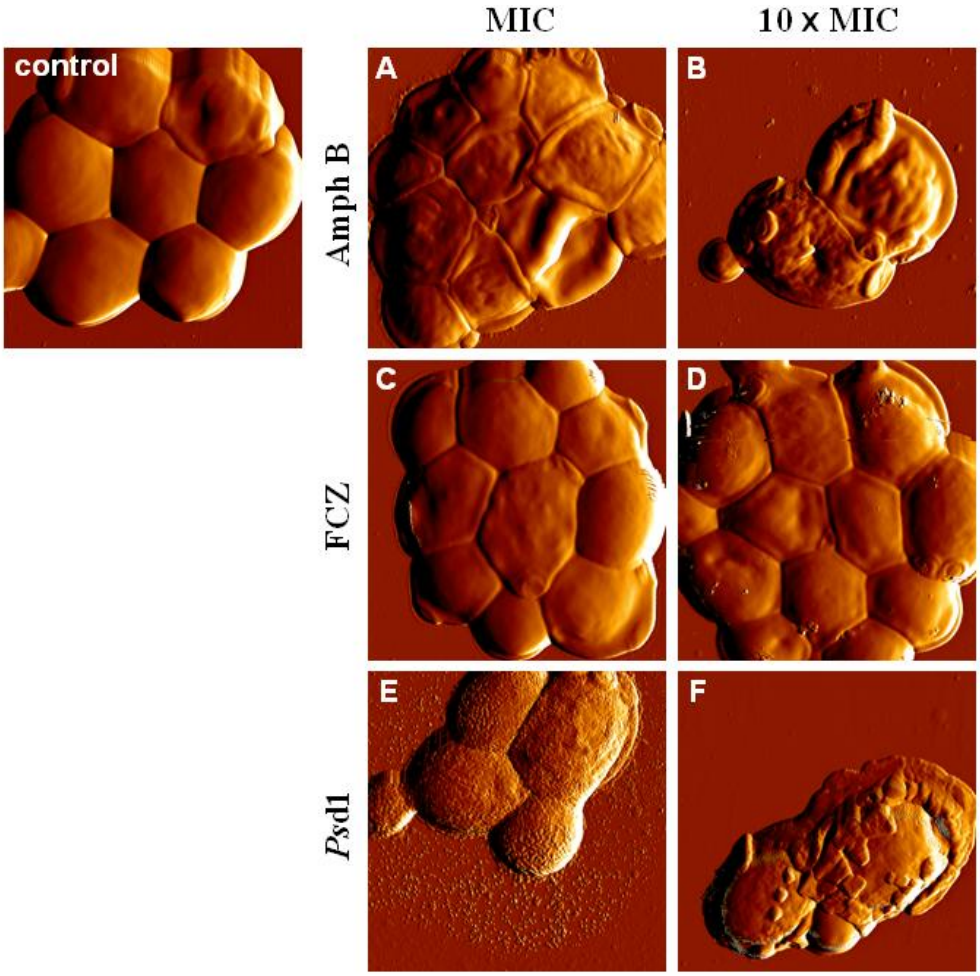

Figure 13. AFM error signal images of clinical isolate cells after 24 h incubation with Amph B, FCZ or *Ps*d1. All images are 10 µm^2.

The height and pseudo-3D representation of the peels when *Ps*d1 concentration is equal to the MIC are shown in Figure 15. When *Ps*d1 concentration is equal to the MIC, the peels height is around 50 nm and, when *Ps*d1 concentration is 10-fold higher, the peels height is around 171 nm (Figure 16). Of the three treatments, *Ps*d1 is the one that has a stronger effect on reducing cells adhesion to each other, which may be the reason why it was difficult to find larger groups of cells gathered on the glass slide, as it was found for the control group and for Amph B and FCZ.

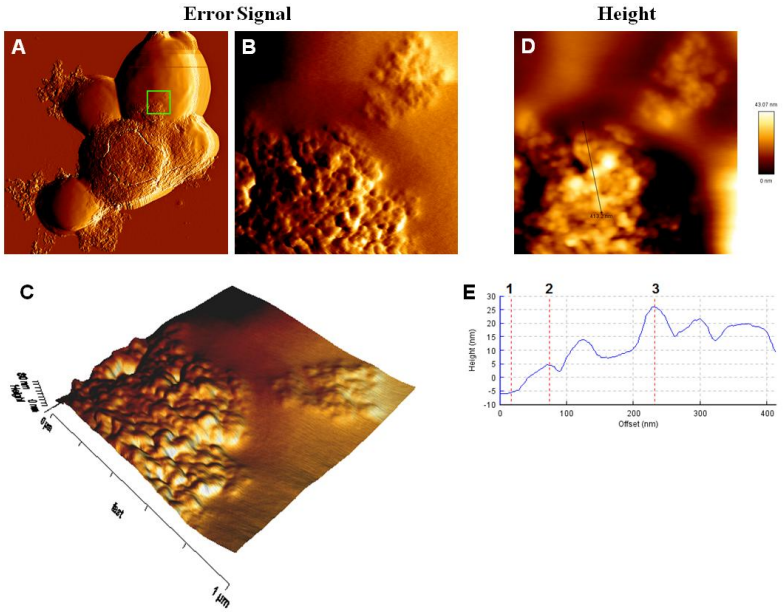

Figure 14. Blebbing detail on clinical isolate cell, after 6 h incubation with *Ps*d1 (10 x MIC). The green square in the error signal image A (10 µm^2) represents a selected new scan area of 1 µm^2. Error signal (B) and height images (D) of the 1 µm^2 selected area were used to make the pseudo-3D representation of the membrane blebs (C). The black line on image D is a cross-section over the blebs on the membrane. The cross-section is represented by the height profile E, which was used to determine the height of the blebs. The difference in height between 1 (cell membrane) and 2 (first bleb in the cross section) is 9.97 nm, while the difference between 1 and 3 (higher point in the bulk of the blebs) is 31.5 nm.

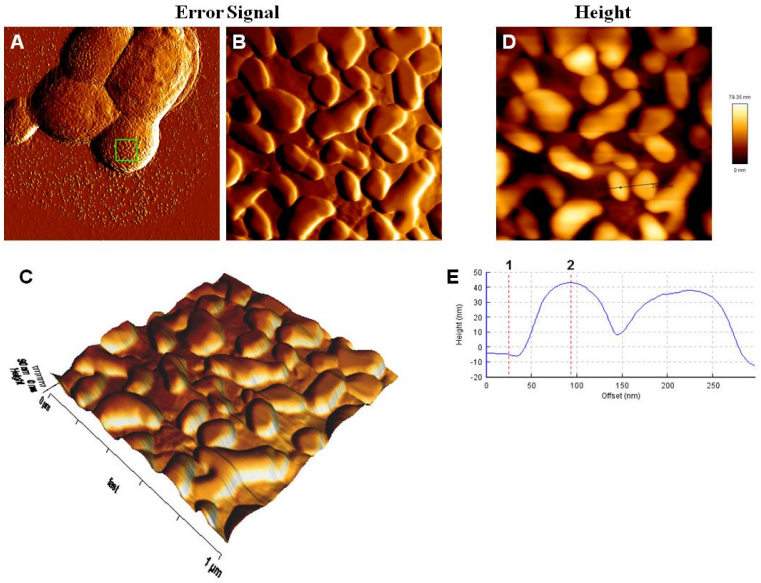

Figure 15. Peeling detail on clinical isolate cell, after 24 h incubation with *Ps*d1 (MIC).

The green square in the error signal image A (10 µm^2) represents a selected new scan area of 1 µm^2. Error signal (B) and height images (D) of the 1 µm^2 selected area were used to make the pseudo-3D representation of the membrane peels (C). The black line on image D is a cross-section over the peels on the membrane. The cross-section is represented by the height profile E, which was used to determine the height of the peels. The difference in height between 1 (base of the peel) and 2 (first peel in the section) is 48.4 nm.

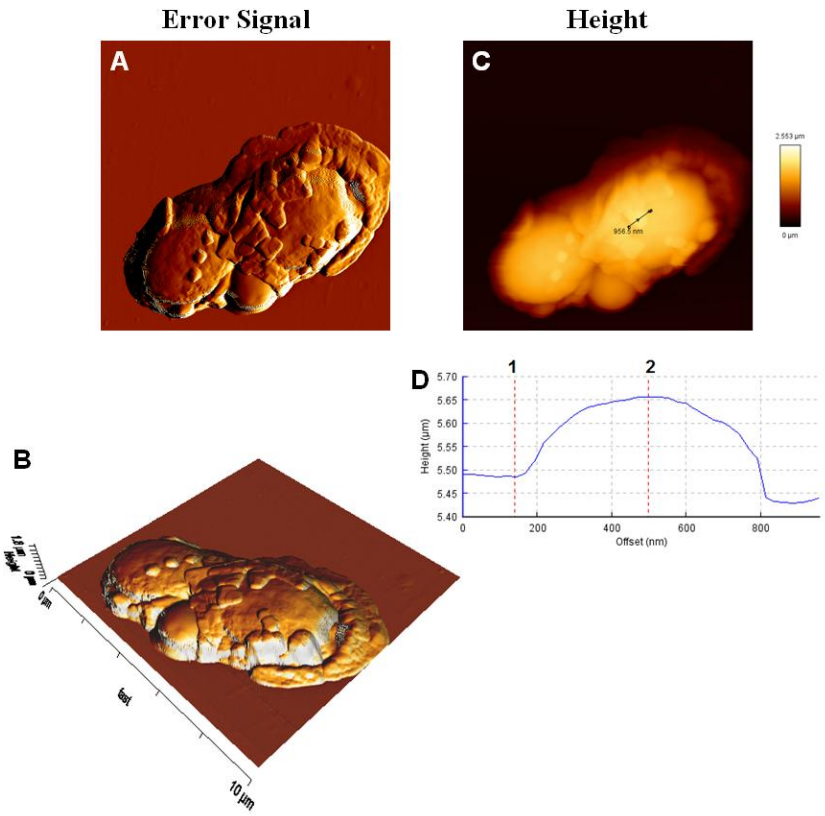

Figure 16. Peeling detail on clinical isolate cell, after 24 h incubation with *Ps*d1 (10 x MIC). Error signal (A) and height images (C) are 10 µm^2 and were used to make a pseudo-3D representation of the membrane blebs (B). A cross-section on image C (black line), corresponding to the height profile D, was traced to determine the height of the peels: the difference in height between 1 (cell membrane) and 2 (peel) is 171 nm.

There are some differences between clinical isolate and WT cells without antifungal treatment. WT cells do not have a regular shape or smooth surface (Figures 17 and 18, control) as clinical isolate cells (Figures 12 and 13, control) and they gather in smaller groups.

After a 6 h incubating with Amph B, there is the appearance of blebs when the drug concentration is equal to the MIC value (Figure 17 A) and the membrane seems to be rougher than the control when the drug reaches a concentration 10-fold higher than the MIC (Figure 17 B). After 24 h of incubation, blebs were not visualized but cells seem to have released an amorphous mass of particles (Figure 18 A-B). For all Amph B conditions, there is a deposition of particles around the cells.

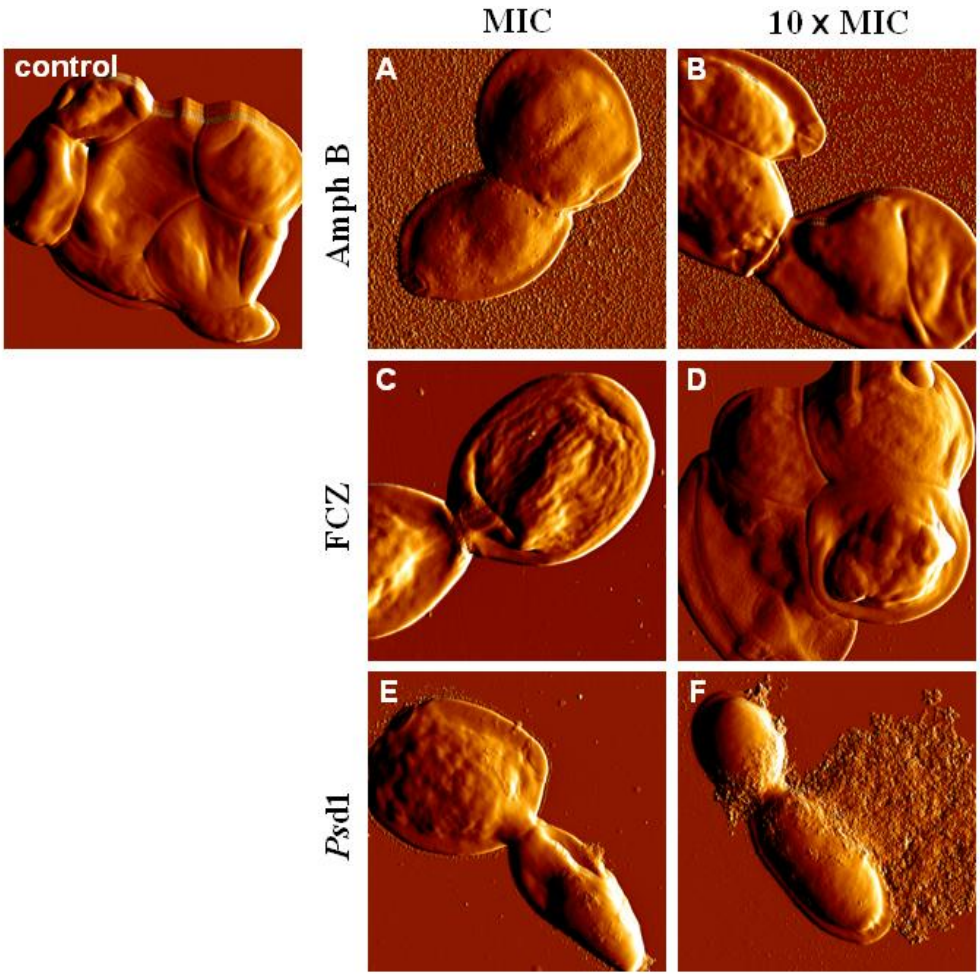

Figure 17. AFM error signal images of WT cells after 6 h incubation with Amph B, FCZ or *Ps*d1. All images are 10 μm^2.

Similarly to the clinical isolate, FCZ is the treatment that had less effect on changing cells morphology for the WT strain. Blebs were not visible in any of the four conditions studied (Figures 17 and 18, C-D), but there is an increase in membrane roughness (evident in Figure 17 C) and loss of cell volume after 6 h of incubation (Figure 17 D). *Ps*d1 causes the appearance of blebs in the membrane of the cells for all conditions tested, as well as increased membrane roughness and cells covered by a bulk mass of debris (Figures 17, 18 E-F, and SF 4 in the Appendix - Supplementary data section) that also covers the surrounding area of the cell (Figures 17 F and 18 E), accompanied by a loss of volume (Figures 18 E and 19).

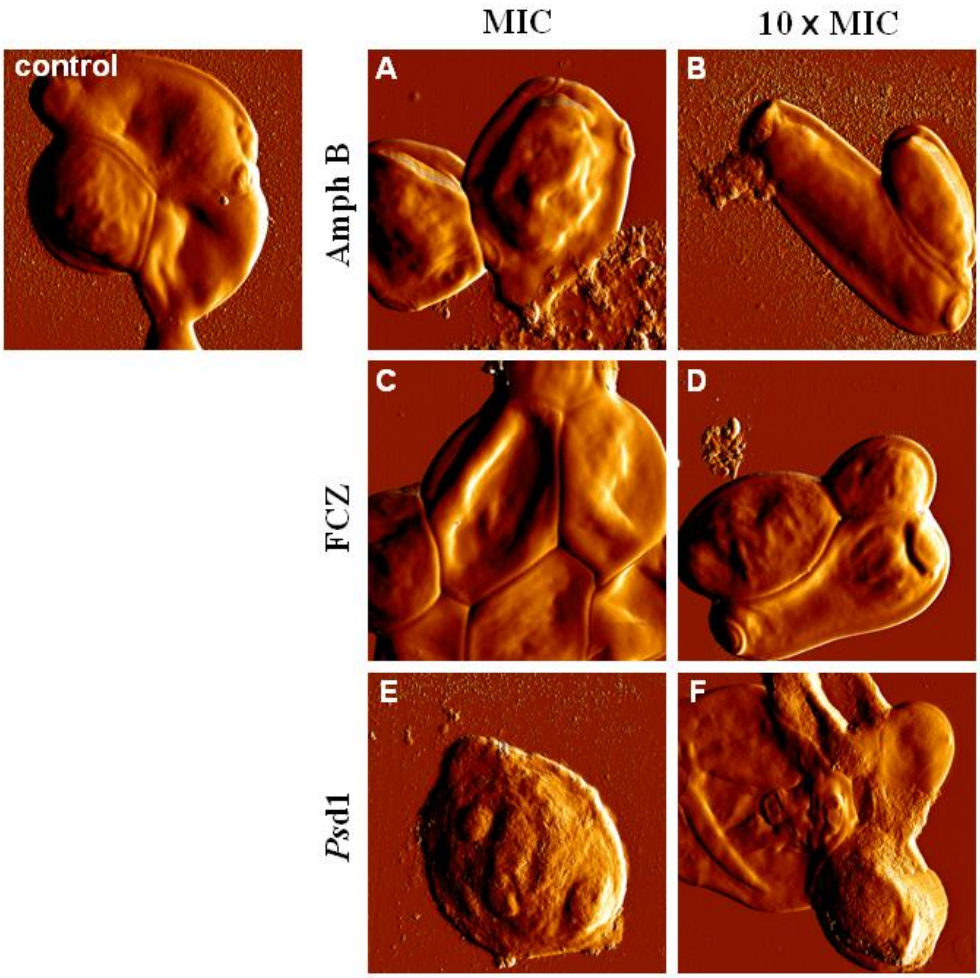

Figure 18. AFM error signal images of WT cells after 24 h incubation with Amph B, FCZ or *Psd*1. All images are 10 μm^2.

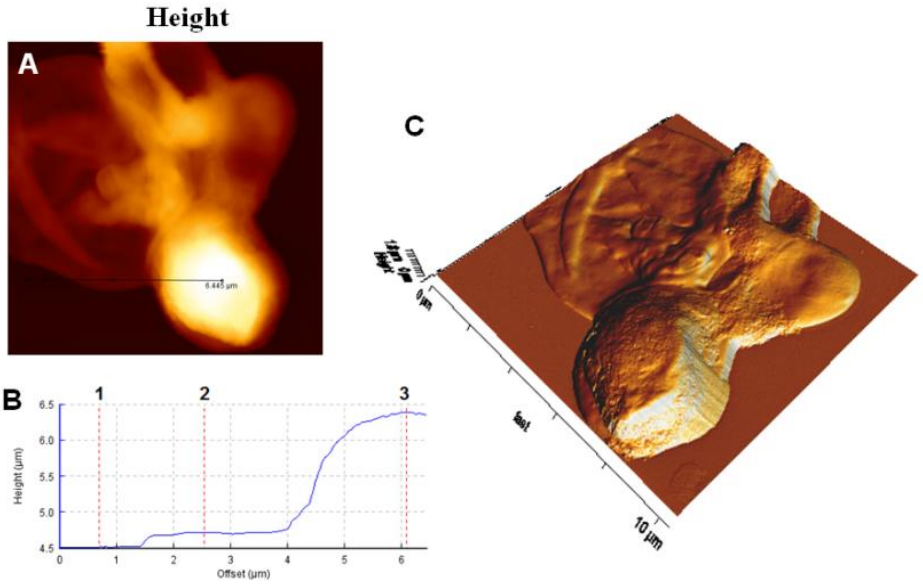

Figure 19. Volume loss suffered by WT cells after 24 h incubation with *Psd*1 (10 x MIC). A cross-section on image A (black line) was used to determine the height of the cells. The difference of height between the points 1 (glass slide) and 2 (collapsed cell) is 203 nm and the difference between the points 1 and 3 (higher cell) is 1.88 μm. C is a pseudo-3D representation of the cells. Images A and C are 10 μm^2.

Compared to clinical isolate and WT cells, untreated mutant cells (control) have an apparent increase in membrane roughness regardless of the incubation time. These cells do not gather in groups and are mostly isolated cells with or without smaller cells budding from the mother cell, in pairs or in groups of three cells, although the latter is less frequent (Figures 20 and 21, control). This observation is the same for any of the treatments for this cell strain.

Amph B effects in mutant cells are more related to the appearance of irregular topography on the cells surface (Figures 20 B and 21 A), although it is also possible to observe the deposit of small debris around the cells, especially when the drug reaches concentrations 10-fold higher than the MIC value (Figures 20 and 21 B). FCZ causes a decrease in cell volume after 6 h of incubation (Figure 20 C-D). When the drug is 10-fold higher than the MIC value, there is also the appearance of blebs in the membrane (Figure 20 D).

After 24 h of incubation with the drug, the most radical effect is when FCZ is 10-fold higher than the MIC value, where it is possible to observe complete cell destruction (Figure 21 D). *Ps*d1 has effects already observed for the other two strains, with blebbing of the membrane (Figures 20 F, 21 E-F and SF 5, in the Appendix - Supplementary data section) and release of vesicles to the surrounding areas when *Ps*d1 reaches the higher concentration (Figures 20 and 21 F).

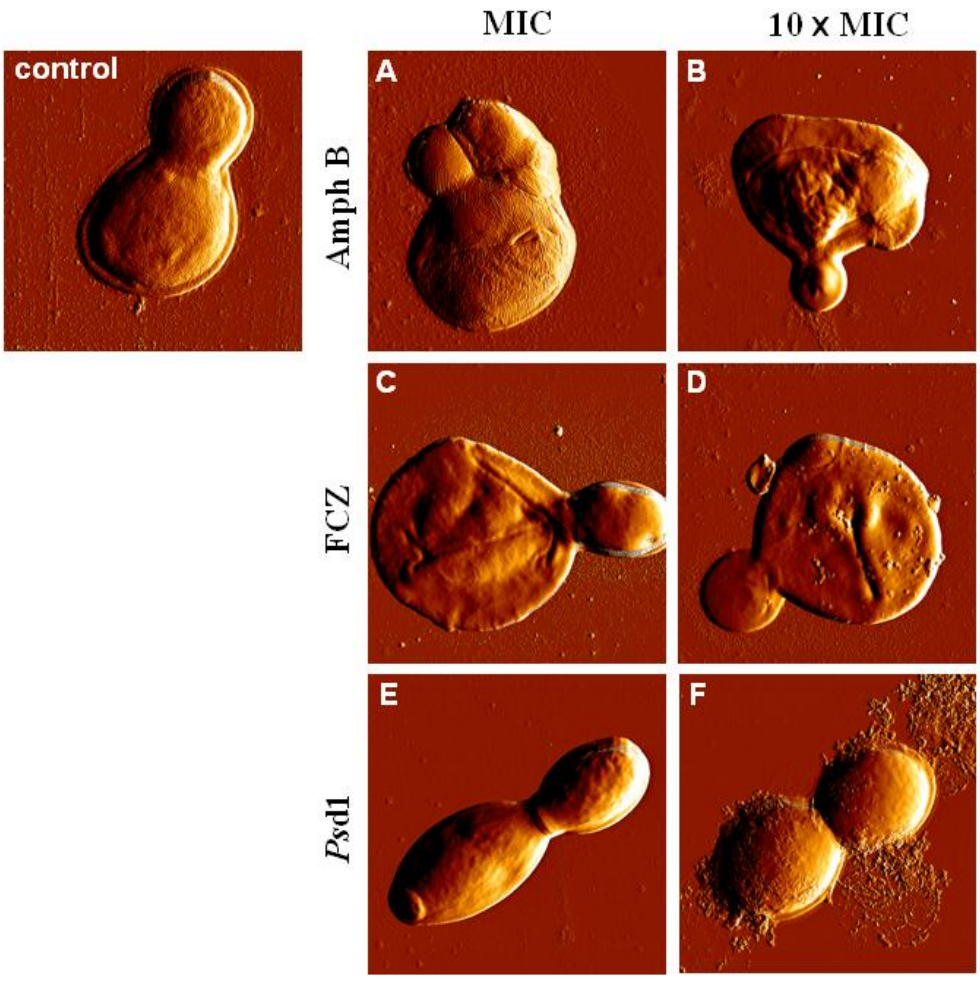

Figure 20. AFM error signal images of Δ*gcs* cells after 6 h incubation with Amph B, FCZ or *Ps*d1. All images are 10 μm^2.

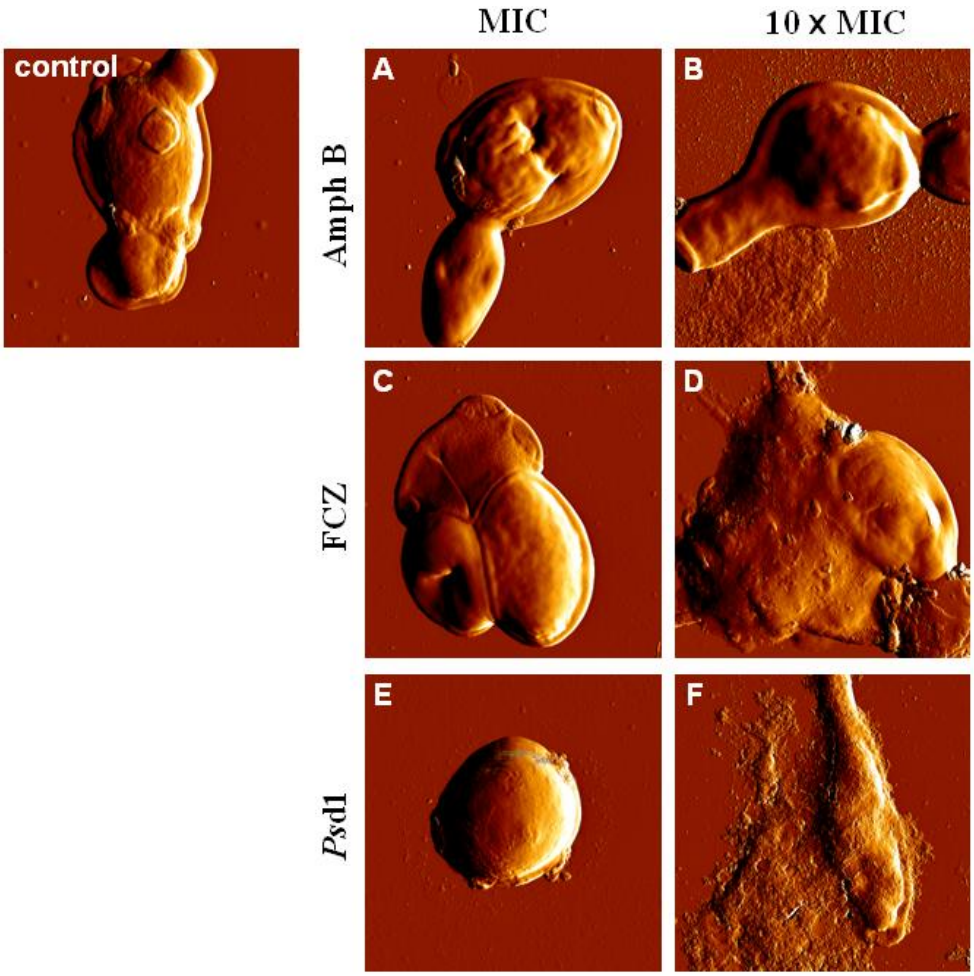

Figure 21. AFM error signal images of Δ*gcs* cells after 24 h incubation with Amph B, FCZ or *Ps*d1. All images are 10 μm^2.

3. *C. albicans* suffers an increase in surface roughness after treatment with Amph B, FCZ or *Ps*d1

There is an overall increase of roughness on all the treatments performed, for all strains. These results (Figure 22), obtained with the RMS formula applied to 1 μm^2 images of the surface of the membrane (Figure SF 6, in the Appendix - Supplementary data section), corroborating all the previous section's observations that membrane roughness increases after cells are submitted to any of the treatments. Regarding the control condition, clinical isolate and WT cells have lower surface roughness values, below 5 nm, whereas Δ*gcs* cells have higher surface roughness values, above 5 nm, being the roughest of the three strains. This relation between the three types of cells has also been concluded from the observation of AFM error signal images, in the previous section. WT cells were the most affected and Δ*gcs* were the least affected, regarding any of the treatments.

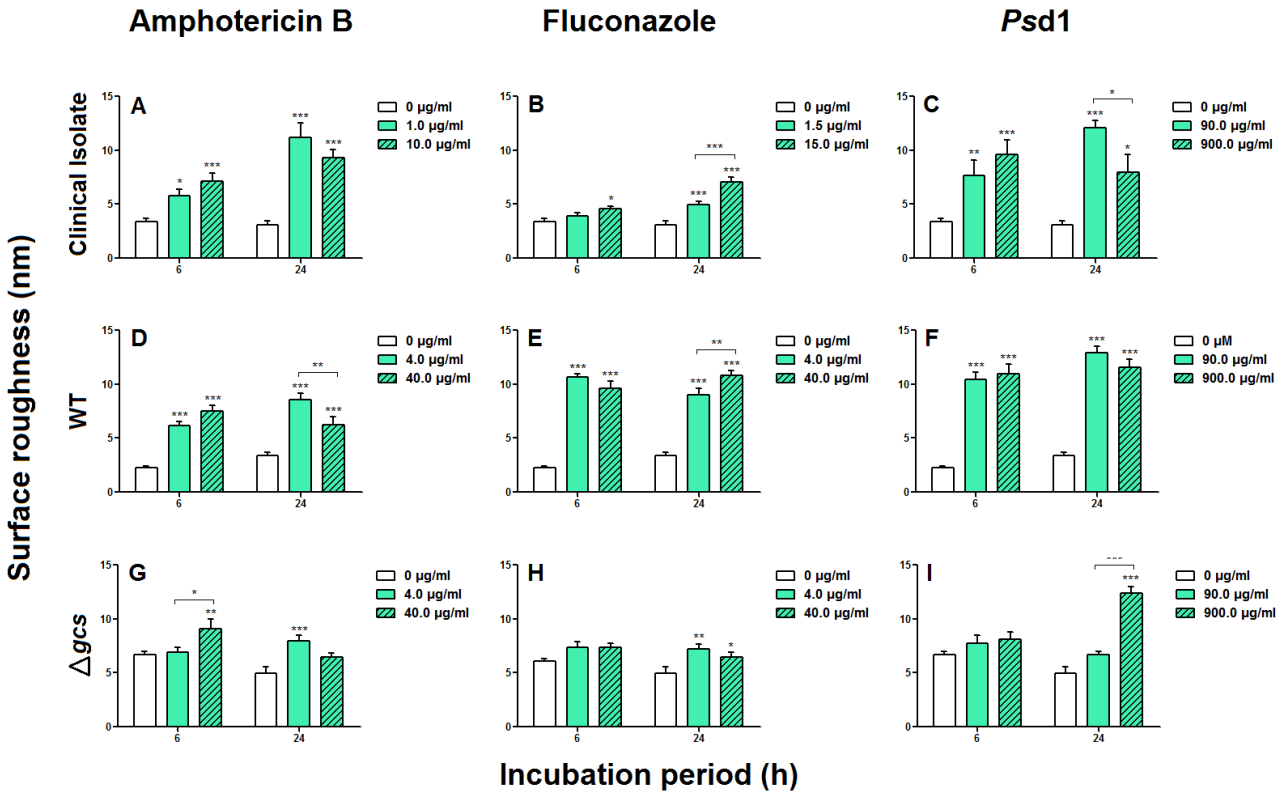

Figure 22. Average surface roughness of *C. albicans* cells after treatment with Amph B, FCZ or *Ps*d1. Two-way ANOVA and Bonferroni post-tests were performed (*p < 0.05, **p < 0.01, ***p < 0.001). Error bars indicate the SEM.

All treatments with Amph B cause a statistically significant increase of membrane roughness on clinical isolate and WT cells. This is not always the case for mutant cells, which although suffering an increase in membrane roughness after 6 h of incubation with a concentration equal to the MIC and 24 h incubation with a concentration 10-fold higher than the MIC (Figure 22 G), this increase in roughness is not statistically significant. When comparing the three cells treated with FCZ, fewer effects on membrane roughness were observed for clinical isolate and mutant cells (Figure 22 B and H). Contrary to this, WT cells were strongly affected by this treatment (Figure 22 E) and all conditions tested resulted in a statistically significant increase in membrane roughness. *Ps*d1 increases clinical isolate's cells roughness in a similar way as Amph B does (Figure 22 A and C), whereas for WT cells the effects of *Ps*d1 are similar in magnitude to those of FCZ (Figure 22 E and F). Again, as it was observed for Amph B and FCZ, mutant cells are the least affected by *Ps*d1 but the defensin manages to strongly increase membrane roughness in these cells after 24 hours of incubation, with a peptide concentration 10-fold higher than the MIC (Figure 22 I).

4. *C. albicans* loses stiffness after treatment with Amph B, FCZ or *Ps*d1

Changes in the stiffness of the cells were assessed in two different ways. One way is based on the determination of the Young's modulus of the membrane, using AFM-based force spectroscopy (for the

three treatments); and the other is based in the observation of AFM phase-contrast images of the cells surface, which allow to visualize and distinguish softer and stiffer areas in the membrane (for *Ps*d1 only).

4.1. Young's Modulus determination

These experiments were performed after 24 h of incubation with an Amph B, FCZ or *Ps*d1 concentration 10-fold higher than the MIC. The clinical isolate has a mean value of membrane stiffness of 354 ± 14 kPa (± standard error), WT has a mean value of 384 ± 14 kPa, and Δ*gcs* has a mean value of 315 ± 21 kPa. When Δ*gcs* cells mean value of stiffness is compared to the same value for WT cell, there is a reduction of 18% (red asterisk in Figure 23; *p < 0.05).

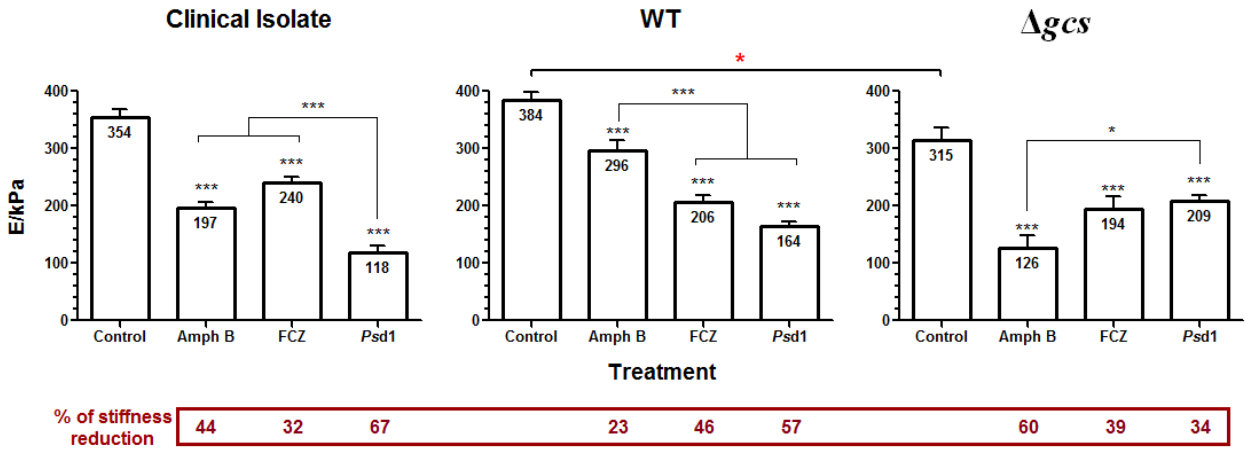

Figure 23. Average stiffness of *C. albicans* cells after treatment with Amph B, FCZ or *Ps*d1. Two-way ANOVA and Bonferroni post-tests were performed (*p < 0.05, **p < 0.01, ***p < 0.001). Error bars indicate the SEM. Values below the graphics, in dark red, are the percentage of reduction in stiffness, relative to the control condition.

The percentage of stiffness reduction was calculated to better understand the different impacts of each treatment (values in the dark red box on the bottom of Figure 23). Amph B effects on cell stiffness were more severe for the mutant cells, with a reduction of 60% of the cell's initial stiffness. WT cells were the less affected by this treatment, with a 23% reduction of the initial stiffness. FCZ was the treatment with less effect on the three strains and its highest reduction on stiffness was registered on the WT cells, to which FCZ caused a reduction to nearly half of the initial stiffness. *Ps*d1, of the three treatments, was the one that caused the highest reduction on stiffness of the clinical isolate, 67%, and WT cells, 57%, whereas for the mutant this was the treatment with a lower effect (34% stiffness reduction). In all cases, the treatment with the antifungal drugs, including *Ps*d1, lead to statistically significant decreases on the cells stiffness (Figure 23, ***p < 0.001).

4.2. Phase contrast imaging of *C. albicans* cells after *Ps*d1 treatment

With this type of AFM images, it is possible to visualize areas in a surface that have different softness (Magonov et al., 1997; Martinez and Garcia, 2006; Garcia et al., 2007; Nie et al., 2011). Phase contrast images of control cells of the three strains all present a homogenous surface. For the three strains, the results observed are roughly the same. Blebs in the membrane caused by the treatment with the peptide are softer than the surrounding membrane (Figures 24, 25 and 26, Phase contrast images) and even when there are no blebs formed, these images allow to distinguish softer and stiffer areas.

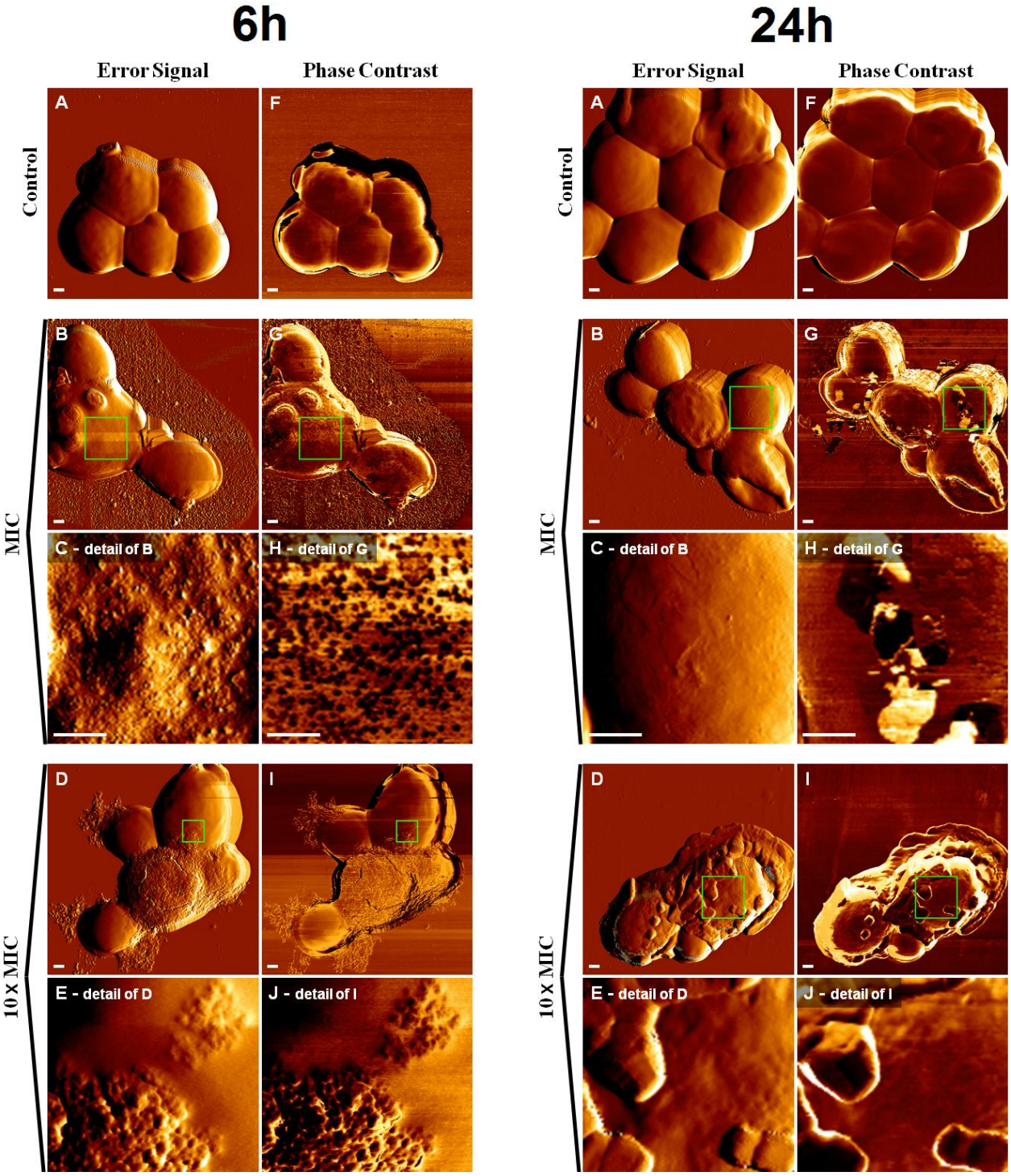

Figure 24. Phase contrast and error signal images of clinical isolate cells after incubation with *Ps*d1. Bars in the lower left corners represent 500 nm.

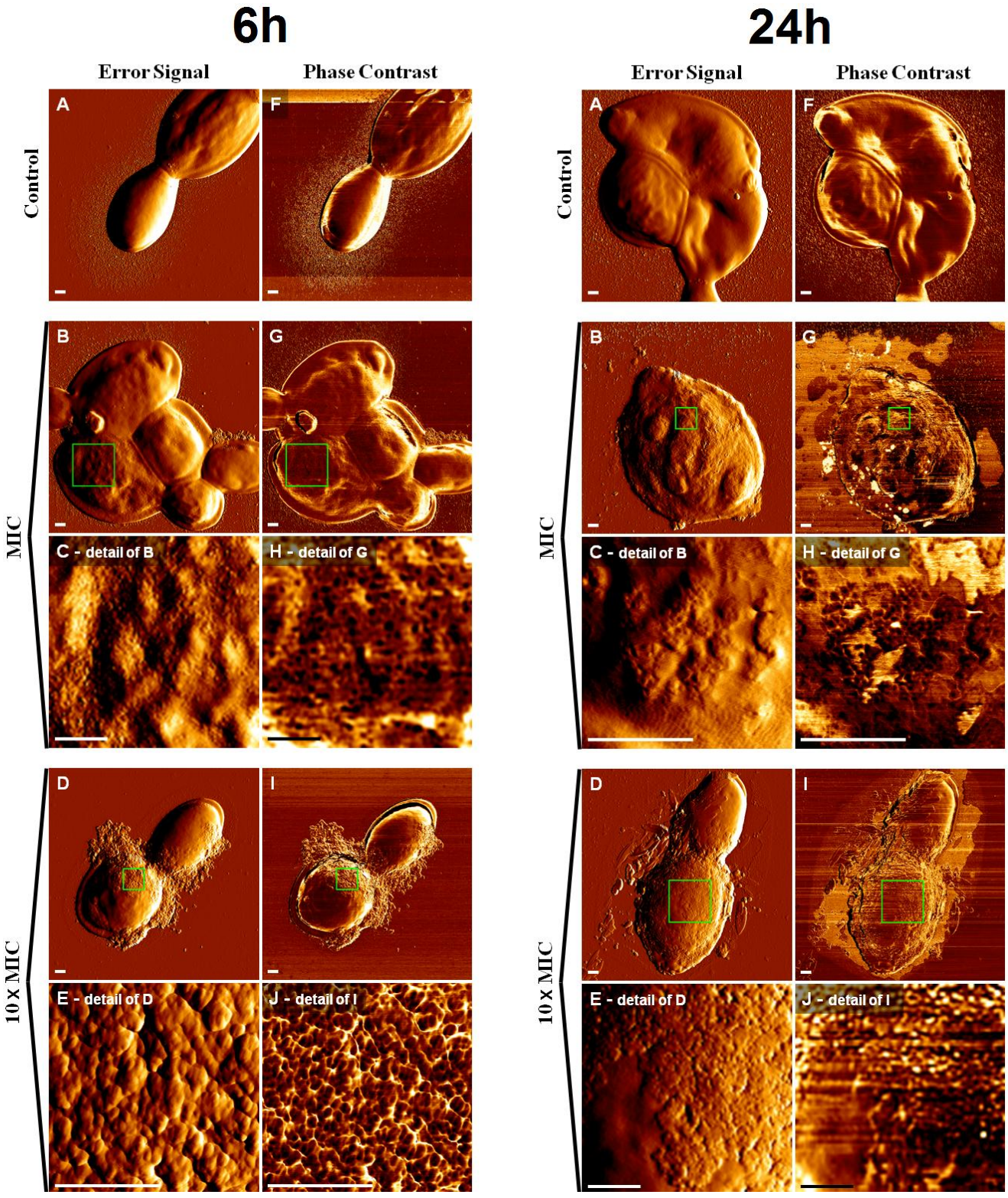

Figure 25. Phase contrast and error signal images of WT cells after incubation with *Psd*1. Bars in the lower left corners represent 500 nm.

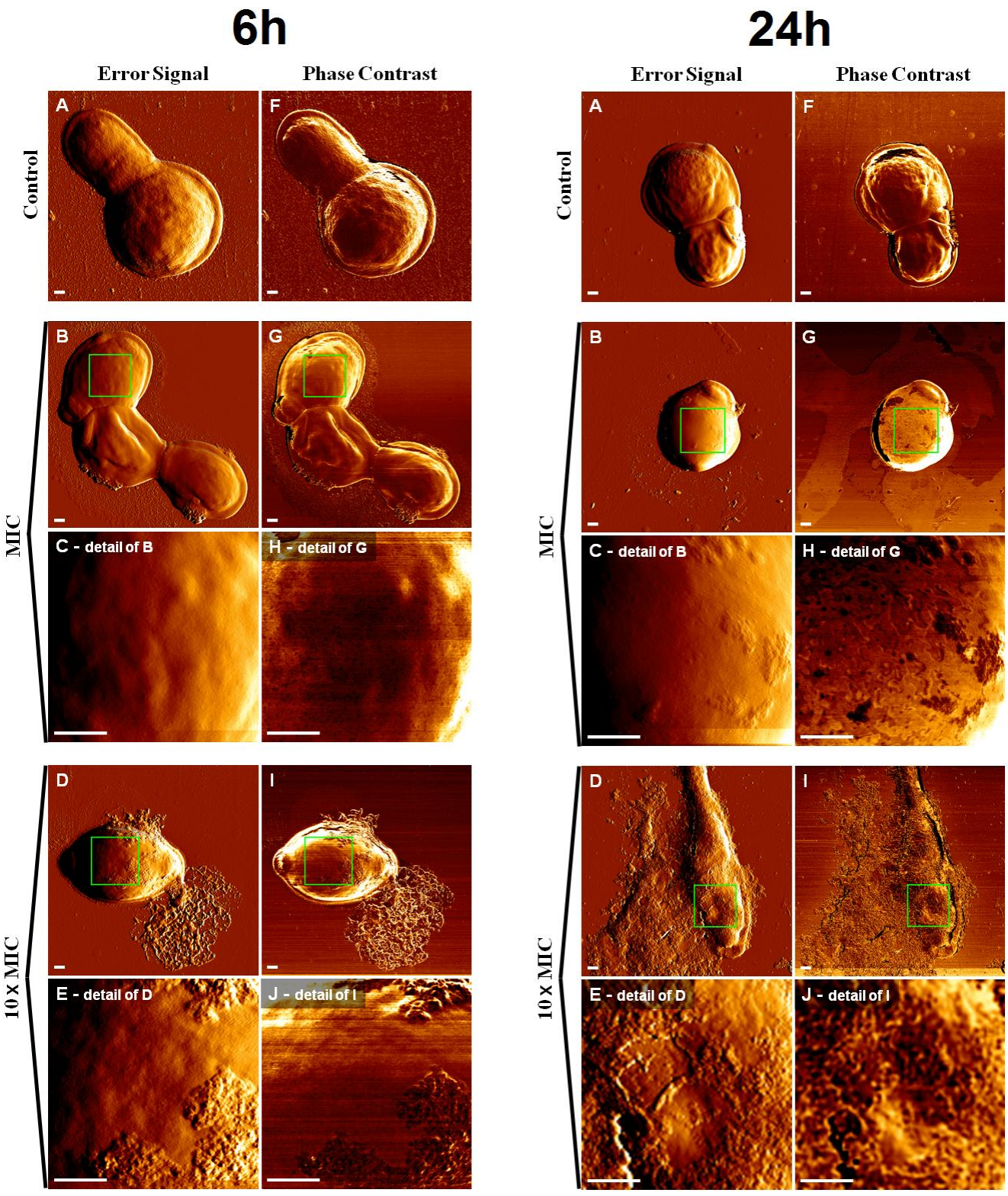

Figure 26. Phase contrast and error signal images of Δ*gcs* cells after incubation with *Psd*1. Bars in the lower left corners represent 500 nm.

5. Amph B, FCZ and *Ps*d1 trigger apoptosis in *C. albicans*

For flow cytometry experiments, WT and Δ*gcs* cells were incubated with a concentration of Amph B, FCZ or *Ps*d1 equal to the MIC, for 24 h. According to the quadrants established (live, dead, necrotic and apoptotic cells), the percentages of apoptotic cells among the WT and Δ*gcs* control samples were determined to be 2.4% and 4.8%, respectively (Figures 27 and 28 C).

Considering the WT cells, Amph B is the treatment with lower effects both in terms of killing cells and apoptosis triggering, having a distribution of cells in the dot plot similar to that of the control (Figure 27 D). FCZ and *Ps*d1 have similar effects in increasing apoptotic cells (Figure 27 E and F), but *Ps*d1 treated cells have a higher percentage of dead cells among them.

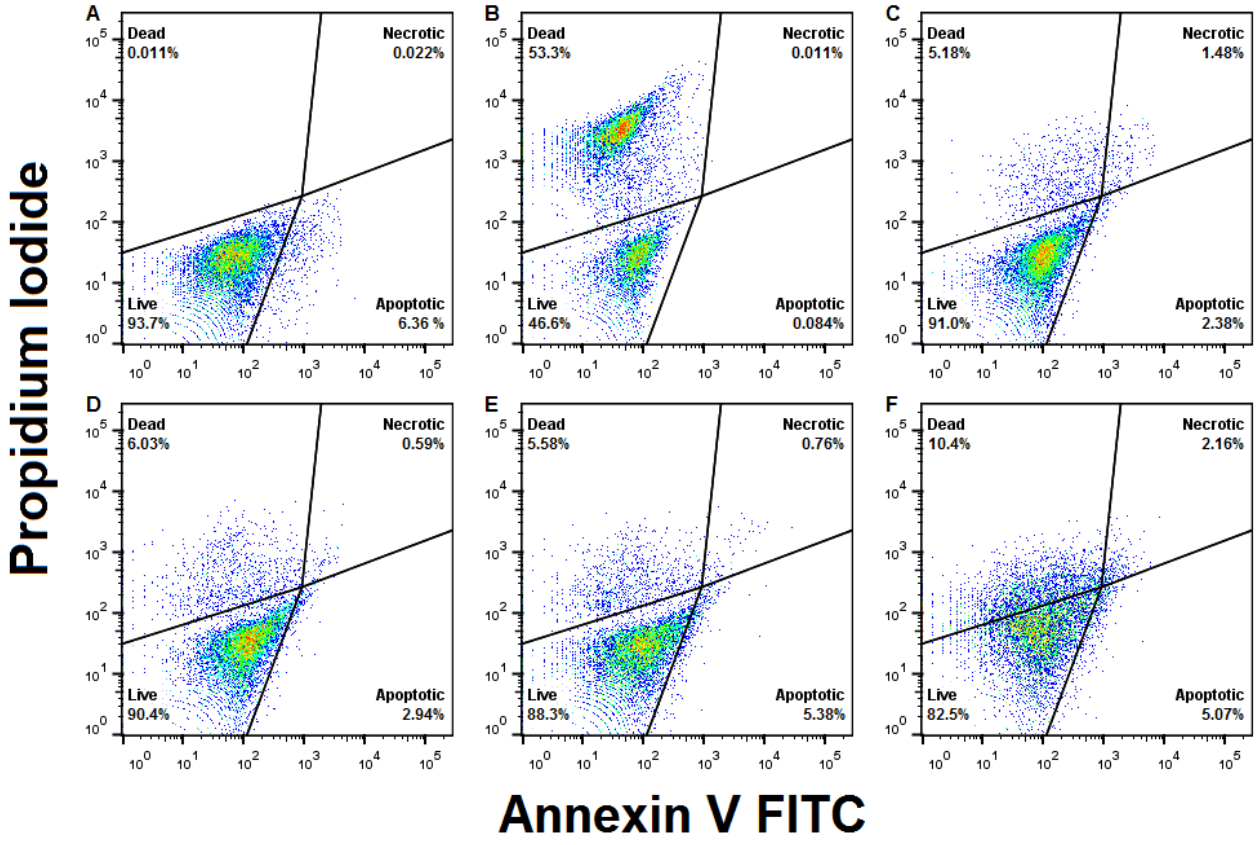

Figure 27. Flow cytometry dot plots of WT cells after treatment with Amph B, FCZ or *Ps*d1. Mix of live and dead cells (1:1) stained with annexin V-FITC (A) or propidium iodide (B); control cells stained with both dyes (C); cells stained with both dyes after 24 h incubation with Amph B (D), FCZ (E) or *Ps*d1 (F).

Δ*gcs* cells treated with Amph B or FCZ (Figure 28 D and E) show an increase in cells with a positive signal for the apoptotic marker, both for the cells still alive (i.e., in the quadrant of apoptotic cells) and dead (i.e., in the quadrant of necrotic cells). *Ps*d1 also causes an increase in apoptotic and necrotic cells (Figure 28 F), but the strongest effect of the peptide is to increase the percentage of dead cells with negative signal for the apoptotic marker, from 11.7% (control) to 36.6%.

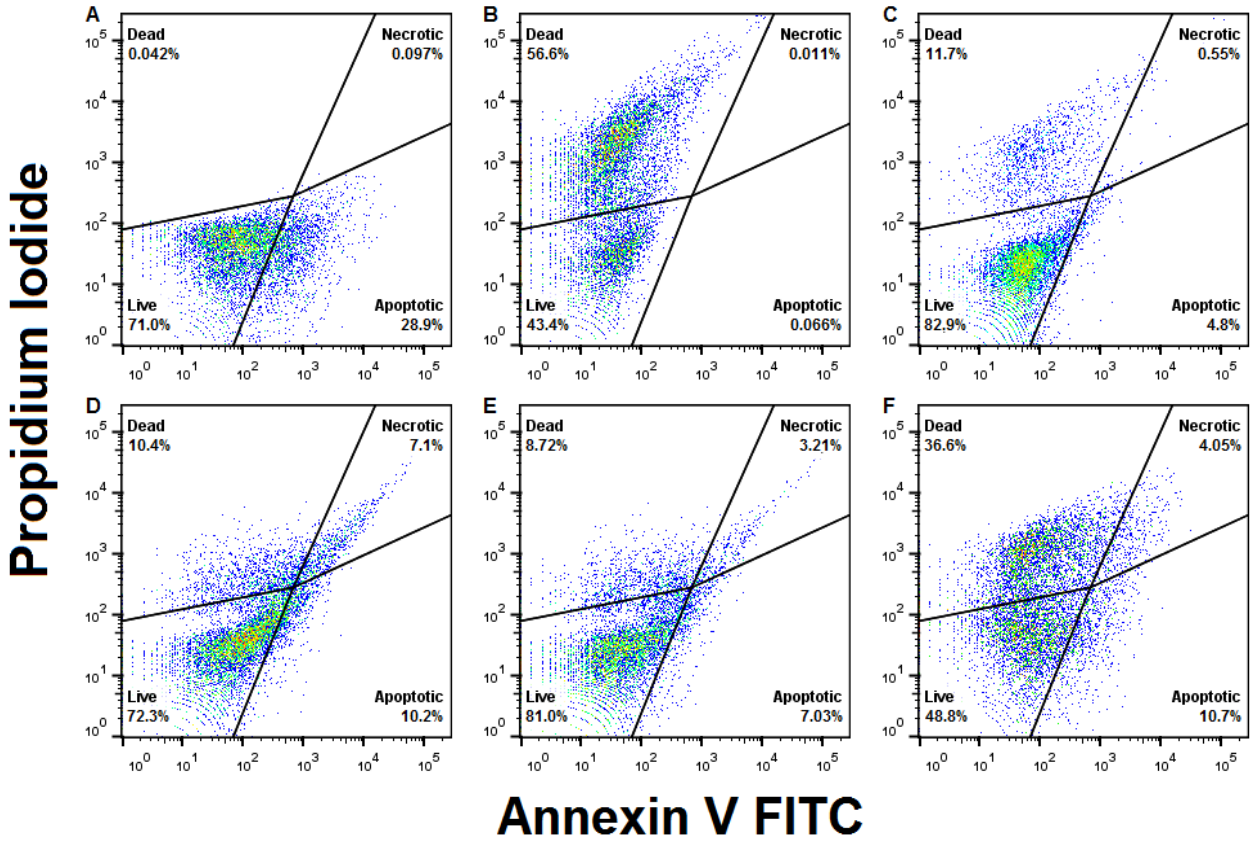

Figure 28. Flow cytometry dot plots of Δ*gcs* cells after treatment with Amph B, FCZ or *Ps*d1. Mix of live and dead cells (1:1) stained with annexin V-FITC (A) or propidium iodide (B); control cells stained with both dyes (C); cells stained with both dyes after 24 h incubation with Amph B (D), FCZ (E) or *Ps*d1 (F).

Discussion

The aim of using a strain of *C. albicans* with a mutation in the GlcCer synthase gene, as well as its wild type counterpart, was to evaluate the role of glucosylceramide in *Ps*d1 antifungal effects against *C. albicans*. As determined previously, this defensin has a weaker effect in inhibiting the growth of *C. albicans* Δ*gcs* compared to the WT strain (de Medeiros, 2009), which after an incubation with 20µM of *Ps*d1 was 70% and 100%, respectively, for each of the strains. In fact, some of the effects reported in this work are compatible with these evidences that *Ps*d1 effects rely on the presence of this glycosphingolipid in the membrane of *C. albicans*. AMPs have been tested for their ability to affect physical properties of cells, such as morphology, size, height, roundness, and stiffness (Canetta et al., 2006; Tyagi and Malik, 2010; Kim et al., 2011; Eaton et al., 2012).

As seen in the section 2 of the Results - *Amph B, FCZ and Psd1 cause morphological alterations in C. albicans*, *Ps*d1 considerably changes the morphology of the three strains used, and these effects can be seen on the lower concentrations, as well as with less time of incubation (i.e., after 6 h of incubation at the MIC). We can see the appearance of blebs in the membrane, the cell surface displays a peeling effect, volume loss, rougher aspect and a lower ability of cells to adhere to each other. The effects induced by Amph B and flucytosine, an azole, were previously imaged by SEM and AFM (Kim et al., 2011), and results similar to those obtained here, for Amph B and FCZ, were observed. Those authors also described a peeling like effect on *C. albicans* cells similar to the visualized here for *Ps*d1.

Considering the most commonly accepted models of AMP mechanisms of action referred in the Introduction - *Models of membrane activity – mechanism of action of AMPs*, the carpet model is the one that causes a larger decrease in membrane homogeneity and, due to a detergent-like micellization, causes a great loss in membrane resistance (Chang et al., 2008). This model (carpet accumulation of peptide in the membrane's surface followed by a disorganization and micellization of the membrane) seems to be the most suitable to explain the blebs appearance and the rougher appearance of the membrane. A weakened membrane could suffer disruption, leading to the leakage of cellular contents, explaining the volume loss observed on some cells. By observing the error signal images, it is also possible to notice that *Ps*d1-treated cells do not aggregate like the control cells, or even like Amph B or FCZ-treated cells. This may be a sign that the defensin has some effect on changing cell's adhesion. This outcome may be explained by the disorganization introduced in the membrane by *Ps*d1 and by its detergent-like action upon the membrane. The ability of planktonic cells to adhere to an abiotic surface and to other cells is an important virulence factor, and it is especially important to the formation of biofilms. By hindering this ability, *Ps*d1 testing against *C. albicans* biofilms becomes highly relevant.

In the third section of the Results - *C. albicans suffers an increase in surface roughness after treatment with Amph B, FCZ or Psd1*, through surface analysis of AFM height (method used by Franquelim et al., 2013), it was possible to quantify the increase in membrane roughness that had been noticed by observing error signal images. All treatments, in a more or less statistically significant manner, increase cells surface roughness and the fact that the mutant cells are the less affected may be due to the

fact that these cells were already rougher than the clinical isolate and WT cells before treatment with Amph B, FCZ or *Ps*d1.

Regarding the Young's Modulus determination in the fourth section of Results - *C. albicans loses stiffness after treatment with Amph B, FCZ or Psd1*, some conclusions may be drawn relatively to the absence of GCS in the mutant's membrane. Δ*gcs* cells have a reduction of 18% in the average cell stiffness, comparing to its WT counterpart and this is expectably due to the lack of glucosylceramides in the membrane. Ceramides are proven to increase membranes rigidity, stability and structural organization of biological membranes (Sullan et al., 2009). When compared to Amph B or FCZ effects in membrane stiffness reduction, *Ps*d1 has a stronger effect both on the clinical isolate and on the WT cells, with decreases of 67% and 57% relative to the control sample, respectively. The fact that *Ps*d1 causes a substantially lower decrease on the stiffness of the mutant cells (34%) is strong evidence that this defensin has glucosylceramide as a molecular target in *C. albicans* membranes. Amph B strong reduction of mutant cells' stiffness (60%) may be due to a synergistic effect between the pores formed by this antifungal drug and the lack of glucosylceramide in the membrane. As the binding of Amph B to ergosterol is irreversible, there is no way for the cell to repair the damage caused and the membrane is rendered with high instability and low resistance.

By observing AFM phase contrast images of *C. albicans* after treatment with *Ps*d1, it is possible to observe softer spots in the membrane, which coincide with the localization of blebs seen in error signal images. These softer areas are probably where the peptide accumulates and interacts with the membrane in a detergent-like manner, causing a disorganization and micellization of the lipids of the membrane and, consequently, a weakened membrane.

*Ps*d1 is a trigger of apoptosis in both *C. albicans* strains tested by flow cytometry. The peptide has a stronger effect than Amph B or FCZ. The comparison of the results obtained for both strains tested are not coincident with the fact that the mutant lacks glucosylceramide in the membrane, indicating that this effect of the peptide does not depend on the existence of GlcCer in the membrane. Probably due to the cell being more fragile without glucosylceramide, the addition of an antifungal peptide would increase cell's susceptibility, hence increasing the percentage of cells undergoing apoptosis. Also, the fact that the flow cytometry dot-plot of *C. albicans* WT only registers 13% of dead cells, when the *Ps*d1 concentration used is equal to the MIC, points out to a non-disruptive mechanism of action of *Ps*d1 (Lobo et al., 2007). This is equally valid for *C. albicans* Δ*gcs*, which registers 41% of dead cells at the same *Ps*d1 concentration. Given that the condition "Dead" in this flow cytometry experiment is defined by the positive signal of the fluorescent stain propidium iodide and that this stain is permeant to cells with corrupted membranes, the previous observation, based on flow cytometry data, indicates that this defensin antifungal action may not be through a membrane disrupting mechanism. Some mechanisms of action of antifungal peptides have been reported, such as binding to the cell wall, induction of signaling cascades and interaction with intracellular targets, which would lead to apoptosis, membrane permeabilization and receptor-mediated internalization (Thevissen et al., 2003; Thevissen et al., 2004; van der Weerden et al., 2013). As previously reported, *Ps*d1 interacts with a *N. crassa* cell cycle protein cyclin F and halts the cell

cycle (Lobo et al., 2007). Due to this, it is possible that *Ps*d1, besides its negative effects observed on the membrane, may also enter into *C. albicans* cells and interact with an intracellular target, causing apoptosis.

Conclusions and future perspective

This work elucidates some aspects of the *Pisum sativum* defensin 1 antifungal activity that had not been investigated so far. It was possible to conclude that the most likely model to explain the mechanism of interaction of the peptide with *Candida albicans* is the carpet model with micellization of the membrane and a detergent-like effect on the membrane surface, which supports the appearance of features in the membrane, such as blebs and an increased membrane roughness. This defensin is likely to interact with glucosylceramide present in *C. albicans* cell membrane, causing a decrease in membrane stiffness. *Ps*d1 is also a triggering agent of apoptosis in this human pathogen.

By hindering cells ability to adhere, *Ps*d1 may also contribute to preventing an infection to proliferate by reducing the adherence of new *C. albicans* to the infected tissue. It is also possible to consider that *Ps*d1 may interfere with biofilm formation, which depends highly on cell-substrate and cell-cell adherence, as well as on quorum sensing (Inigo et al., 2012). In fact, a research line with this focus has already been set in motion. *Ps*d1 is being tested against *C. albicans* biofilms to evaluate its ability to eradicate a biofilm, and the peptide is also being tested for its ability to prevent biofilm formation upon being added to the cells before the biofilm is formed.

The knowledge on antimicrobial peptides has been increasing considerably during the last 20 years. This increased knowledge lead to the notion that AMPs have much more than just strict antimicrobial activity, presenting a broad spectrum of physiological functions. In general, AMPs may have limitations in terms of new drug development, due to their cationic, amphiphilic and protease labile nature, leading to a low serum half-life that limits their systemic administration (Maisetta et al., 2008). This limitation can be overcome by the use of peptidomimetics, like the substitution of natural occurring L-amino acids by D-amino acids or unusual ones (Oren et al., 1997; McPhee et al., 2005). Defensins bare a favorable characteristic against this problem, as their disulphide-stabilized structure confers an increased protease-resistance (Wu et al., 2003). Apart from the need to check their citotoxicity to human cells, the fact that some AMPs (e.g., LL-37) have the ability to translocate into cells and inside the nucleus (Sandgren et al., 2004) needs to be taken into account as well.

Nonetheless, AMPs may combine targeted antimicrobial activity with the capacity to positively modulate the immune system and have proven to be effective across Life evolution, making these peptides highly appealing as an anti-infective strategy. The molecular design and synthesis of new molecules inspired on AMPs structure and sequence seem to be a promising approach to open a new and extensive field of applications, ranging from antimicrobial therapy, to their possible use as vaccine adjuvants. Therefore, a better understanding of function and mechanism of action of host defense peptides is a great promise in anti-infective and immunomodulatory therapeutics.

References

Aaronson, L.R., and Martin, C.E. (1983). Temperature-induced modifications of glycosphingolipids in plasma membranes of *Neurospora crassa*. *Biochim. Biophys. Acta* **735**: 252-258.

Aerts, A.M., Bammens, L., Govaert, G., Carmona-Gutierrez, D., Madeo, F., Cammue, B.P., and Thevissen, K. (2011). The Antifungal Plant Defensin HsAFP1 from *Heuchera sanguinea* Induces Apoptosis in *Candida albicans*. *Front. Microbiol.* **2**: 47.

Aerts, A.M., Carmona-Gutierrez, D., Lefevre, S., Govaert, G., Francois, I.E., Madeo, F., Santos, R., Cammue, B.P., and Thevissen, K. (2009). The antifungal plant defensin RsAFP2 from radish induces apoptosis in a metacaspase independent way in *Candida albicans*. *FEBS Lett.* **583**: 2513-2516.

Aerts, A.M., Francois, I.E., Meert, E.M., Li, Q.T., Cammue, B.P., and Thevissen, K. (2007). The antifungal activity of RsAFP2, a plant defensin from *Raphanus sativus*, involves the induction of reactive oxygen species in *Candida albicans*. *J. Mol. Microbiol. Biotechnol.* **13**: 243-247.

Alba, A., Lopez-Abarrategui, C., and Otero-Gonzalez, A.J. (2012). Host defense peptides: an alternative as antiinfective and immunomodulatory therapeutics. *Biopolymers* **98**: 251-267.

Almeida, M.S., Cabral, K.M., Kurtenbach, E., Almeida, F.C., and Valente, A.P. (2002). Solution structure of *Pisum sativum* defensin 1 by high resolution NMR: plant defensins, identical backbone with different mechanisms of action. *J. Mol. Biol.* **315**: 749-757.

Almeida, M.S., Cabral, K.M., Zingali, R.B., and Kurtenbach, E. (2000). Characterization of two novel defense peptides from pea (*Pisum sativum*) seeds. *Arch. Biochem. Biophys.* **378**: 278-286.

Alves, C.S., Melo, M.N., Franquelim, H.G., Ferre, R., Planas, M., Feliu, L., Bardaji, E., Kowalczyk, W., Andreu, D., Santos, N.C., Fernandes, M.X., and Castanho, M.A. (2010). *Escherichia coli* cell surface perturbation and disruption induced by antimicrobial peptides BP100 and pepR. *J. Biol. Chem.* **285**: 27536-27544.

Andrews, J.M. (2001). Determination of minimum inhibitory concentrations. *J. Antimicrob. Chemother.* **48 Suppl 1**: 5-16.

Argimon, S., Fanning, S., Blankenship, J.R., and Mitchell, A.P. (2011). Interaction between the *Candida albicans* High-Osmolarity Glycerol (HOG) Pathway and the Response to Human beta-Defensins 2 and 3. *Eukaryot. Cell* **10**: 272-275.

Aumelas, A., Mangoni, M., Roumestand, C., Chiche, L., Despaux, E., Grassy, G., Calas, B., and Chavanieu, A. (1996). Synthesis and solution structure of the antimicrobial peptide protegrin-1. *Eur. J. Biochem.* **237**: 575-583.

Ayroza, G., Ferreira, I.L., Sayegh, R.S., Tashima, A.K., and da Silva Junior, P.I. (2012). Juruin: an antifungal peptide from the venom of the Amazonian Pink Toe spider, *Avicularia juruensis*, which contains the inhibitory cystine knot motif. *Front. Microbiol.* **3**: 324.

Bagnat, M., Chang, A., and Simons, K. (2001). Plasma membrane proton ATPase Pma1p requires raft association for surface delivery in yeast. *Mol. Biol. Cell* **12**: 4129-4138.

Bagnat, M., Keranen, S., Shevchenko, A., and Simons, K. (2000). Lipid rafts function in biosynthetic delivery of proteins to the cell surface in yeast. *Proc. Natl. Acad. Sci. U. S. A.* **97**: 3254-3259.

Bagnat, M., and Simons, K. (2002). Lipid rafts in protein sorting and cell polarity in budding yeast *Saccharomyces cerevisiae*. *Biol. Chem.* **383**: 1475-1480.

Bechinger, B., and Lohner, K. (2006). Detergent-like actions of linear amphipathic cationic antimicrobial peptides. *Biochim. Biophys. Acta* **1758**: 1529-1539.

Behnsen, J., Hartmann, A., Schmaler, J., Gehrke, A., Brakhage, A.A., and Zipfel, P.F. (2008). The opportunistic human pathogenic fungus *Aspergillus fumigatus* evades the host complement system. *Infect. Immun.* **76**: 820-827.

Berman, J. (2012). *Candida albicans*. *Curr. Biol.* **22**: R620-622.

Berman, J., and Sudbery, P.E. (2002). *Candida albicans*: a molecular revolution built on lessons from budding yeast. *Nat. Rev. Genet.* **3**: 918-930.

Binnig, G., Quate, C.F., and Gerber, C. (1986). Atomic force microscope. *Phys. Rev. Lett.* **56**: 930-933.

Binnig, G., and Rohrer, H. (1982). Scanning tunneling microcopy. *Surf. Sci.* **126**: 236-244.

Bourbigot, S., Dodd, E., Horwood, C., Cumby, N., Fardy, L., Welch, W.H., Ramjan, Z., Sharma, S., Waring, A.J., Yeaman, M.R., and Booth, V. (2009). Antimicrobial peptide RP-1 structure and interactions with anionic versus zwitterionic micelles. *Biopolymers* **91**: 1-13.

Brand, A., Shanks, S., Duncan, V.M., Yang, M., Mackenzie, K., and Gow, N.A. (2007). Hyphal orientation of *Candida albicans* is regulated by a calcium-dependent mechanism. *Curr. Biol.* **17**: 347-352.

Brock, M. (2009). Fungal metabolism in host niches. *Curr. Opin. Microbiol.* **12**: 371-376.

Bulet, P., and Stocklin, R. (2005). Insect antimicrobial peptides: structures, properties and gene regulation. *Protein Pept. Lett.* **12**: 3-11.

Bulychev, S.I., Alekhin, V.P., Shorshorov, M.K., Ternovskii, A.P., and Shnyrev, G.D. (1975). Determining Young's modulus from the indentor penetration diagram. *Zavodskaya Laboratoriya* **41**: 1137–1140.

Buttner, S., Eisenberg, T., Herker, E., Carmona-Gutierrez, D., Kroemer, G., and Madeo, F. (2006). Why yeast cells can undergo apoptosis: death in times of peace, love, and war. *J. Cell Biol.* **175**: 521-525.

Cabral, K.M., Almeida, M.S., Valente, A.P., Almeida, F.C., and Kurtenbach, E. (2003). Production of the active antifungal *Pisum sativum* defensin 1 (*Ps*d1) in *Pichia pastoris*: overcoming the inefficiency of the STE13 protease. *Protein Expr. Purif.* **31**: 115-122.

Caiado, F., Carvalho, T., Rosa, I., Remédio, L., Costa, A., Matos, J., Heissig, B., Yagita, H., Hattori, K., da Silva, J.P., Fidalgo, P., Pereira, A.D., and Dias, S. (2013). Bone Marrow-Derived CD11b+Jagged2+ Cells Promote Epithelial-to-Mesenchymal Transition and Metastasization in Colorectal Cancer. *Cancer Res.* **73**: 4233-4246.

Calderone, R.A., and Clancy, C.J. (2012). *Candida and Candidiasis.* ASM Press.

Campanella, R. (1992). Membrane lipids modifications in human gliomas of different degree of malignancy. *J. Neurosurg. Sci.* **36**: 11-25.

Canetta, E., Adya, A.K., and Walker, G.M. (2006). Atomic force microscopic study of the effects of ethanol on yeast cell surface morphology. *FEMS Microbiol. Lett.* **255**: 308-315.

Carmona-Gutierrez, D., Eisenberg, T., Buttner, S., Meisinger, C., Kroemer, G., and Madeo, F. (2010). Apoptosis in yeast: triggers, pathways, subroutines. *Cell Death Differ.* **17**: 763-773.

Carrillo-Munõz, A.J., Giusiano, G., Ezkurra, P.A., and Quindos, G. (2006). Antifungal agents: mode of action in yeast cells. *Rev. Esp. Quimioter.* **19**: 130-139.

Carvalho, F.A., Connell, S., Miltenberger-Miltenyi, G., Pereira, S.V., Tavares, A., Ariens, R.A., and Santos, N.C. (2010). Atomic force microscopy-based molecular recognition of a fibrinogen receptor on human erythrocytes. *ACS Nano* **4**: 4609-4620.

Carvalho, F.A., de Oliveira, S., Freitas, T., Goncalves, S., and Santos, N.C. (2011). Variations on fibrinogen-erythrocyte interactions during cell aging. *PLoS ONE* **6**: e18167.

Carvalho, F.A., Martins, I.C., and Santos, N.C. (2013). Atomic force microscopy and force spectroscopy on the assessment of protein folding and functionality. *Arch. Biochem. Biophys.* **531**: 116-127.

Carvalho, F.A., and Santos, N.C. (2012). Atomic force microscopy-based force spectroscopy--biological and biomedical applications. *IUBMB Life* **64**: 465-472.

Chang, W.K., Wimley, W.C., Searson, P.C., Hristova, K., and Merzlyakov, M. (2008). Characterization of antimicrobial peptide activity by electrochemical impedance spectroscopy. *Biochim. Biophys. Acta* **1778**: 2430-2436.

Chen, Y., Zeng, H., Tian, J., Ban, X., Ma, B., and Wang, Y. (2013). Antifungal mechanism of essential oil from *Anethum graveolens* seeds against *Candida albicans*. *J. Med. Microbiol.* **62**: 1175-1183.

Chiantia, S., and London, E. (2013). Sphingolipids and membrane domains: recent advances. *Handb. Exp. Pharmacol.*: 33-55.
Cho, J., Hwang, I.S., Choi, H., Hwang, J.H., Hwang, J.S., and Lee, D.G. (2012). The novel biological action of antimicrobial peptides via apoptosis induction. *J Microbiol Biotechnol* **22**: 1457-1466.
Citiulo, F., Jacobsen, I.D., Miramon, P., Schild, L., Brunke, S., Zipfel, P., Brock, M., Hube, B., and Wilson, D. (2012). *Candida albicans* scavenges host zinc via Pra1 during endothelial invasion. *PLoS Pathog.* **8**: e1002777.
Clardy, J., Fischbach, M.A., and Currie, C.R. (2009). The natural history of antibiotics. *Curr. Biol.* **19**: R437-441.
Cornet, B., Bonmatin, J.M., Hetru, C., Hoffmann, J.A., Ptak, M., and Vovelle, F. (1995). Refined three-dimensional solution structure of insect defensin A. *Structure* **3**: 435-448.
da Silva, A.F., Rodrigues, M.L., Farias, S.E., Almeida, I.C., Pinto, M.R., and Barreto-Bergter, E. (2004). Glucosylceramides in *Colletotrichum gloeosporioides* are involved in the differentiation of conidia into mycelial cells. *FEBS Lett.* **561**: 137-143.
Daniotti, J.L., and Iglesias-Bartolome, R. (2011). Metabolic pathways and intracellular trafficking of gangliosides. *IUBMB Life* **63**: 513-520.
De, A. (2013). Current laboratory diagnosis of opportunistic enteric parasites in human immunodeficiency virus-infected patients. *Trop Parasitol* **3**: 7-16.
de Coninck, B., Cammue, B.P.A., and Thevissen, K. (2013). Modes of antifungal action and in planta functions of plant defensins and defensin-like peptides. *Fungal Biol. Rev.* **26**: 109-120.
de Medeiros, L.N. (2009). *Interação da defensina Psd1 com a monohexosil ceramida (CMH) isolada do fungo Fusarium solani.* Doutor em Química Biológica, Universidade Federal do Rio de Janeiro.
de Medeiros, L.N., Angeli, R., Sarzedas, C.G., Barreto-Bergter, E., Valente, A.P., Kurtenbach, E., and Almeida, F.C. (2010). Backbone dynamics of the antifungal *Ps*d1 pea defensin and its correlation with membrane interaction by NMR spectroscopy. *Biochim. Biophys. Acta* **1798**: 105-113.
DeGarmo, E.P., Black, J.T., and Kohser, R.A. (2003). *Materials and Processes in Manufacturing.* John Wiley & Sons.
den Hertog, A.L., van Marle, J., van Veen, H.A., Van't Hof, W., Bolscher, J.G., Veerman, E.C., and Nieuw Amerongen, A.V. (2005). Candidacidal effects of two antimicrobial peptides: histatin 5 causes small membrane defects, but LL-37 causes massive disruption of the cell membrane. *Biochem. J.* **388**: 689-695.
den Hertog, A.L., van Marle, J., Veerman, E.C., Valentijn-Benz, M., Nazmi, K., Kalay, H., Grun, C.H., Van't Hof, W., Bolscher, J.G., and Nieuw Amerongen, A.V. (2006). The human cathelicidin peptide LL-37 and truncated variants induce segregation of lipids and proteins in the plasma membrane of *Candida albicans*. *Biol. Chem.* **387**: 1495-1502.
Derrick, S.C., Yabe, I.M., Yang, A., Kolibab, K., Hollingsworth, B., Kurtz, S.L., and Morris, S. (2013). Immunogenicity and protective efficacy of novel *Mycobacterium tuberculosis* antigens. *Vaccine*.
Eaton, P., Zuzarte-Luis, V., Mota, M.M., Santos, N.C., and Prudencio, M. (2012). Infection by *Plasmodium* changes shape and stiffness of hepatic cells. *Nanomed.* **8**: 17-19.
Ehrenstein, G., and Lecar, H. (1977). Electrically gated ionic channels in lipid bilayers. *Q. Rev. Biophys.* **10**: 1-34.
Epand, R.F., Maloy, L., Ramamoorthy, A., and Epand, R.M. (2010). Amphipathic helical cationic antimicrobial peptides promote rapid formation of crystalline states in the presence of phosphatidylglycerol: lipid clustering in anionic membranes. *Biophys. J.* **98**: 2564-2573.
Fadel, V., Bettendorff, P., Herrmann, T., de Azevedo, W.F., Jr., Oliveira, E.B., Yamane, T., and Wuthrich, K. (2005). Automated NMR structure determination and disulfide bond identification of the myotoxin crotamine from *Crotalus durissus terrificus*. *Toxicon* **46**: 759-767.
Faustino, A.F., Carvalho, F.A., Martins, I.C., Castanho, M.A., Mohana-Borges, R., Almeida, F.C., da Poian, A.T., and Santos, N.C. (2013). Dengue virus capsid protein interacts specifically with very low-density lipoproteins. *Nanomed.*
Feinstein, M.B., Fernandez, S.M., and Sha'afi, R.I. (1975). Fluidity of natural membranes and phosphatidylserine and ganglioside dispersions. Effect of local anesthetics, cholesterol and protein. *Biochim. Biophys. Acta* **413**: 354-370.
Fink, S.L., and Cookson, B.T. (2005). Apoptosis, pyroptosis, and necrosis: mechanistic description of dead and dying eukaryotic cells. *Infect. Immun.* **73**: 1907-1916.
Finkel, J.S., and Mitchell, A.P. (2010). Genetic control of *Candida albicans* biofilm development. *Nat. Rev. Microbiol.* **9**: 109-118.
Fleck, C.B., Schobel, F., and Brock, M. (2011). Nutrient acquisition by pathogenic fungi: nutrient availability, pathway regulation, and differences in substrate utilization. *Int. J. Med. Microbiol.* **301**: 400-407.
Franquelim, H.G., Gaspar, D., Veiga, A.S., Santos, N.C., and Castanho, M.A. (2013). Decoding distinct membrane interactions of HIV-1 fusion inhibitors using a combined atomic force and fluorescence microscopy approach. *Biochim. Biophys. Acta* **1828**: 1777-1785.
Fry, B.G., Roelants, K., Champagne, D.E., Scheib, H., Tyndall, J.D., King, G.F., Nevalainen, T.J., Norman, J.A., Lewis, R.J., Norton, R.S., Renjifo, C., and de la Vega, R.C. (2009). The toxicogenomic multiverse: convergent recruitment of proteins into animal venoms. *Annu. Rev. Genomics Hum. Genet.* **10**: 483-511.
Gank, K.D., Yeaman, M.R., Kojima, S., Yount, N.Y., Park, H., Edwards, J.E., Filler, S.G., and Fu, Y. (2008). SSD1 is integral to host defense peptide resistance in *Candida albicans*. *Eukaryot. Cell* **7**: 1318-1327.
Ganz, T. (2003). The role of antimicrobial peptides in innate immunity. *Integr. Comp. Biol.* **43**: 300-304.
Ganz, T. (2004). Defensins: antimicrobial peptides of vertebrates. *C. R. Biol.* **327**: 539-549.
Ganz, T., and Lehrer, R.I. (1998). Antimicrobial peptides of vertebrates. *Curr. Opin. Immunol.* **10**: 41-44.
Gao, B., and Zhu, S. (2012). Alteration of the mode of antibacterial action of a defensin by the amino-terminal loop substitution. *Biochem. Biophys. Res. Commun.* **426**: 630-635.
Garcia, R., Magerle, R., and Perez, R. (2007). Nanoscale compositional mapping with gentle forces. *Nat. Mater.* **6**: 405-411.
Gaspar, D., Veiga, A.S., and Castanho, M.A. (2013). From antimicrobial to anticancer peptides. A review. *Front Microbiol* **4**: 294.
Ghannoum, M.A., and Rice, L.B. (1999). Antifungal agents: mode of action, mechanisms of resistance, and correlation of these mechanisms with bacterial resistance. *Clin. Microbiol. Rev.* **12**: 501-517.
Gonçalves, J.M., and Polson, A. (1947). The electrophoretic analysis of snake venoms. *Arch. of Biochem.* **13**: 253-259.
Gonçalves, S., Abade, J., Teixeira, A., and Santos, N.C. (2012a). Lipid composition is a determinant for human defensin HNP1 selectivity. *Biopolymers* **98**: 313-321.
Gonçalves, S., Teixeira, A., Abade, J., de Medeiros, L.N., Kurtenbach, E., and Santos, N.C. (2012b). Evaluation of the membrane lipid selectivity of the pea defensin *Ps*d1. *Biochim. Biophys. Acta* **1818**: 1420-1426.
Graham, M.D. (2003). The Coulter Principle: Foundation of an Industry. *JALA* **8**: 72-81.
Gunn, J.S., Ryan, S.S., Van Velkinburgh, J.C., Ernst, R.K., and Miller, S.I. (2000). Genetic and functional analysis of a PmrA-PmrB-regulated locus necessary for lipopolysaccharide modification, antimicrobial peptide resistance, and oral virulence of *Salmonella enterica* serovar typhimurium. *Infect. Immun.* **68**: 6139-6146.
Guo, M.L., Wei, J.G., Huang, X.H., Huang, Y.H., and Qin, Q.W. (2012). Antiviral effects of beta-defensin derived from orange-spotted grouper (*Epinephelus coioides*). *Fish Shellfish Immunol.* **x32**: 828-838.
Hakomori, S. (2003). Structure, organization, and function of glycosphingolipids in membrane. *Curr. Opin. Hematol.* **10**: 16-24.
Hakomori, S.I. (2008). Structure and function of glycosphingolipids and sphingolipids: recollections and future trends. *Biochim. Biophys. Acta* **1780**: 325-346.
Halter, D., Neumann, S., van Dijk, S.M., Wolthoorn, J., de Maziere, A.M., Vieira, O.V., Mattjus, P., Klumperman, J., van Meer, G., and Sprong, H. (2007). Pre- and post-Golgi translocation of glucosylceramide in glycosphingolipid synthesis. *J. Cell Biol.* **179**: 101-115.
Hancock, R.E., and Rozek, A. (2002). Role of membranes in the activities of antimicrobial cationic peptides. *FEMS Microbiol. Lett.* **206**: 143-149.

Hazlett, L., and Wu, M. (2011). Defensins in innate immunity. *Cell Tissue Res.* **343**: 175-188.
Heymann, P., Gerads, M., Schaller, M., Dromer, F., Winkelmann, G., and Ernst, J.F. (2002). The siderophore iron transporter of *Candida albicans* (Sit1p/Arn1p) mediates uptake of ferrichrome-type siderophores and is required for epithelial invasion. *Infect. Immun.* **70**: 5246-5255.
Hoskin, D.W., and Ramamoorthy, A. (2008). Studies on anticancer activities of antimicrobial peptides. *Biochim. Biophys. Acta* **1778**: 357-375.
Hwang, J.S., Lee, J., Kim, Y.J., Bang, H.S., Yun, E.Y., Kim, S.R., Suh, H.J., Kang, B.R., Nam, S.H., Jeon, J.P., Kim, I., and Lee, D.G. (2009). Isolation and Characterization of a Defensin-Like Peptide (Coprisin) from the Dung Beetle, *Copris tripartitus*. *Int. J. Pept.* **2009**.
Inigo, M., Peman, J., and Del Pozo, J.L. (2012). Antifungal activity against *Candida* biofilms. *Int. J. Artif. Organs* **35**: 780-791.
Islam, D., Bandholtz, L., Nilsson, J., Wigzell, H., Christensson, B., Agerberth, B., and Gudmundsson, G.H. (2001). Downregulation of bactericidal peptides in enteric infections: A novel immune escape mechanism with bacterial DNA as a potential regulator. *Nat. Med.* **7**: 180-185.
Jung, S.I., Finkel, J.S., Solis, N.V., Chaili, S., Mitchell, A.P., Yeaman, M.R., and Filler, S.G. (2013). Bcr1 Functions Downstream of Ssd1 To Mediate Antimicrobial Peptide Resistance in *Candida albicans*. *Eukaryot. Cell* **12**: 411-419.
Katzung, B.G., Masters, S.B., and Trevor, A.J. (2011). *Basic & Clinical Pharmacology*. Lange.
Khan, S.A., Fidel, P.L., Jr., Thunayyan, A.A., Varlotta, S., Meiller, T.F., and Jabra-Rizk, M.A. (2013). Impaired Histatin-5 Levels and Salivary Antimicrobial Activity against in HIV Infected Individuals. *J. AIDS Clin. Res.* **4**.
Kim, K.S., Kim, Y.S., Han, I., Kim, M.H., Jung, M.H., and Park, H.K. (2011). Quantitative and qualitative analyses of the cell death process in *Candida albicans* treated by antifungal agents. *PLoS ONE* **6**: e28176.
Kobayashi, Y., Takashima, H., Tamaoki, H., Kyogoku, Y., Lambert, P., Kuroda, H., Chino, N., Watanabe, T.X., Kimura, T., Sakakibara, S., and et al. (1991). The cystine-stabilized alpha-helix: a common structural motif of ion-channel blocking neurotoxic peptides. *Biopolymers* **31**: 1213-1220.
Koopman, G., Reutelingsperger, C.P., Kuijten, G.A., Keehnen, R.M., Pals, S.T., and van Oers, M.H. (1994). Annexin V for flow cytometric detection of phosphatidylserine expression on B cells undergoing apoptosis. *Blood* **84**: 1415-1420.
Kumamoto, C.A. (2008). Molecular mechanisms of mechanosensing and their roles in fungal contact sensing. *Nat. Rev. Microbiol.* **6**: 667-673.
Kuzhir, P., Volynets, N., Maksimenko, S., Kaplas, T., and Svirko, Y. (2013). Multilayered graphene in K(a)-band: nanoscale coating for aerospace applications. *J. Nanosci. Nanotechnol.* **13**: 5864-5867.
Kuznetsova, T.G., Starodubtseva, M.N., Yegorenkov, N.I., Chizhik, S.A., and Zhdanov, R.I. (2007). Atomic force microscopy probing of cell elasticity. *Micron* **38**: 824-833.
Ladokhin, A.S., Selsted, M.E., and White, S.H. (1999). CD spectra of indolicidin antimicrobial peptides suggest turns, not polyproline helix. *Biochemistry* **38**: 12313-12319.
Lai, Y.P., and Gallo, R.L. (2009). AMPed up immunity: how antimicrobial peptides have multiple roles in immune defense. *Trends Immunol.* **30**: 131-141.
Lam, W.A., Rosenbluth, M.J., and Fletcher, D.A. (2007). Chemotherapy exposure increases leukemia cell stiffness. *Blood* **109**: 3505-3508.
Lambert, R.J., and Pearson, J. (2000). Susceptibility testing: accurate and reproducible minimum inhibitory concentration (MIC) and non-inhibitory concentration (NIC) values. *J. Appl. Microbiol.* **88**: 784-790.
Lande, R., Gregorio, J., Facchinetti, V., Chatterjee, B., Wang, Y.H., Homey, B., Cao, W., Su, B., Nestle, F.O., Zal, T., Mellman, I., Schroder, J.M., Liu, Y.J., and Gilliet, M. (2007). Plasmacytoid dendritic cells sense self-DNA coupled with antimicrobial peptide. *Nature* **449**: 564-569.
Landon, C., Sodano, P., Hetru, C., Hoffmann, J., and Ptak, M. (1997). Solution structure of drosomycin, the first inducible antifungal protein from insects. *Protein Sci.* **6**: 1878-1884.
Lay, F.T., and Anderson, M.A. (2005). Defensins - Components of the innate immune system in plants. *Curr. Protein Pept. Sci.* **6**: 85-101.
Lee, J., Hwang, J.S., Hwang, I.S., Cho, J., Lee, E., Kim, Y., and Lee, D.G. (2012). Coprisin-induced antifungal effects in *Candida albicans* correlate with apoptotic mechanisms. *Free Radic. Biol. Med.* **52**: 2302-2311.
Lehrer, R.I. (2004). Primate defensins. *Nat. Rev. Microbiol.* **2**: 727-738.
Lehrer, R.I., and Ganz, T. (1999). Antimicrobial peptides in mammalian and insect host defence. *Curr. Opin. Immunol.* **11**: 23-27.
Lehrer, R.I., and Lu, W. (2011). α-Defensins in human innate immunity. *Immunol. Rev.* **245**: 84-112.
Leipelt, M., Warnecke, D., Zahringer, U., Ott, C., Muller, F., Hube, B., and Heinz, E. (2001). Glucosylceramide synthases, a gene family responsible for the biosynthesis of glucosphingolipids in animals, plants, and fungi. *J. Biol. Chem.* **276**: 33621-33629.
Li, M., Lai, Y.P., Villaruz, A.E., Cha, D.J., Sturdevant, D.E., and Otto, M. (2007). Gram-positive three-component antimicrobial peptide-sensing system. *Proc. Natl. Acad. Sci. U. S. A.* **104**: 9469-9474.
Li, R., Kumar, R., Tati, S., Puri, S., and Edgerton, M. (2013). *Candida albicans* Flu1-Mediated Efflux of Salivary Histatin 5 Reduces Its Cytosolic Concentration and Fungicidal Activity. *Antimicrob. Agents Chemother.* **57**: 1832-1839.
Li, Y., Xiang, Q., Zhang, Q., Huang, Y., and Su, Z. (2012). Overview on the recent study of antimicrobial peptides: origins, functions, relative mechanisms and application. *Peptides* **37**: 207-215.
Lin, D.C., Dimitriadis, E.K., and Horkay, F. (2007). Robust strategies for automated AFM force curve analysis--I. Non-adhesive indentation of soft, inhomogeneous materials. *J. Biomech. Eng.* **129**: 430-440.
Lindquist, S. (1992). Heat-shock proteins and stress tolerance in microorganisms. *Curr. Opin. Genet. Dev.* **2**: 748-755.
Lobo, D.S., Pereira, I.B., Fragel-Madeira, L., Medeiros, L.N., Cabral, L.M., Faria, J., Bellio, M., Campos, R.C., Linden, R., and Kurtenbach, E. (2007). Antifungal *Pisum sativum* defensin 1 interacts with *Neurospora crassa* cyclin F related to the cell cycle. *Biochemistry* **46**: 987-996.
Madeo, F., Frohlich, E., and Frohlich, K.U. (1997). A yeast mutant showing diagnostic markers of early and late apoptosis. *J. Cell Biol.* **139**: 729-734.
Madeo, F., Herker, E., Maldener, C., Wissing, S., Lachelt, S., Herlan, M., Fehr, M., Lauber, K., Sigrist, S.J., Wesselborg, S., and Frohlich, K.U. (2002). A caspase-related protease regulates apoptosis in yeast. *Mol. Cell* **9**: 911-917.
Magonov, S.N., Elings, V., and Whangbo, M.-H. (1997). Phase imaging and stiffness in tapping-mode atomic force microscopy. *Surf. Sci.* **375**: L385-L391.
Maisetta, G., Di Luca, M., Esin, S., Florio, W., Brancatisano, F.L., Bottai, D., Campa, M., and Batoni, G. (2008). Evaluation of the inhibitory effects of human serum components on bactericidal activity of human beta defensin 3. *Peptides* **29**: 1-6.
Martinez, N.F., and Garcia, R. (2006). Measuring phase shifts and energy dissipation with amplitude modulation atomic force microscopy. *Nanotechnology* **17**: S167-172.
Marvin, M.E., Williams, P.H., and Cashmore, A.M. (2003). The *Candida albicans* CTR1 gene encodes a functional copper transporter. *Microbiology* **149**: 1461-1474.
Maurya, I.K., Thota, C.K., Sharma, J., Tupe, S.G., Chaudhary, P., Singh, M.K., Thakur, I.S., Deshpande, M., Prasad, R., and Chauhan, V.S. (2013). Mechanism of action of novel synthetic dodecapeptides against *Candida albicans*. *Biochim. Biophys. Acta* **1830**: 5193-5203.
Mayer, F.L., Wilson, D., and Hube, B. (2012). *Candida albicans* pathogenicity mechanisms. *Virulence* **4**: 119-128.
McPhee, J.B., Scott, M.G., and Hancock, R.E. (2005). Design of host defence peptides for antimicrobial and immunity enhancing activities. *Comb. Chem. High Throughput Screen.* **8**: 257-272.
Mehra, T., Koberle, M., Braunsdorf, C., Mailander-Sanchez, D., Borelli, C., and Schaller, M. (2012). Alternative approaches to antifungal therapies. *Exp. Dermatol.* **21**: 778-782.

Meiller, T.F., Hube, B., Schild, L., Shirtliff, M.E., Scheper, M.A., Winkler, R., Ton, A., and Jabra-Rizk, M.A. (2009). A novel immune evasion strategy of *Candida albicans*: proteolytic cleavage of a salivary antimicrobial peptide. *PLoS ONE* **4**: e5039.
Mochon, A.B., and Liu, H. (2008). The antimicrobial peptide histatin-5 causes a spatially restricted disruption on the *Candida albicans* surface, allowing rapid entry of the peptide into the cytoplasm. *PLoS Pathog.* **4**: e1000190.
Mookherjee, N., and Hancock, R.E.W. (2007). Cationic host defence peptides: Innate immune regulatory peptides as a novel approach for treating infections. *Cell. Mol. Life Sci.* **64**: 922-933.
Mor, A., Nguyen, V.H., Delfour, A., Migliorесamour, D., and Nicolas, P. (1991). Isolation, Amino-Acid-Sequence, and Synthesis of Dermaseptin, a Novel Antimicrobial Peptide of Amphibian Skin. *Biochemistry* **30**: 8824-8830.
Mygind, P.H., Fischer, R.L., Schnorr, K.M., Hansen, M.T., Sonksen, C.P., Ludvigsen, S., Raventos, D., Buskov, S., Christensen, B., De Maria, L., Taboureau, O., Yaver, D., Elvig-Jorgensen, S.G., Sorensen, M.V., Christensen, B.E., Kjaerulff, S., Frimodt-Moller, N., Lehrer, R.I., Zasloff, M., and Kristensen, H.H. (2005). Plectasin is a peptide antibiotic with therapeutic potential from a saprophytic fungus. *Nature* **437**: 975-980.
Nicastro, G., Franzoni, L., de Chiara, C., Mancin, A.C., Giglio, J.R., and Spisni, A. (2003). Solution structure of crotamine, a Na+ channel affecting toxin from *Crotalus durissus terrificus* venom. *Eur. J. Biochem.* **270**: 1969-1979.
Nie, H.Y., Taylor, A.R., Lau, W.M., and MacFabe, D.F. (2011). Subcellular features revealed on unfixed rat brain sections by phase imaging. *Analyst* **136**: 2270-2276.
Nimrichter, L., Burdick, M.M., Aoki, K., Laroy, W., Fierro, M.A., Hudson, S.A., Von Seggern, C.E., Cotter, R.J., Bochner, B.S., Tiemeyer, M., Konstantopoulos, K., and Schnaar, R.L. (2008). E-selectin receptors on human leukocytes. *Blood* **112**: 3744-3752.
Nimrichter, L., and Rodrigues, M.L. (2011). Fungal glucosylceramides: from structural components to biologically active targets of new antimicrobials. *Front. Microbiol.* **2**: 212.
Nobile, C.J., Nett, J.E., Hernday, A.D., Homann, O.R., Deneault, J.S., Nantel, A., Andes, D.R., Johnson, A.D., and Mitchell, A.P. (2009). Biofilm matrix regulation by *Candida albicans* Zap1. *PLoS Biol.* **7**: e1000133.
Noble, S.M., French, S., Kohn, L.A., Chen, V., and Johnson, A.D. (2010). Systematic screens of a *Candida albicans* homozygous deletion library decouple morphogenetic switching and pathogenicity. *Nat. Genet.* **42**: 590-598.
Norris, J.A., Stabile, K.J., and Jinnah, R.H. (2008). An introduction to tribology. *J. Surg. Orthop. Adv.* **17**: 2-5.
Oberparleiter, C., Kaiserer, L., Haas, H., Ladurner, P., Andratsch, M., and Marx, F. (2003). Active internalization of the *Penicillium chrysogenum* antifungal protein PAF in sensitive aspergilli. *Antimicrob. Agents Chemother.* **47**: 3598-3601.
Oeemig, J.S., Lynggaard, C., Knudsen, D.H., Hansen, F.T., Norgaard, K.D., Schneider, T., Vad, B.S., Sandvang, D.H., Nielsen, L.A., Neve, S., Kristensen, H.H., Sahl, H.G., Otzen, D.E., and Wimmer, R. (2012). Eurocin, a New Fungal Defensin STRUCTURE, LIPID BINDING, AND ITS MODE OF ACTION. *J. Biol. Chem.* **287**: 42361-42372.
Oren, Z., Hong, J., and Shai, Y. (1997). A repertoire of novel antibacterial diastereomeric peptides with selective cytolytic activity. *J. Biol. Chem.* **272**: 14643-14649.
Osborn, R.W., De Samblanx, G.W., Thevissen, K., Goderis, I., Torrekens, S., Van Leuven, F., Attenborough, S., Rees, S.B., and Broekaert, W.F. (1995). Isolation and characterisation of plant defensins from seeds of Asteraceae, Fabaceae, Hippocastanaceae and Saxifragaceae. *FEBS Lett.* **368**: 257-262.
Ouellette, A.J., and Selsted, M.E. (1996). Paneth cell defensins: endogenous peptide components of intestinal host defense. *FASEB J.* **10**: 1280-1289.
Pang, H.B., Hevroni, L., Kol, N., Eckert, D.M., Tsvitov, M., Kay, M.S., and Rousso, I. (2013). Virion stiffness regulates immature HIV-1 entry. *Retrovirology* **10**: 4.
Pasupuleti, M., Schmidtchen, A., and Malmsten, M. (2011). Antimicrobial peptides: key components of the innate immune system. *Crit. Rev. Biotechnol.* **32**: 143-171.
Phan, Q.T., Fratti, R.A., Prasadarao, N.V., Edwards, J.E., Jr., and Filler, S.G. (2005). N-cadherin mediates endocytosis of *Candida albicans* by endothelial cells. *J. Biol. Chem.* **280**: 10455-10461.
Pinto, M.R., Rodrigues, M.L., Travassos, L.R., Haido, R.M., Wait, R., and Barreto-Bergter, E. (2002). Characterization of glucosylceramides in *Pseudallescheria boydii* and their involvement in fungal differentiation. *Glycobiology* **12**: 251-260.
Poulain, D. (2012). *Candida albicans*, plasticity and pathogenesis. *Crit. Rev. Microbiol.*
Pujari, S.P., Li, Y., Regeling, R., and Zuilhof, H. (2013). Tribology and Stability of Organic Monolayers on CrN: A Comparison among Silane, Phosphonate, Alkene, and Alkyne Chemistries. *Langmuir* **29**: 10405-10415.
Rahman, A.H. (2013). Flow cytometric methods for the assessment of allergic disease. *Methods Mol. Biol.* **1032**: 297-313.
Reddy, K.V., Yedery, R.D., and Aranha, C. (2004). Antimicrobial peptides: premises and promises. *Int. J. Antimicrob. Agents* **24**: 536-547.
Ren, Q., Li, M., Zhang, C.Y., and Chen, K.P. (2011). Six defensins from the triangle-shell pearl mussel *Hyriopsis cumingii*. *Fish Shellfish Immunol.* **31**: 1232-1238.
Rittershaus, P.C., Kechichian, T.B., Allegood, J.C., Merrill, A.H., Jr., Hennig, M., Luberto, C., and Del Poeta, M. (2006). Glucosylceramide synthase is an essential regulator of pathogenicity of *Cryptococcus neoformans*. *J. Clin. Invest.* **116**: 1651-1659.
Rodrigues, M.L., Shi, L., Barreto-Bergter, E., Nimrichter, L., Farias, S.E., Rodrigues, E.G., Travassos, L.R., and Nosanchuk, J.D. (2007). Monoclonal antibody to fungal glucosylceramide protects mice against lethal *Cryptococcus neoformans* infection. *Clin. Vaccine Immunol.* **14**: 1372-1376.
Rosenbluth, M.J., Lam, W.A., and Fletcher, D.A. (2006). Force microscopy of nonadherent cells: a comparison of leukemia cell deformability. *Biophys. J.* **90**: 2994-3003.
Ruhnke, M., and Maschmeyer, G. (2002). Management of mycoses in patients with hematologic disease and cancer -- review of the literature. *Eur. J. Med. Res.* **7**: 227-235.
Sahl, H.G., Pag, U., Bonness, S., Wagner, S., Antcheva, N., and Tossi, A. (2005). Mammalian defensins: structures and mechanism of antibiotic activity. *J. Leukoc. Biol.* **77**: 466-475.
Saito, K., Takakuwa, N., Ohnishi, M., and Oda, Y. (2006). Presence of glucosylceramide in yeast and its relation to alkali tolerance of yeast. *Appl. Microbiol. Biotechnol.* **71**: 515-521.
Sandgren, S., Wittrup, A., Cheng, F., Jonsson, M., Eklund, E., Busch, S., and Belting, M. (2004). The human antimicrobial peptide LL-37 transfers extracellular DNA plasmid to the nuclear compartment of mammalian cells via lipid rafts and proteoglycan-dependent endocytosis. *J. Biol. Chem.* **279**: 17951-17956.
Santos, N.C., and Castanho, M.A. (2004). An overview of the biophysical applications of atomic force microscopy. *Biophys. Chem.* **107**: 133-149.
Schneider, T., Kruse, T., Wimmer, R., Wiedemann, I., Sass, V., Pag, U., Jansen, A., Nielsen, A.K., Mygind, P.H., Raventos, D.S., Neve, S., Ravn, B., Bonvin, A.M., De Maria, L., Andersen, A.S., Gammelgaard, L.K., Sahl, H.G., and Kristensen, H.H. (2010). Plectasin, a fungal defensin, targets the bacterial cell wall precursor Lipid II. *Science* **328**: 1168-1172.
Schroder, J.M., and Harder, J. (1999). Human beta-defensin-2. *Int. J. Biochem. Cell Biol.* **31**: 645-651.
Seibold, M., Wolschann, P., Bodevin, S., and Olsen, O. (2011). Properties of the bubble protein, a defensin and an abundant component of a fungal exudate. *Peptides* **32**: 1989-1995.
Semple, F., and Dorin, J.R. (2012). β-Defensins: multifunctional modulators of infection, inflammation and more? *J. Innate Immun.* **4**: 337-348.
Semple, F., Webb, S., Li, H.N., Patel, H.B., Perretti, M., Jackson, I.J., Gray, M., Davidson, D.J., and Dorin, J.R. (2010). Human beta-defensin 3 has immunosuppressive activity in vitro and in vivo. *Eur. J. Immunol.* **40**: 1073-1078.
Severin, F.F., and Hyman, A.A. (2002). Pheromone induces programmed cell death in *S. cerevisiae*. *Curr. Biol.* **12**: R233-235.

Shai, Y. (1999). Mechanism of the binding, insertion and destabilization of phospholipid bilayer membranes by alpha-helical antimicrobial and cell non-selective membrane-lytic peptides. *Biochim. Biophys. Acta* **1462**: 55-70.
Shai, Y. (2002). Mode of action of membrane active antimicrobial peptides. *Biopolymers* **66**: 236-248.
Si, H., Hernday, A.D., Hirakawa, M.P., Johnson, A.D., and Bennett, R.J. (2013). *Candida albicans* white and opaque cells undergo distinct programs of filamentous growth. *PLoS Pathog.* **9**: e1003210.
Simson, E. (2013). Wallace Coulter's life and his impact on the world. *Int J Lab Hematol* **35**: 230-236.
Staubach, S., and Hanisch, F.G. (2011). Lipid rafts: signaling and sorting platforms of cells and their roles in cancer. *Expert Rev. Proteomics* **8**: 263-277.
Sullan, R.M., Li, J.K., and Zou, S. (2009). Quantification of the nanomechanical stability of ceramide-enriched domains. *Langmuir* **25**: 12874-12877.
Szafranski-Schneider, E., Swidergall, M., Cottier, F., Tielker, D., Roman, E., Pla, J., and Ernst, J.F. (2012). Msb2 shedding protects *Candida albicans* against antimicrobial peptides. *PLoS Pathog.* **8**: e1002501.
Ternovskii, A.P., Alekhin, V.P., Shorshorov, M.K., Khrushchov, M.M., and Skvortsov, V.N. (1974). Micromechanical testing of materials by depression. *Zavodskaya Laboratoriya* **39**: 1242-1247.
Terras, F.R., Schoofs, H.M., De Bolle, M.F., Van Leuven, F., Rees, S.B., Vanderleyden, J., Cammue, B.P., and Broekaert, W.F. (1992). Analysis of two novel classes of plant antifungal proteins from radish (*Raphanus sativus* L.) seeds. *J. Biol. Chem.* **267**: 15301-15309.
Thevissen, K., Ferket, K.K., Francois, I.E., and Cammue, B.P. (2003). Interactions of antifungal plant defensins with fungal membrane components. *Peptides* **24**: 1705-1712.
Thevissen, K., Tavares, P.D., Xu, D.M., Blankenship, J., Vandenbosch, D., Idkowiak-Baldys, J., Govaert, G., Bink, A., Rozental, S., de Groot, P.W.J., Davis, T.R., Kumamoto, C.A., Vargas, G., Nimrichter, L., Coenye, T., Mitchell, A., Roemer, T., Hannun, Y.A., and Cammue, B.P.A. (2012). The plant defensin RsAFP2 induces cell wall stress, septin mislocalization and accumulation of ceramides in *Candida albicans*. *Mol. Microbiol.* **84**: 166-180.
Thevissen, K., Terras, F.R., and Broekaert, W.F. (1999). Permeabilization of fungal membranes by plant defensins inhibits fungal growth. *Appl. Environ. Microbiol.* **65**: 5451-5458.
Thevissen, K., Warnecke, D.C., Francois, E.J.A., Leipelt, M., Heinz, E., Ott, C., Zahringer, U., Thomma, B.P.H.J., Ferkel, K.K.A., and Cammue, B.P.A. (2004). Defensins from insects and plants interact with fungal glucosylceramides. *J. Biol. Chem.* **279**: 3900-3905.
Thomma, B.P.H.J., Cammue, B.P.A., and Thevissen, K. (2002). Plant defensins. *Planta* **216**: 193-202.
Tyagi, A.K., and Malik, A. (2010). In situ SEM, TEM and AFM studies of the antimicrobial activity of lemon grass oil in liquid and vapour phase against *Candida albicans*. *Micron* **41**: 797-805.
Ulm, H., Wilmes, M., Shai, Y., and Sahl, H.G. (2012). Antimicrobial host defensins - specific antibiotic activities and innate defense modulation. *Front. Immunol.* **3**: 249.
Vachova, L., and Palkova, Z. (2005). Physiological regulation of yeast cell death in multicellular colonies is triggered by ammonia. *J. Cell Biol.* **169**: 711–717.
van der Weerden, N.L., Bleackley, M.R., and Anderson, M.A. (2013). Properties and mechanisms of action of naturally occurring antifungal peptides. *Cell. Mol. Life Sci.* **70**: 3545-3570.
van Dijk, A., Veldhuizen, E.J., and Haagsman, H.P. (2008). Avian defensins. *Vet. Immunol. Immunopathol.* **124**: 1-18.
Verstrepen, K.J., and Klis, F.M. (2006). Flocculation, adhesion and biofilm formation in yeasts. *Mol. Microbiol.* **60**: 5-15.
Vylkova, S., Carman, A.J., Danhof, H.A., Collette, J.R., Zhou, H., and Lorenz, M.C. (2011). The fungal pathogen *Candida albicans* autoinduces hyphal morphogenesis by raising extracellular pH. *MBio* **2**: e00055-00011.
Vylkova, S., Jang, W.S., Li, W., Nayyar, N., and Edgerton, M. (2007). Histatin 5 initiates osmotic stress response in *Candida albicans* via activation of the Hog1 mitogen-activated protein kinase pathway. *Eukaryot. Cell* **6**: 1876-1888.
Wachtler, B., Wilson, D., Haedicke, K., Dalle, F., and Hube, B. (2011). From attachment to damage: defined genes of *Candida albicans* mediate adhesion, invasion and damage during interaction with oral epithelial cells. *PLoS ONE* **6**: e17046.
Wang, D.Y.C., Kumar, S., and Hedges, S.B. (1999). Divergence time estimates for the early history of animal phyla and the origin of plants, animals and fungi. *Proc. Biol. Sci.* **266**: 163-171.
Weinberger, M., Ramachandran, L., Feng, L., Sharma, K., Sun, X., Marchetti, M., Huberman, J.A., and Burhans, W.C. (2005). Apoptosis in budding yeast caused by defects in initiation of DNA replication. *J. Cell Sci.* **118**: 3543-3553.
Westerhoff, H.V., Zasloff, M., Rosner, J.L., Hendler, R.W., De Waal, A., Vaz Gomes, A., Jongsma, P.M., Riethorst, A., and Juretic, D. (1995). Functional synergism of the magainins PGLa and magainin-2 in *Escherichia coli*, tumor cells and liposomes. *Eur. J. Biochem.* **228**: 257-264.
Wimley, W.C., and Hristova, K. (2011). Antimicrobial peptides: successes, challenges and unanswered questions. *J. Membr. Biol.* **239**: 27-34.
Wu, Z.B., Hoover, D.M., Yang, D., Boulegue, C., Santamaria, F., Oppenheim, J.J., Lubkowski, J., and Lu, W.Y. (2003). Engineering disulfide bridges to dissect antimicrobial and chemotactic activities of human beta-defensin 3. *Proc. Natl. Acad. Sci. U. S. A.* **100**: 8880-8885.
Yamane, E.S., Bizerra, F.C., Oliveira, E.B., Moreira, J.T., Rajabi, M., Nunes, G.L.C., de Souza, A.O., da Silva, I.D.C.G., Yamane, T., Karpel, R.L., Silva, P.I., and Hayashi, M.A.F. (2013). Unraveling the antifungal activity of a South American rattlesnake toxin crotamine. *Biochimie* **95**: 231-240.
Yamasaki, K., Di Nardo, A., Bardan, A., Murakami, M., Ohtake, T., Coda, A., Dorschner, R.A., Bonnart, C., Descargues, P., Hovnanian, A., Morhenn, V.B., and Gallo, R.L. (2007). Increased serine protease activity and cathelicidin promotes skin inflammation in rosacea. *Nat. Med.* **13**: 975-980.
Yang, L., Weiss, T.M., Lehrer, R.I., and Huang, H.W. (2000). Crystallization of antimicrobial pores in membranes: magainin and protegrin. *Biophys. J.* **79**: 2002-2009.
Yeaman, M.R., Soldan, S.S., Ghannoum, M.A., Edwards, J.E., Filler, S.G., and Bayer, A.S. (1996). Resistance to platelet microbicidal protein results in increased severity of experimental *Candida albicans* endocarditis. *Infect. Immun.* **64**: 1379-1384.
Yeaman, M.R., and Yount, N.Y. (2003). Mechanisms of antimicrobial peptide action and resistance. *Pharmacol. Rev.* **55**: 27-55.
Yount, N.Y., and Yeaman, M.R. (2005). Immunocontinuum: perspectives in antimicrobial peptide mechanisms of action and resistance. *Protein Pept. Lett.* **12**: 49-67.
Zasloff, M. (2002). Antimicrobial peptides of multicellular organisms. *Nature* **415**: 389-395.
Zheng, X., and Wang, Y. (2004). Hgc1, a novel hypha-specific G1 cyclin-related protein regulates *Candida albicans* hyphal morphogenesis. *EMBO J.* **23**: 1845-1856.
Zhu, S.Y., and Gao, B. (2013). Evolutionary origin of beta-defensins. *Dev. Comp. Immunol.* **39**: 79-84.
Zhu, W., and Filler, S.G. (2009). Interactions of *Candida albicans* with epithelial cells. *Cell. Microbiol.* **12**: 273-282.

Appendix

This section includes information and results that complement the text of the previous chapters. The reader will find some of the outcomes of this work in terms of publications and communications, which include two abstract of posters presented in congress and the abstract of a review article focused in antifungal defensins. Also in this section is an original article that studies the effects of the AMP $rBPI_{21}$ against *Escherichia coli* and *Staphylococcus aureus*, that relies on some of the techniques employed in this thesis. Furthermore, the data presented in this thesis will also be converted in an additional manuscript, to be submitted to an international peer-reviewed journal during the upcoming months.

Supplementary data

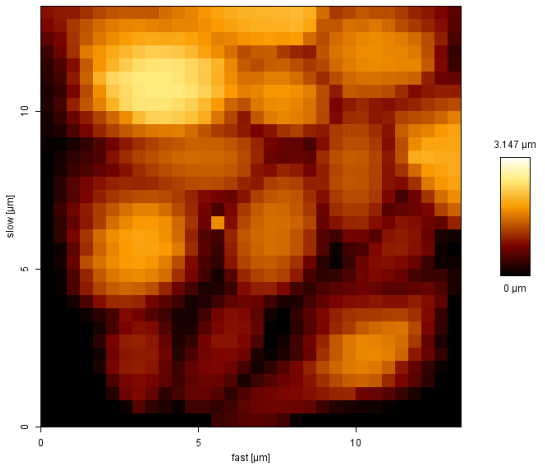

Figure SF1. Force map of *C. albicans* WT cells after 24 h incubation with Amph B.
These cells were treated with an Amph B concentration 10-fold higher than the MIC. Force maps like the one exemplified here were used to perform AFM-based force spectroscopy assays for the Young's Modulus determination. Each pixel (square) in the image has a coordinate and the highest pixel (the lighter the color, the higher the coordinate) in each cell was chosen to perform force-distance curves over it, in triplicate.

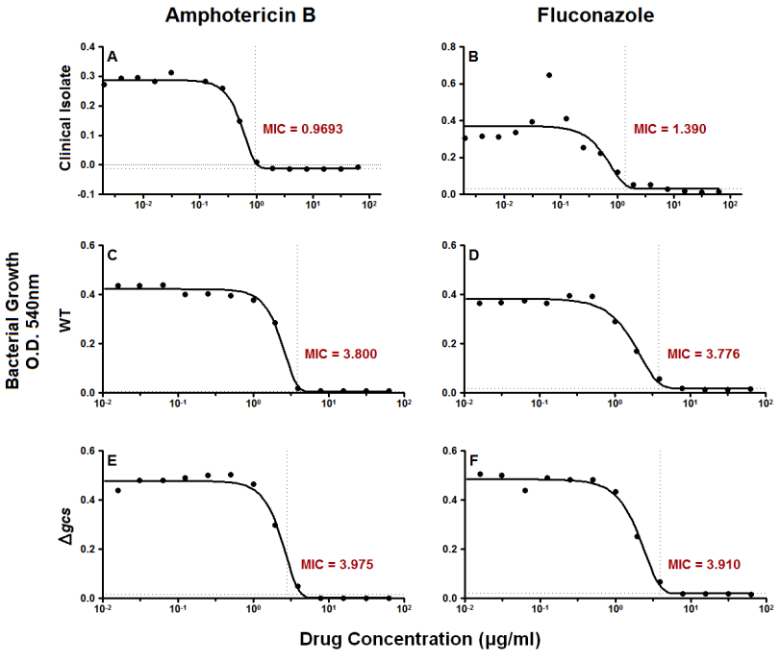

Figure SF2. Susceptibility curves of Amph B or FCZ against the *C. albicans* clinical isolate, WT and Δ*gcs* cells.
Curves were fitted and the MIC value was obtained using the Gompertz equation.

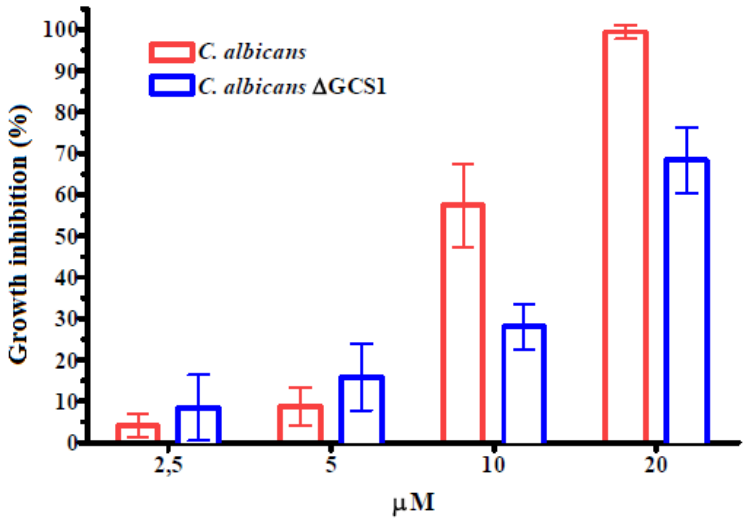

Figure SF3. Growth inhibition curve of *C. albicans* WT and Δ*gcs* by *Ps*d1. Results represent four independent experiments, made in duplicate. Determined by Luciano de Medeiros and included in his doctoral thesis (de Medeiros, 2009).

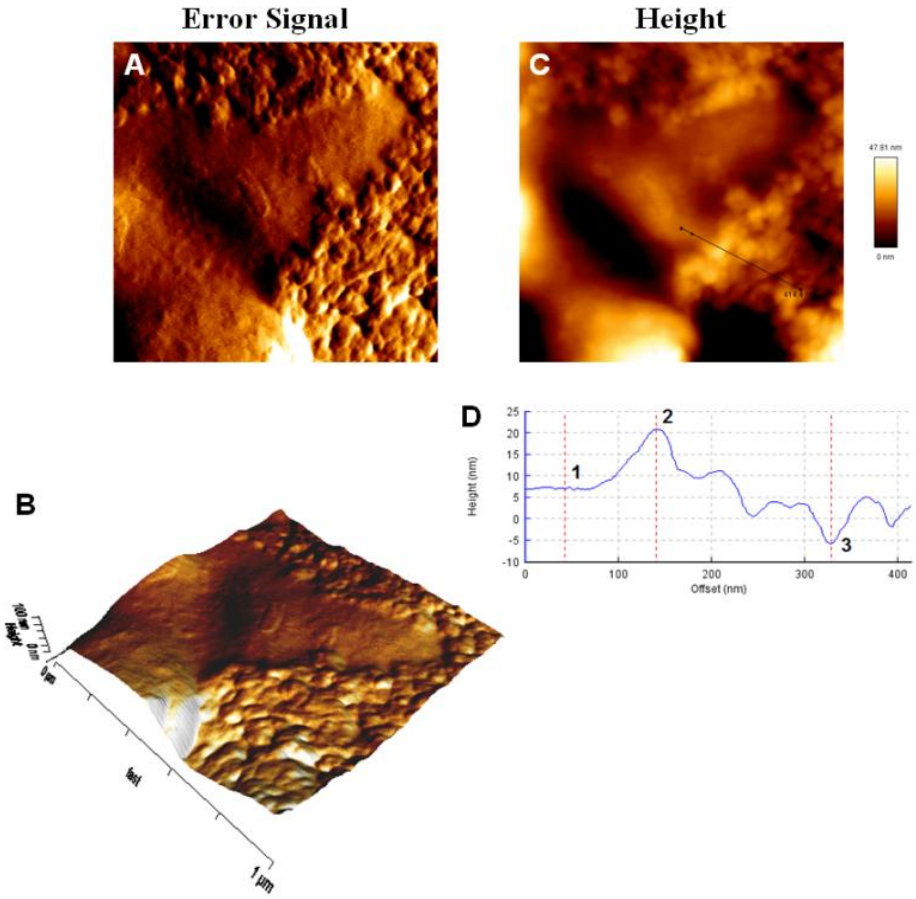

Figure SF4. Blebbing detail of *C. albicans* WT cell after 24 h incubation with *Ps*d1 (10 x MIC). Error signal (A) and height images (C) are 1μm^2 and were used to make a pseudo-3D representation of the membrane blebs (B). Cross-section of image C (black line), represented by the height profile D, was traced to determine the height of the blebs: the difference in height between 1 (cell membrane) and 2 (first bleb in the cross section) is 13.8 nm, while the difference between 1 and 3 (lower point in the bulk of blebs) is 12.8 nm.

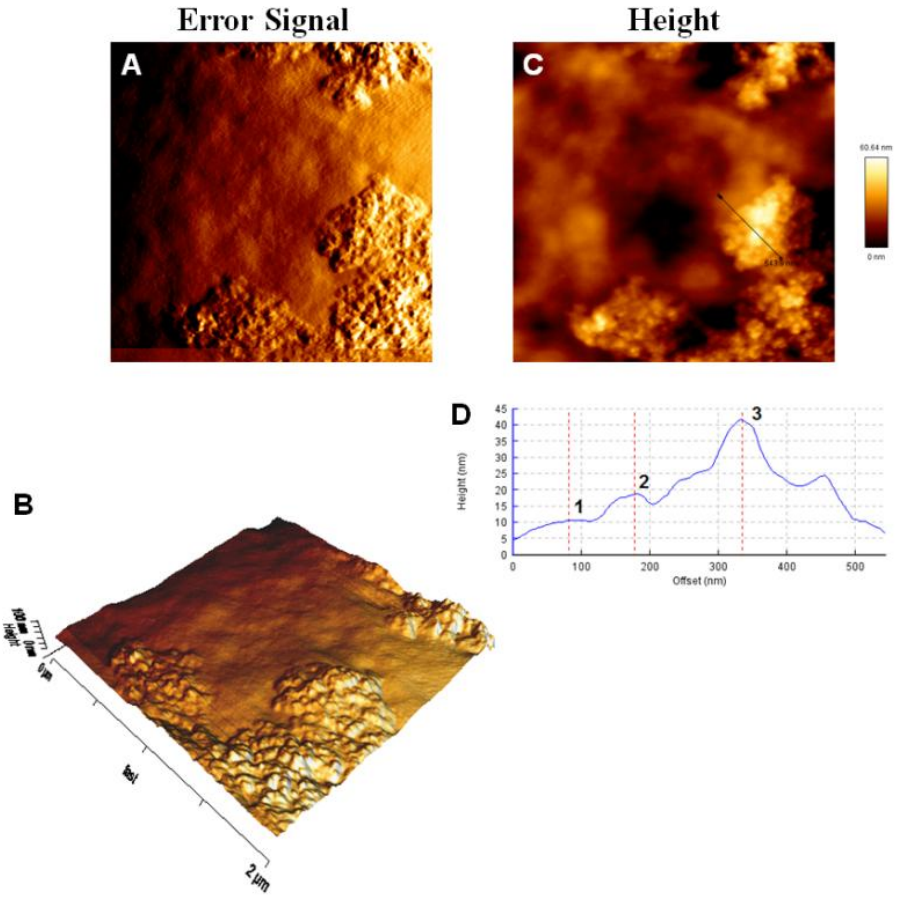

Figure SF5. Blebbing detail of *C. albicans* Δ*gcs* cell, after 24 h incubation with *Ps*d1 (10 x MIC). Error signal (A) and height images (C) are 2 µm^2 and were used to make a pseudo-3D representation of the membrane blebs (B). A cross-section on image C (black line), represented by the height profile D, was used to determine the height of the blebs: the difference of height between 1 (cell membrane) and 2 (first bleb in the cross section) is 7.83 nm, while the difference between 1 and 3 (higher point in the bulk of blebs) is 36.5 nm.

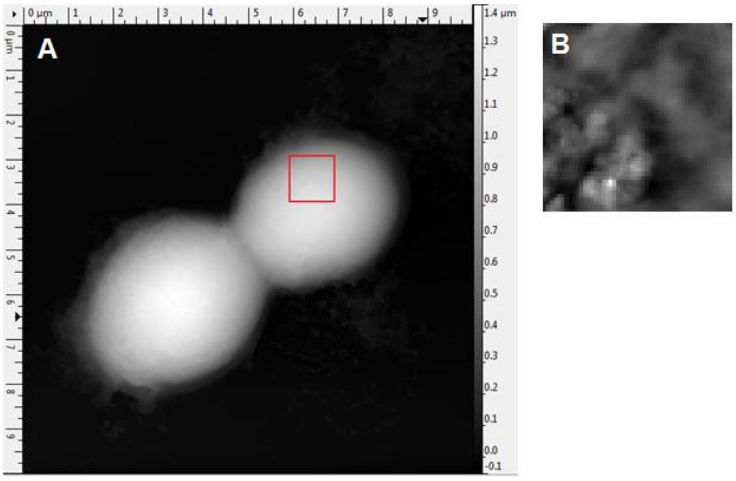

Figure SF6. Height images of *C. albicans* Δ*gcs* cells after 6 h treatment with Psd1 (10 x MIC). The red square in A is 1 µm^2 and B is the cropped area of the red square after leveling. Several crops like this over one cell were used to calculate the RMS of the membrane surface, as described in the Methodology section.

Outcomes of the present thesis

The following first two abstracts are relative to the posters presented by me and Sónia Gonçalves, respectively, at the 9th European Biophysics Congress – EBSA 2013, published in the *European Biophysical Journal*.

Antifungal defensin *Ps*d1 increases membrane roughness and promotes apoptosis in *Candida albicans*

Patrícia M. Silva [a], Sónia Gonçalves [a], Luciano Neves de Medeiros [b], Eleonora Kurtenbach [b], Nuno C. Santos [a]

[a] Instituto de Medicina Molecular, Faculdade de Medicina da Universidade de Lisboa, Lisbon, Portugal
[b] Instituto de Biofísica Carlos Chagas Filho, Universidade Federal do Rio de Janeiro, Rio de Janeiro, Brazil

*Ps*d1 is a defensin, isolated from *Pisum sativum* seeds, previously shown to have a strong interaction with fungal-specific membrane components [1]. *Candida albicans* is an important human pathogen, causing oral, genital and systemic opportunistic infections, which are especially relevant clinically in immunocompromised patients, such as HIV-infected individuals. We tested the effects of this antimicrobial peptide, comparing it with the antifungal drugs amphotericine B and fluconazole, at the minimal inhibitory concentration (MIC) and at a 10-fold higher concentration. By atomic force microscopy (AFM) imaging we assessed morphological changes on *C. albicans* cells. SYTO-9 and propidium iodide allowed us to image live and dead cells by confocal microscopy and to quantify their ratio. Our results show that, with increasing incubation times and *Ps*d1 concentrations, there is an increased cell death and surface roughness, with the appearance of apoptotic features, such as membrane blebs, cell size alterations, membrane disruption and leakage of cellular contents. Thus, we were able to visualize the action of *Ps*d1 against a relevant fungal human pathogen, aiming at its possible use as a natural antimycotic agent.

[1] Gonçalves *et al.* (2012) *Biochim Biophys Acta* 1818:1420

Biofilm formation by different *Candida albicans* variants and their antifungal agents' susceptibility

Sónia Gonçalves [a], Patrícia M. Silva [a], Luciano Neves de Medeiros [b], Eleonora Kurtenbach [b], Nuno C. Santos [a]

[a] Instituto de Medicina Molecular, Faculdade de Medicina da Universidade de Lisboa, Lisbon, Portugal
[b] Instituto de Biofísica Carlos Chagas Filho, Universidade Federal do Rio de Janeiro, Rio de Janeiro, Brazil

Biofilms represent the most common type of microbial growth in nature and are crucial to the development of clinical infections. Candidiasis associated with intravenous lines and bioprosthetic devices is problematic, since these devices can act as substrates for biofilm growth. In the present work *Candida albicans* biofilm formation was studied in the absence and in presence of a defensin, *Ps*d1 [1], and two current antimicotic drugs: amphotericine B and fluconazole. Three *C. albicans* variants were studied, one of them a mutant deficient in glucosylceramide synthase, conferring resistance to *Ps*d1 antifungal action. Differences in the biofilm formation were encountered for the variants studied. Atomic force microscopy (AFM) images showed that during the biofilm growth a structured mesh of fungal cells is formed with 1.2-1.5 μM height (single cell have 500-600 nm). The action of the three antifungal agents was evaluated both in terms of inhibition of the biofilm formation and disruption of previously formed biofilm.

[1] Gonçalves *et al.* (2012) *Biochim Biophys Acta* 1818:1420

Next are the abstracts of the two manuscripts I am co-author of. The third abstract is of a review with a subject closely related to this thesis work, which is submitted for publication in the journal *Frontiers in Antimicrobials, Resistance and Chemotherapy*. The manuscript is under editorial revision and was considered as acceptable with minor changes.

Defensins: antifungal lessons from eukaryotes

Patrícia M. Silva, Sónia Gonçalves, Nuno C. Santos

Instituto de Medicina Molecular, Faculdade de Medicina, Universidade de Lisboa, Lisbon, Portugal

Pathogenic fungi resistance to conventional antimycotic drugs is becoming a major problem as fungal infections in immunocompromised patients, as well as infections caused by primary pathogenic fungi, are leading to clinical situations hard to overcome. Furthermore, in agriculture, phytopathogenic fungi lower crop yields and increase food stock price, resulting in an enormous economic burden. Over the last years, antimicrobial peptides (AMPs) have been the focus of intense research towards finding a viable alternative to current antifungal drugs. Defensins are cysteine-stabilized AMPs found in plants, animals and fungi, which provide an important first line of host defense against microorganisms, demonstrating a relevant effect against pathogenic fungi. The fact that defensins act as an important vehicle of information between innate and adaptive immune system and that there are structural homologies between defensins from diverse eukaryotic origins demonstrate the difficulty of microorganisms in facing this host shield. Defensins, as other AMPs, may become the basis for effective antimycotic therapies.

Keywords: antimicrobial peptides; defensins; antifungal; resistance; host defense peptides.

The fourth abstract, although of a manuscript not related to this thesis, employs some of the same techniques to study another AMP. It was submitted for publication in the journal *Nanomedicine (NBM)* and is under editorial revision after the submission of a revised version. It was also considered acceptable with minor changes.

Antimicrobial protein $rBPI_{21}$-induced surface changes on Gram-negative and Gram-positive bacteria

Marco M. Domingues, Patrícia M. Silva, Henri G. Franquelim, Filomena A. Carvalho, Miguel A.R.B. Castanho, Nuno C. Santos

Instituto de Medicina Molecular, Faculdade de Medicina, Universidade de Lisboa, Av. Prof. Egas Moniz, 1649-028 Lisbon, Portugal.

New classes of antibiotics, such as antimicrobial peptides or proteins (AMPs), with new modes of action, are crucial to deal with threatening bacterial diseases. $rBPI_{21}$ is an AMP based on the human neutrophil BPI protein, with potential clinical use for meningitis. We studied the membrane perturbations promoted by $rBPI_{21}$ on Gram-negative *Escherichia coli* and Gram-positive *Staphyloccoccus aureus*. Its interaction with bacteria was also studied in the presence of lipopolysaccharide (LPS), $rBPI_{21}$ major ligand. Flow cytometry analysis of both *E. coli* and *S. aureus* shows that $rBPI_{21}$ induces membrane depolarization. $rBPI_{21}$ increases the negative surface charge of both bacteria toward positive values, as shown by zeta-potential measurements. This charge modification is followed by surface perturbations, culminating in cell lysis, as visualized by atomic force microscopy (AFM). Force spectroscopy measurements show that soluble LPS decreases the interaction of $rBPI_{21}$ with bacteria, being this effect more pronounced for *S. aureus*. This indicates that $rBPI_{21}$ is able to interact with Gram-positive bacteria using the same domain involved on LPS-binding.

Keywords: Lipopolysaccharide; $rBPI_{21}$; atomic force microscopy.

U LISBOA | UNIVERSIDADE DE LISBOA

2013